

Durham E-Theses

Synthesis and characterisation of new amphiphilic molecules for non-linear optics

Grainger, Andrew McAngus

How to cite:

Grainger, Andrew McAngus (1991) *Synthesis and characterisation of new amphiphilic molecules for non-linear optics*, Durham theses, Durham University. Available at Durham E-Theses Online: <http://etheses.dur.ac.uk/6028/>

Use policy

The full-text may be used and/or reproduced, and given to third parties in any format or medium, without prior permission or charge, for personal research or study, educational, or not-for-profit purposes provided that:

- a full bibliographic reference is made to the original source
- a [link](#) is made to the metadata record in Durham E-Theses
- the full-text is not changed in any way

The full-text must not be sold in any format or medium without the formal permission of the copyright holders.

Please consult the [full Durham E-Theses policy](#) for further details.

The copyright of this thesis rests with the author.
No quotation from it should be published without
his prior written consent and information derived
from it should be acknowledged.

SYNTHESIS AND CHARACTERISATION OF NEW AMPHIPHILIC MOLECULES
FOR NON-LINEAR OPTICS

by

Andrew McAngus Grainger, B. Sc.

Department of Chemistry
University of Durham

A Thesis submitted for the degree of
Doctor of Philosophy at the University of Durham.

October 1991



- 8 JUL 1992

STATEMENT OF COPYRIGHT

The copyright of this thesis rests with the author. No quotation from it should be published without his prior written consent, and information derived from it should be acknowledged.

DECLARATION

The work described in this thesis was carried out by the author, in the Department of Chemistry, University of Durham and the Centre for Molecular Electronics, Cranfield Institute of Technology, Cranfield, between October 1988 and October 1991.

ABSTRACT

SYNTHESIS AND CHARACTERISATION OF NEW AMPHIPHILIC MOLECULES FOR NON-LINEAR OPTICS

New amphiphilic donor- π -acceptor chromophores have been prepared and characterised. The LB film forming and second order non-linear optical properties of these amphiphiles have been investigated.

New electron acceptors have been prepared using the reagent 2-chlorobenzylthiocyanate. The scope of the reagent for the preparation of TCNQ derivatives has been investigated. New DCNQI and N,7,7-tricyanoquinomethaneimines have been prepared and characterised. Attempts to prepare novel donor- π -acceptor compounds from these electron acceptors were unsuccessful.

The synthesis, LB deposition and CT spectra of R-Q3CNQ (R = C₆H₁₃ to C₂₀H₄₁) and four substituted analogues have been studied. The second harmonic intensity from Z-type films of C₁₆H₃₃-Q3CNQ was found to increase quadratically with the number of LB layers.

Zwitterionic amphiphiles with benzothiazolium and thiazolium donor groups (C₁₆H₃₃-BT3CNQ and C₆H₁₃-T3CNQ) have been prepared and characterised. No SHG was observed from films of C₆H₁₃-T3CNQ. Films of C₁₆H₃₃-BT3CNQ are Y-type and optical SHG has been observed from odd numbers of layers. A variation in SH intensity with the number of laser pulses has been observed.

The synthesis, CT spectra and LB deposition of some new hemicyanine derivatives have been studied. The LB films have a Y-type structure and SHG was observed from films with odd numbers of layers.

Novel push-pull chromophores with the 1,3-dithiole donor group have been prepared and characterised. The LB deposition, CT spectra and NLO properties have been studied.

AKNOWLEDGEMENTS

I would like to thank the following:

My joint supervisors, Dr. Martin R. Bryce (Durham University) and Dr. Geoffrey J. Ashwell (Cranfield Institute of Technology) for their help and encouragement. Dr. Masihul Hasan and Dr. Stephen R. Davies for help relating to the synthesis of electron acceptors. Dr. Mike Jones for obtaining mass spectra and Dr. Ray Matthews for NMR services. Michael B. Hursthouse, Paul Bates and Mohammed Mazid for the X-ray structural analyses. Finally, to Heather.

CONTENTS

	<u>PAGE</u>
CHAPTER ONE - INTRODUCTION TO NON-LINEAR OPTICS	
1.1 THE ORIGIN OF NON-LINEAR OPTICAL EFFECTS	2
1.2 MACROSCOPIC NON-LINEARITIES	4
1.3 MATERIALS FOR NON-LINEAR OPTICS	7
1.4 DETERMINATION OF SECOND ORDER HYPERPOLARISABILITIES	12
1.5 THE LANGMUIR BLODGETT TECHNIQUE	15
1.6 DEPOSITION TECHNIQUES	18
1.7 NON-LINEAR OPTICAL STUDIES OF LB FILMS	19
1.8 ORGANIC CRYSTALS FOR NON-LINEAR OPTICS	31
1.9 POLYMERS FOR NON-LINEAR OPTICS	35
CHAPTER TWO - NEW DERIVATIVES OF 7, 7, 8, 8-TETRACYANO- -P-QUINODIMETHANE, <u>N, N'</u> -DICYANOQUINONEDIIMINE AND <u>N, 7, 7</u> -TRICYANOQUINOMETHANEIMINE SYSTEMS	
2.1 INTRODUCTION	38
2.2 SYNTHETIC STUDIES	44
2.3 X-RAY CRYSTAL STRUCTURE OF 2, 5-DIBROMO-TCNQ (41d)	47
2.4 THE SYNTHESIS, ELECTROCHEMISTRY AND X-RAY CRYSTAL STRUCTURE OF SOME NEW <u>N, 7, 7</u> -TRICYANO- QUINOMETHANEIMINES.	49
2.5 INTRODUCTION	49

2.6 SYNTHESIS OF N, 7, 7-TRICYANOQUINOMETHANEIMINES (72h-72r)	50
2.7 ELECTROCHEMICAL STUDIES	54
2.8 X-RAY CRYSTAL STRUCTURES OF COMPOUNDS (72m) AND (72n)	58
2.9 VARIABLE TEMPERATURE PROTON NMR SPECTRA OF (72n) AND (72p)	59

CHAPTER THREE - SYNTHESIS, LB DEPOSITION AND NLO
PROPERTIES OF R-Q3CNQ CHROMOPHORES

3.1 INTRODUCTION	61
3.2 SYNTHESIS OF R-Q3CNQ DERIVATIVES	63
3.3 LANGMUIR BLODGETT FILMS OF R-Q3CNQ	65
3.4 CHARGE TRANSFER SPECTRA	66
3.5 ANALOGUES OF C ₁₆ H ₃₃ -Q3CNQ (20)	70
3.6 NON-LINEAR OPTICAL PROPERTIES	71

CHAPTER FOUR - SYNTHESIS, LB DEPOSITION AND NLO
PROPERTIES OF R-BT3CNQ AND R-T3CNQ CHROMOPHORES

4.1 INTRODUCTION	74
4.2 SYNTHETIC STUDIES	79
4.3 LANGMUIR BLODGETT DEPOSITION OF C ₁₆ H ₃₃ -BT3CNQ (91)	81

4.4 LB UV-VIS SPECTRA AND OPTICAL SECOND HARMONIC GENERATION.	83
4.5 LANGMUIR BLODGETT DEPOSITION OF C ₆ H ₁₃ -T3CNQ (92)	86
4.6 LB UV-VIS SPECTRA AND OPTICAL SECOND HARMONIC GENERATION.	87

CHAPTER FIVE - SYNTHESIS, LB DEPOSITION AND NLO PROPERTIES OF SOME NEW HEMICYANINE DERIVATIVES

5.1 INTRODUCTION	89
5.2 SYNTHETIC STUDIES	95
5.3 LANGMUIR BLODGETT ALIGNMENT OF C ₂ -HEMICYANINE (118)	97
5.4 LANGMUIR BLODGETT DEPOSITION OF HEMICYANINE (113a) AND HEMICYANINE (113b)	97
5.5 UV-VIS SOLUTION AND LB SPECTRA	101
5.6 OPTICAL SECOND HARMONIC GENERATION	102

CHAPTER SIX - SYNTHESIS, LB DEPOSITION AND NLO PROPERTIES OF CHROMOPHORES WITH THE 1,3-DITHIOLE DONOR GROUP

6.1 INTRODUCTION	103
6.2 SYNTHESIS	110

6.3 LANGMUIR BLODGETT FILMS OF CHROMOPHORES (128) AND (129)	114
6.4 OPTICAL SECOND HARMONIC GENERATION	115
CHAPTER SEVEN - EXPERIMENTAL	
7.1 GENERAL METHODS	118
7.2 EXPERIMENTAL TO CHAPTER 2	119
7.2.1 Methyl-2,5-di(bromomethyl)benzoate (63f)	119
7.2.2 Methyl-2,5-di(cyanomethyl)benzoate (64f)	119
7.2.3 Preparation of TCNQ derivatives using 2-chlorobenzylthiocyanate	120
7.2.3.1 General procedure	120
7.2.3.2 2,5-Dichloro-TCNQ (41c)	120
7.2.3.3 2,5-Dibromo-TCNQ (41d)	121
7.2.3.4 2,5-Dimethoxy-TCNQ (41e)	121
7.2.3.5 2-Methoxycarbonyl-TCNQ (41f)	121
7.2.3.6 11,11,12,12-Tetracyano-1,4-naphtho- quinodimethane (67)	121
7.2.3.7 11,11,12,12-Tetracyano-2,7-naphtho- quinodimethane (69)	121
7.2.3.8 1-Cyanomethyl-4-(dicyanomethyl)tetra- chlorobenzene (70)	121

7.2.4	Preparation of mono(dicyanomethylated)-p- benzoquinones	122
7.2.4.1	General procedure	122
7.2.4.2	1-Oxo-4-dicyanomethylene-2,5-cyclohexadiene (74h)	122
7.2.4.3	1-Oxo-2,3,5,6-tetramethyl-4-dicyanomethyl- ene-2,5-cyclohexadiene (74m)	123
7.2.4.4	1-Oxo-2,3,6-trimethyl-4-dicyanomethylene -2,5-cyclohexadiene (74n)	123
7.2.4.5	1-Oxo-2,6-dimethyl-4-dicyanomethylene -2,5-cyclohexadiene (74p)	124
7.2.4.6	Benzo[1,2-b,4,5-b']bis[1,4]dithiin-5-oxo -10-dicyanomethylene 2,3,7,8-tetrahydro (74q)	125
7.2.4.7	Naphtho[2,3-b][1,4]dithiin-5-dicyano- methylene-10-one 2,3-tetrahydro (74r)	126
7.2.5	Preparation of <u>N</u> ,7,7-tricyanoquinomethane -imines	127
7.2.5.1	General procedure	127
7.2.5.2	<u>N</u> -Cyano-4-dicyanomethylene-cyclohexa- 2,5-dienylideneamine (72h)	127

7. 2. 5. 3	<u>N</u> -Cyano-2, 3, 5, 6-tetramethyl-4-dicyano- methylene-cyclohexa-2, 5-dienylideneam- ine (72m)	128
7. 2. 5. 4	<u>N</u> -Cyano-2, 3, 6-trimethyl-4-dicyanomethyl- ene-cyclohexa-2, 5-dienylideneamine (72n)	128
7. 2. 5. 5	<u>N</u> -Cyano-2, 6-dimethyl-4-dicyanomethylene cyclohexa-2, 5-dienylideneamine (72p)	129
7. 2. 5. 6	Benzo[1, 2-b, 4, 5-b']bis[1, 4]dithiin-5- <u>N</u> - cyanoimine-10-dicyanomethylene 2, 3, 7, 8- tetrahydro (72q)	129
7. 2. 5. 7	Naphtho[2, 3-b][1, 4]dithiin-5-dicyanomethyl- ene-10- <u>N</u> -cyanoimine 2, 3-tetrahydro (72r)	130
7. 2. 6	Preparation of <u>N, N'</u> -dicyano-p-quinodimethanes	130
7. 2. 6. 1	Benzo[1, 2-b, 4, 5-b']bis[1, 4]dithiin- <u>N, N'</u> - dicyano-5, 10-diimine 2, 3, 7, 8-tetrahydro (80)	130
7. 2. 6. 2	Naphtho[2, 3-b][1, 4]dithiin-5- <u>N</u> -cyanoimine -10-one 2, 3-tetrahydro (81) and naphtho [2, 3-b][1, 4]dithiin- <u>N, N'</u> -dicyano-5, 10- diimine 2, 3-tetrahydro (79)	131
7. 4	EXPERIMENTAL TO CHAPTER 4	
7. 4. 1	<u>N</u> -n-Hexadecyl-2-methylbenzothiazolium iodide (94)	132

7. 4. 2	Z- β -(<u>N</u> -n-Hexadecyl-2-benzothiazolium)- α -cyano 4-styryldicyanomethanide (91)	132
7. 4. 3	2-Methyl-4-n-hexylthiazole (104)	133
7. 4. 4	2, 3-Dimethyl-4-n-hexylthiazolium methylsulphate (105)	133
7. 4. 5	Z- β -(<u>N</u> -Methyl-4-n-hexylthiazolium)- α -cyano -4-styryldicyanomethanide (92)	134
Table 7. 1:	Spectroscopic and analytical data for R-BT3CNQ chromophores	135
7. 5 EXPERIMENTAL TO CHAPTER 5		
7. 5. 1	Preparation of Hemicyanines (113a-113d)	136
7. 5. 1. 1	General procedure	136
7. 5. 1. 2	2-[2-(4-Octadecylaminophenyl)ethenyl] -3- <u>N</u> -methylbenzothiazolium iodide (113a)	136
7. 5. 1. 3	2-[2-(4-Octadecylaminophenyl)ethenyl] -2- <u>N</u> -n-hexadecylbenzothiazolium iodide (113b)	137
7. 5. 1. 4	2-[2-(4-Octadecylaminophenyl)ethenyl] -3- <u>N</u> -methyl-benzoxazolium iodide (113c)	137
7. 5. 1. 5	2-[2-(4-Octadecylaminophenyl)ethenyl] 3- <u>N</u> -methyl-4-methylthiazolium iodide (113d)	138
7. 5. 1. 6	2-[2-(4-Octadecylaminophenyl)ethenyl] -3- <u>N</u> -methyl-4-n-hexylthiazolium methylsulphate (118)	138

7.6 EXPERIMENTAL TO CHAPTER 6

7.6.1	2-Methylthio-4-n-hexyl-1,3-dithiolium methylsulphate (132)	139
7.6.2	4-n-Hexyl-2-(4-dicyanomethylene-2,5-cyclo- hexadiene)-1,3-dithiole (128)	139
7.6.3	1-Bromo-2-dodecanol (136)	140
7.6.4	1-Bromo-2-dodecanone (137)	140
7.6.5	<u>Q</u> -Ethyl-1-xanthyl-dodecan-2-one (138)	141
7.6.6	4-n-Decyl-1,3-dithiole-2-thione (139)	141
7.6.7	4-n-Decyl-2-methylthio-1,3-dithiolium tetrafluoroborate (140)	142
7.6.8	4-n-Decyl-2-methylthio-2 <u>H</u> -1,3-dithiole (141)	143
7.6.9	4-n-Decyl-1,3-dithiolium tetrafluoroborate (142)	143
7.6.10	4-n-Decyl-2-formylmethylene-1,3-dithiole (143)	144
7.6.11	4-n-Decyl-2-(dicyanomethylene)methylene-1,3- dithiole (129)	144

APPENDICES	146
APPENDIX I - X-RAY CRYSTAL DATA	146
A. CRYSTAL DATA FOR 2,5-DIBROMO-TCNQ (41d)	146
B. CRYSTAL DATA, INTENSITY DATA, COLLECTION PARAMETERS AND DETAILS OF REFINEMENT FOR COMPOUND (72m)	148
C. CRYSTAL DATA, INTENSITY DATA, COLLECTION PARAMETERS AND DETAILS OF REFINEMENT FOR COMPOUND (72n)	150
APPENDIX II - COLLOQUIA, LECTURES AND SEMINARS GIVEN BY INVITED SPEAKERS IN THE DEPARTMENT OF CHEMISTRY DURING THE PERIOD 1ST AUGUST 1988 TO 31ST JULY 1991.	152
APPENDIX III - REFERENCES	158

CHAPTER ONE

INTRODUCTION TO NON-LINEAR OPTICS

INTRODUCTION

Interest in non-linear optics has grown in recent years because optical technologies have taken over many areas in which electronic techniques traditionally dominated. The increased use of fibre-optic technologies in the telecommunications industry stimulated the need for optical switching and processing devices. In non-linear optics, the interactions of electromagnetic radiation in various media to produce new electromagnetic fields altered in amplitude, frequency or phase, or other propagation characteristics, are studied. The greatest interest is in the media in which these effects occur; new materials for non-linear optics are of primary importance.

1.1 The Origin Of Non-linear Optical Effects

The origin of non-linear optical effects can be explained if one considers equation (1.1) where the polarisation, P , induced in a molecule by a local electric field, E , is expanded in powers of the electric field.

$$P = \alpha E + \beta E^2 + \gamma E^3 \dots \dots \dots (1.1)$$

The polarisation, P , is a vector quantity but to simplify the analysis it is easier to assume it is a scalar quantity. The coefficient α is the linear polarisation. The coefficients α , β and γ are complex numbers, for α the real part is the



refractive index and the imaginary part corresponds to an absorption of a photon by the molecule. When an electromagnetic field is applied to media consisting of many molecules the field polarises the molecules. The oscillating dipoles emit E-M radiation which can be detected at some point outside the medium. The frequency of E-M radiation emitted corresponds to the vibrational frequency of the dipoles. If the vibrating dipoles have more than a single frequency component all of these are present in the emitted radiation. If the first non-linear term (β) makes a significant contribution then the medium exhibits an asymmetric non-linear optical response to the applied field $E(\omega)$. Such a medium may consist of molecules with an asymmetric charge distribution aligned in the crystal so polar orientation is maintained in the crystal. If the medium is centrosymmetric then $\beta \equiv 0$. This can be argued as follows. If a field $+E$ is applied then the induced polarisation P from the first non-linear term is $+\beta E^2$. If a field $-E$ is applied the polarisation P predicted by equation (1.1) is still $+\beta E^2$. But if the medium is centrosymmetric the polarisation should be $-\beta E^2$. Only if $\beta \equiv 0$ can the contradiction be resolved. By a similar argument for the next higher order term, γ is the first non zero non-linear term in centrosymmetric media.

1.2 Macroscopic Non-linearities

Non-linear optical properties are measured on samples that consist of many individual molecules. On the macroscopic scale the polarisation induced in a medium by an external field is given by equation (1.2).

$$P = \epsilon_0 (\chi_1 E + \chi_2 E^2 + \chi_3 E^3 \dots) \dots \dots (1.2)$$

E is the applied field and the χ_n terms have meanings similar to the molecular coefficients in (1.1). The odd terms in this expression contribute to the polarisation of all materials but the values of the even order coefficients χ_2 , χ_4 etc. are only non zero if the medium lacks a centre of symmetry. These non-linear terms give rise to effects which may be useful in modern electro-optic communications. Second order (χ_2) effects are especially important. One such effect is the Pockels effect.

Pockels effect modulators can be used to couple electrical and optical transmission media. The modulators operate through synchronous refractive index changes in the modulator media with the digitally coded electric field of the transmission signal. The refractive index of the media must vary with the applied field. This effect can be achieved if the modulator material has a large second order

non-linear susceptibility. Restricting equation (1.2) to two terms gives equation (1.3).

$$P = \epsilon_0 (\chi_1 E + \chi_2 E^2) \dots (1.3)$$

which may be rewritten as equation (1.4).

$$P = \epsilon_0 \chi E \dots (1.4)$$

where $\chi = \chi_1 + \chi_2 E \dots (1.5)$ But the refractive index (n) can be related to χ_1 through equation (1.6).

$$n^2 = 1 + \chi_1 \dots (1.6)$$

Substitution of (1.6) into (1.5) gives equation (1.7) which describes a field dependent refractive index which is the requirement for the modulator.

$$n = (\chi_1 + 1 - \chi_2 E)^{1/2} \dots (1.7)$$

Second harmonic generation (SHG) is another effect that can be observed from materials with large χ_2 . The effect may be explained by the use of equation (1.3). Suppose a sinusoidal laser source of frequency ω is applied which may be described by equation (1.8).

$$E = E_\omega \sin(2\pi\omega t) \dots (1.8)$$

which by substitution into equation (1.3) gives equation (1.9).

$$P = \epsilon_0 (\chi_1 E_\omega \sin(2\pi\omega t) + \chi_2 E_\omega^2 \sin^2(2\pi\omega t)) \dots (1.9)$$

By using the familiar cosine formula $\cos 2\omega = 1 - 2\sin^2\omega$ the E^2 term in equation (1.9) becomes: -

$$\frac{1}{2}\epsilon_0 \chi_2 E_\omega^2 (1 - \cos(4\pi\omega t))$$

This term represents an oscillating polarisation at the doubled frequency.

A variety of other non-linear optical effects can occur through χ_2 and χ_3 depending on the input frequencies, the proximity of vibrational or electronic resonances to the input frequencies, or frequency combinations and the phase matching conditions. A wide variety of conditions can lead to interesting non-linear effects. Various susceptibility functions and frequency arguments are given in Table 1.1 for χ_2 and χ_3 .

Table 1.1: Electric susceptibility functions $\chi_r(\omega_1; \omega_2, \omega_3)$ for various interacting fields. ω_1 = resultant field; ω_2, ω_3 = input frequencies.

<u>Susceptibility</u>	<u>Effect</u>	<u>Application</u>
$\chi_2(0, \omega_2, -\omega_3)$	Optical Rectification	Hybrid bistable Device
$\chi_2(-\omega_1, \omega_2, 0)$	Pockels Effect	Modulators
$\chi_2(-2\omega_1, \omega_2, \omega_3)$	Frequency Doubling	Harmonic Generation
$\chi_2(-\omega_1, \omega_2, \omega_3)$	Frequency Amplification	Parametric Amplification

1.3 Materials For Non-linear Optics

The properties of materials are vitally important to the advancement of the non-linear optics field. Currently three main material types are under investigation.

(1) Multilayered semiconductor structures (called multiquantum wells (MQW)) and other semiconductors. Methods of structure production are highly sophisticated involving molecular beam epitaxy (MBE) or chemical vapour deposition (CVD).

(2) Lithium niobate devices - this technology is advanced and devices are at the production stage. The devices are, however, large as the non-linearity is small.

(3) Organic materials - currently the area of greatest interest. As mentioned previously, in the design of

materials with large second order non-linear optical properties, the molecular hyperpolarisability must be optimised and then oriented in a medium (polymer, crystal, or LB film). Studies have shown that molecules containing conjugated π -electrons with charge asymmetry exhibit extremely large values of β .¹ The largest values are obtained when the molecule contains substituents that lead to low-lying charge transfer resonance states (Figure 1.1).

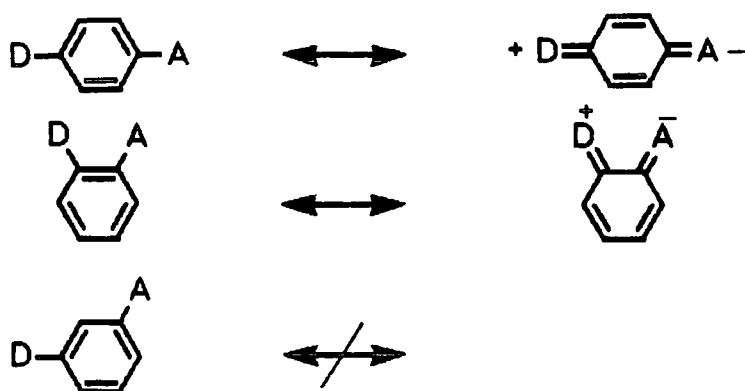


Figure 1.1: Charge transfer resonant states of disubstituted benzenes.

The polarisation arises from substituent-induced asymmetry of π -electrons, as well as the electric field-induced charge transfer resonance state making a contribution to the ground state electronic configuration. For the nitroanilines the charge transfer and substituent-induced asymmetry contributions to the molecular hyperpolarisability (β) have been separated into two parts β_{ada} and β_{et} (equation 1.10).²

$$\beta = \beta_{add} + \beta_{ct} \dots (1.10)$$

The experimental values of β for a series of nitroanilines are given in Table 1.2. Values of β_{add} were obtained by vector addition of measured values of β for nitrobenzene and aniline. Values for β_{ct} were obtained from a quantum mechanical calculation based on a charge resonance two-level model. There is very good agreement between the experimentally determined values for the disubstituted systems and the calculations.

β_{ct} has been accounted for by many different quantum mechanical calculations (e.g. Pariser-Pople-Parr calculations³ and other SCF-LCAO methods^{4,5}). One particularly useful approach is the two-level model previously mentioned which predicts that β_{ct} is given by equation (1.11).

$$\beta_{ct} = \frac{3e^2h^2}{8\pi^2m} F(\omega)f \Delta U_{g,e} \dots (1.11)$$

$$\text{where } F(\omega) = \frac{W}{(W - (2h\nu)^2)(W^2 - (h\nu)^2)}$$

W = the energy of the optical transition.

f = oscillator strength.

$\Delta U_{g,e}$ = difference between ground and excited state dipole moments.

$F(\omega)$ is a dispersion term and enhances β_{ct} as the fundamental frequency approaches the energy of the charge transfer function (Resonant enhancement).

Table 1.2 : Second order hyperpolarisabilities for ortho-, meta- and para-nitroanilines plus aniline and nitrobenzene, determined by experiment. β_{add} and β_{ct} are also given (Values $\times 10^{30}/\text{esu}$).

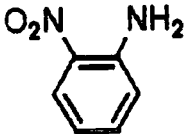
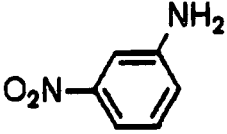
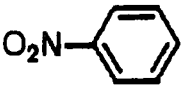
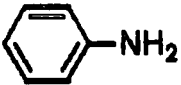
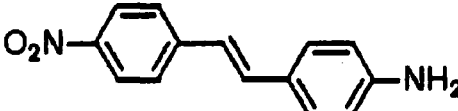
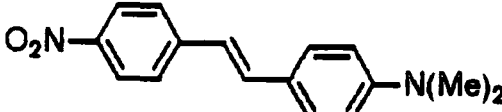
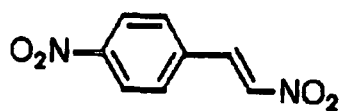
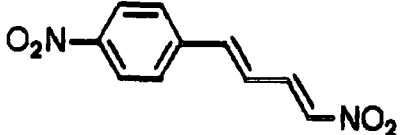
	β_{exp}	β_{add}	β_{ct}
	34.5	3.4	19.6
	10.2	1.7	10.9
	6.0	3.3	4.0
	2.2	--	--
	1.1	--	--

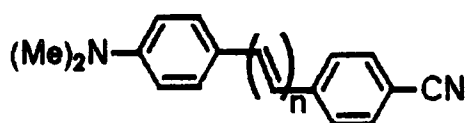
Table 1.3 : Calculated values of β_{calc} and experimental values of β for a series of stilbene and benzene derivatives
 (Values $\times 10^{30}$ /esu).

	β_{calc}	β_{exp}
	19	34.5
	227	260
	383	450
	217	220
	715	650

Good agreement was obtained between β_{calc} and β_{exp} for a series of disubstituted benzene and stilbene derivatives assuming that $\beta_{\text{calc}} = \beta_{\text{exp}}$ (Table 1.3). Dulcic et al have found for compounds (1a-1c) that β depends on the length of the conjugated π system.⁶ An empirical law was found to be obeyed (Equation 1.12).

$$\mu_{\text{e}}\beta = Cn^k \dots\dots (1.12)$$

where $k \approx 2$ and n = number of conjugated double bonds in (1).



- (1) : (a) $n=1$
 (b) $n=2$
 (c) $n=3$

1.4. Determination Of Second Order Hyperpolarisabilities

Currently there are three experimental methods for the determination of second order hyperpolarisabilities. They are the EFISH technique (Electric Field Induced Second Harmonic Generation), the Kurtz Powder technique and monolayer second harmonic generation (MSHG).

In the EFISH technique, a DC electric field is applied to a liquid or a solution of the molecules of interest.⁷ The

electric field produces alignment of the molecular dipoles in the medium and removes orientational averaging effects. The induced second order non-linearity can then produce a signal at 2ω from which β can be obtained.

In a typical experimental set-up the output of a Nd:YAG laser ($1.064\mu\text{m}$) is split and directed into reference and sample cell. The sample cell is translated by a stepper motor across the beam. A high voltage DC pulse is applied to the sample cell and simultaneously the cell is irradiated with laser pulses. The second harmonic (532nm) is separated from the fundamental (1064nm) by a system of monochromators and filters. The second harmonic is detected by a photomultiplier tube. The reference beam is directed into a crystal, such as quartz, whose second order properties are well known. From the signal ratio of the sample and the reference material, the value of the non-linear coefficient may be obtained.

The Kurtz powder technique is a convenient method for screening large numbers of powdered materials for second order non-linear optical activity without needing to grow large single crystals.⁶ The technique involves directing laser light onto the powdered sample and the emitted light is detected by a photomultiplier tube. The method enables material selection for single crystal studies. From a study of second harmonic intensity versus particle size it is

possible to distinguish between phase matchable and non-phase matchable crystalline powders (Figure 1.2).

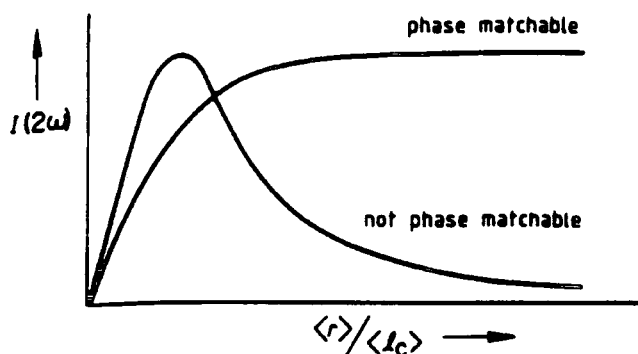


Figure 1.2 : Dependence of second harmonic intensity on $\langle r \rangle / \langle l_c \rangle$ where $\langle r \rangle$ is the average particle size and $\langle l_c \rangle$ is the average length.

Phase matchable conditions exist in birefringent crystalline powders where it is possible to find a direction in a crystal in which a component of the non-linear tensor χ_2 will produce a harmonic wave that propagates with the same effective refractive index as the fundamental beam.

The latest method of β evaluation is monolayer second harmonic generation. For MSHG the chromophore is derivatised with a long alkyl chain, typically $C_{20}H_{41}$. A dilute solution of the amphiphilic chromophore is spread on the water surface to form an oriented monolayer. The monolayer is transferred to a glass or quartz slide and irradiated with laser light; the second harmonic is detected by a photomultiplier tube. This new technique has a number

of advantages over the EFISH technique. The experiment yields a direct value of β and there is very little absorption of the fundamental and second harmonic because the films are thin. Unlike EFISH, the molecular environment of densely-packed chromophores in MSHG more nearly resembles what it would be in an efficient non-linear optical material. Compared to EFISH, the new technique does require extra synthetic effort in attaching the long aliphatic chain to the chromophore.

1.5 The Langmuir Blodgett Technique

The self assembly method of providing ultrathin organic films was first reported by K.B. Blodgett in 1935.¹⁰ The LB technique involves the formation of mono/multi layers of molecular thickness films at an air/water interface. Monolayer forming molecules typically possess hydrophilic and hydrophobic end groups. A dilute solution of the amphiphile in a volatile organic solvent is used to spread a monolayer on the water surface.

The monolayer on the water surface consists of dispersed amphiphiles and forms a two-dimensional solid of oriented molecules on compression (Figure 1.3). The dispersed monolayer may be viewed as a two-dimensional gas and if the surface pressure (Π) is small the gas obeys the equation (1.13).¹¹

$$\Pi A = kT \dots (1.13)$$

Figure 1.3 : The compression of dispersed amphiphiles on a water subphase.

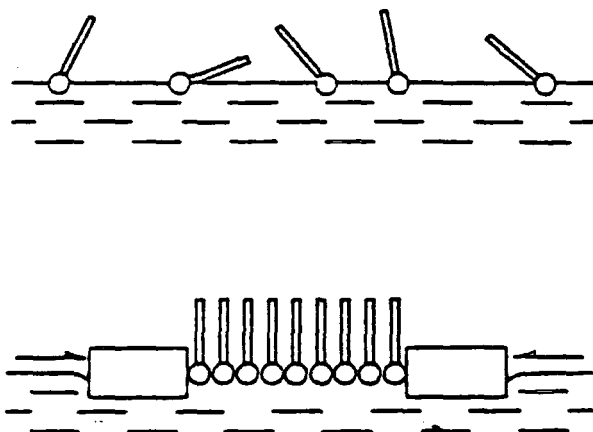


Figure 1.4 : Schematic representation of an "ideal" Π - A isotherm

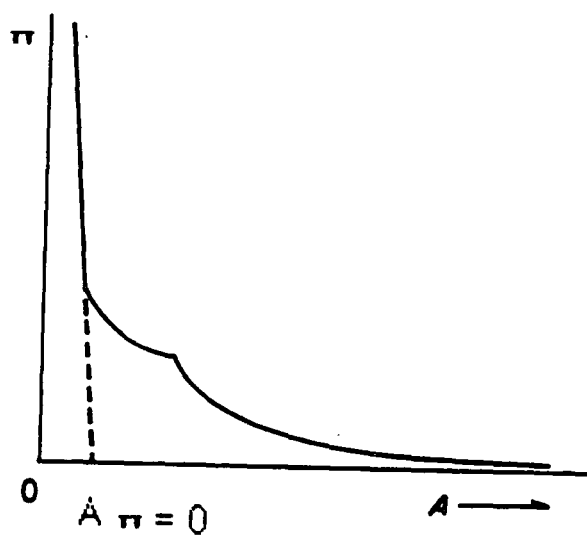


Figure 1.5 : LB deposition of a compressed monolayer.

(Illustrated for Y type deposition)

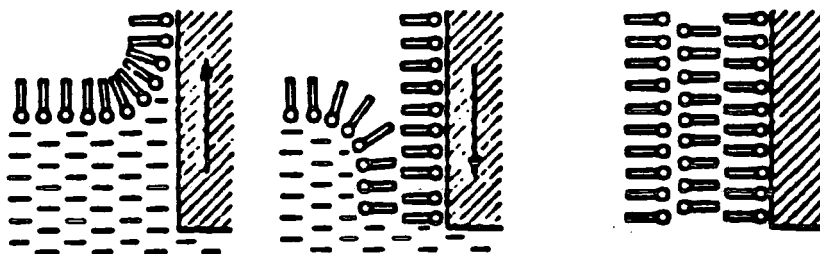
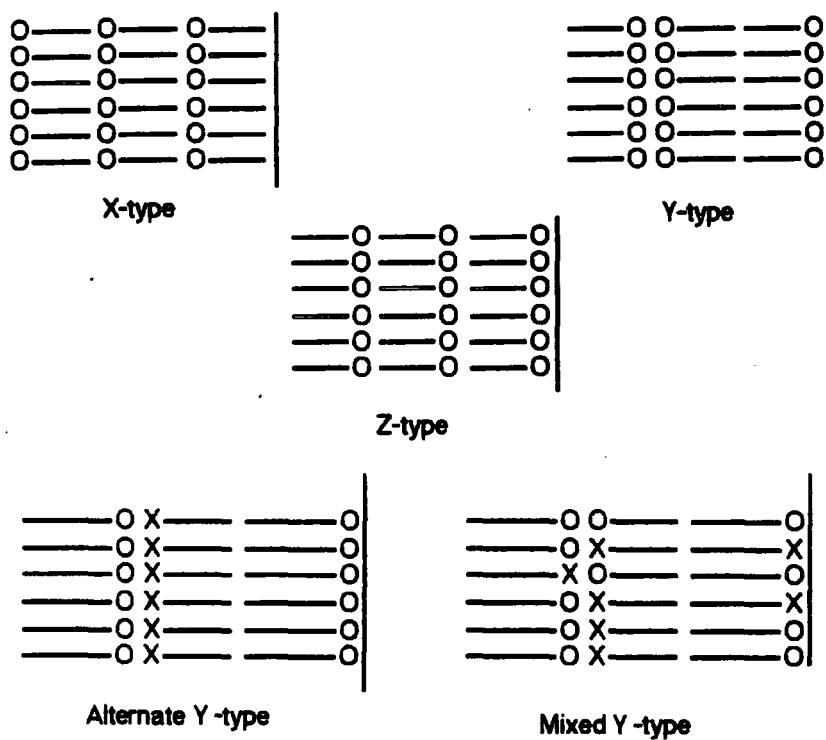


Figure 1.6 : LB deposition modes.



where A = area per molecule, K = Boltzmann's constant and T = absolute temperature. If the surface pressure Π is increased, the monolayer is transformed into the ordered solid state and Π and A are approximately linearly related. A schematic representation of a typical Π - A isotherm is given in Figure 1.4. The extrapolation of the linear portion of the curve to $\Pi = 0$ gives the area at zero pressure which is assumed to correspond to the cross-sectional area of a monolayer-forming molecule.

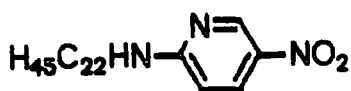
1.6 Deposition Techniques

The steps involved in monolayer and LB film formation are shown in Figure 1.5. After spreading and compression the monolayer may be transferred onto a substrate by dipping the substrate perpendicularly through the amphiphile-water interface. Repeated dipping allows the formation of multilayers. Different molecular orientations can be achieved depending on whether the deposition is on the up or the down stroke of the substrate. The different molecular orientations which are obtained are designated X-, Y- or Z-type structures (Figure 1.6). Also, mixed and alternate layer LB structures can be obtained. For non-linear optical applications, and particularly for SHG, an accentric film structure is desirable.¹² Thus, monolayer, X or Z, alternate film and the Y-type herringbone structures are the structures of interest.

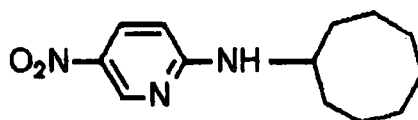
1.7 Non-linear Optical studies Of LB Films

Since the report by Aktsipetrov et al of significant optical second harmonic generation from a Langmuir Blodgett film, further investigations of second order non-linear optical effects in LB films have indicated that such films have excellent non-linear optical properties.^{13, 14}

Tieke et al reported optical second harmonic generation from LB films of 2-docosylamino-5-nitropyridine (2) (DCANP).¹⁵ The amphiphile gives a well ordered LB film which does not exhibit a head to tail arrangement of the molecule; it may be viewed as a long chain analogue of 2-cyclooctylamino-5-nitropyridine (3) which has a large second order susceptibility in the crystalline state.¹⁶



(2)



(3)

The material (2) forms a stable monolayer on pure water. Tieke deduced from the molecular packing density at film collapse, that a highly tilted arrangement of alkyl chains exists in the film structure and that the possible average orientation of molecules of (2) on the water subphase may be represented as in Figure 1.7.

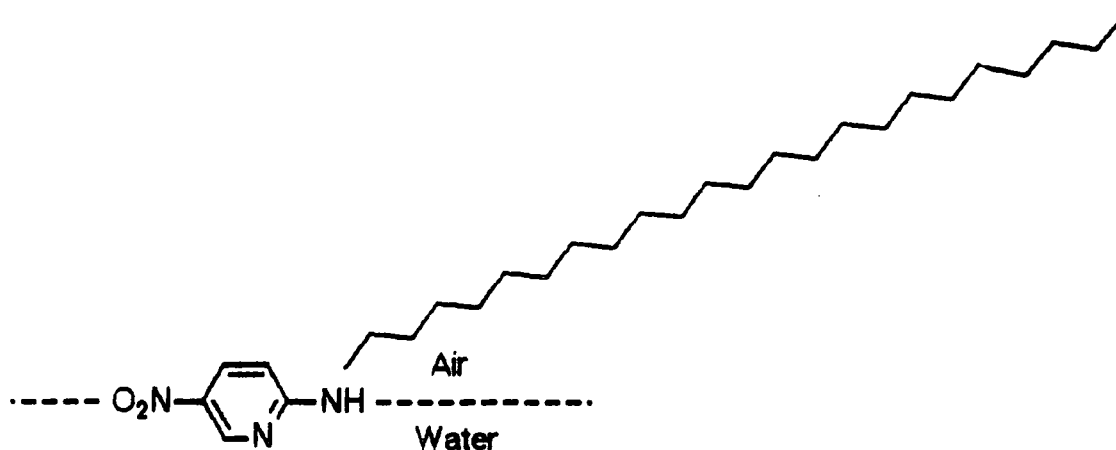


Figure 1.7 : The orientation of a DCANP amphiphile on a water subphase.

Consistent with theory, the SHG increases quadratically with the number of layers of (2).¹⁷ Structural studies of the LB films, using small angle X-ray scattering, indicates a highly ordered Y-type structure with a large tilt angle of approximately 40° (Figure 1.8).

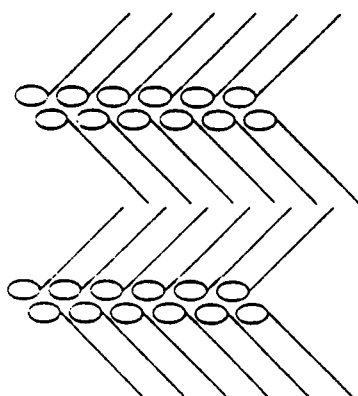
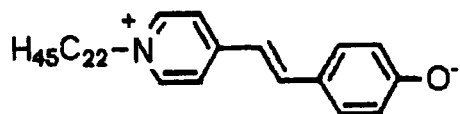


Figure 1.8 : Structural model for DCANP — a tilted Y type bilayer.

This material is the first that demonstrated optical second harmonic generation from LB films that do not have an X or Z type structure.

The zwitterionic merocyanine dye (4) was one of the first amphiphiles studied after Aksipetrovs' report: a high second order hyperpolarisability (β) of $1000 \times 10^{-30} \text{ cm}^5 \text{ esu}^{-1}$ was found.¹⁸

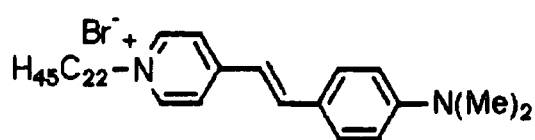


(4)

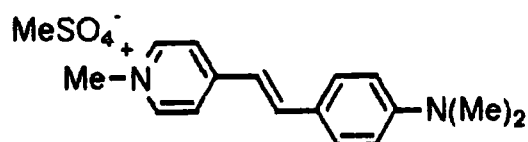
Multilayers of the merocyanine dye (4) are unstable and for device applications thick films are required ($1\mu\text{m}$).¹⁹ Alternating films of ω -tricosenoic acid and the merocyanine dye (4) were studied with this in mind. Unfortunately, the dye has limited device potential since it exhibits a Y type (centrosymmetric) LB structure and the dye is unstable (it is readily protonated in air). During all optical measurements films of the merocyanine dye (4) were kept in a cell containing ammonia vapour to prevent protonation.

Girling et al studied the hemicyanine dye (5).²⁰ Other workers have studied the methylsulphate salt of the hemicyanine dye (6) which crystallises as a mixed crystal with N,N-dimethylaminobenzaldehyde (7) and found a high value of χ_2 ($\sim 10^{-5} \text{ esu}$).²¹ It is assumed that the hemicyanine dye (6) has the largest β value and makes the greatest

contribution to χ_2 . Monolayers of the hemicyanine dye (5) and alternating multilayers of the dye (5) and ω -tricosenoic acid were studied.



(5)



(6)



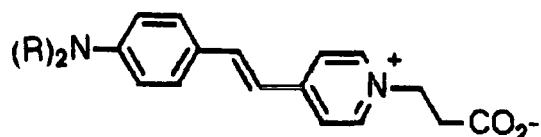
(7)

For monolayers of the hemicyanine dye (5), the optical second harmonic intensity was found to be more than a factor of 10 larger than for the merocyanine dye (4) under comparable conditions. In addition, films of the hemicyanine dye (5) showed no deterioration on exposure to air in contrast to the merocyanine dye (4). The alternating multilayer structures did not show the coherent n^2 dependence for the optical second harmonic intensity. The reduction in the second harmonic intensity is explained by in-plane order which is averaged out as the number of layers is increased and effectively changes the distribution of dye orientations. Studies of the symmetrical bilayer of dye (5) found the unexpected observation of SHG which indicates that there must be a difference between the two layers.

The second order non-linear optical properties of mixed films of hemicyanine dye (5) and poly(octadecylmethacrylate)

and hemicyanine(5)-behenic acid have been studied by Hayden et al.²² Poly(octadecylmethacrylate) is known to deposit as Z type layers with the alkyl side chains oriented perpendicular to the subphase. Non-linear optical measurements and Π -A isotherms established that the hemicyanine(5) - poly(octadecylmethacrylate) system is immiscible and hemicyanine(5)-behenic acid system is miscible.

A series of amphiphilic twin-tailed dyes (8) were studied by Girling et al.²³ The principle motive for the investigation of the LB film forming and optical properties of these materials was the possibility that these materials would form more fluid films, and hence the speed of deposition could be increased so that thicker films for waveguiding devices may be obtained.

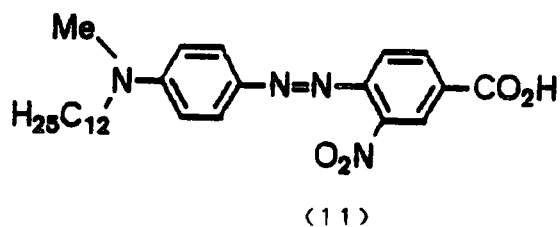
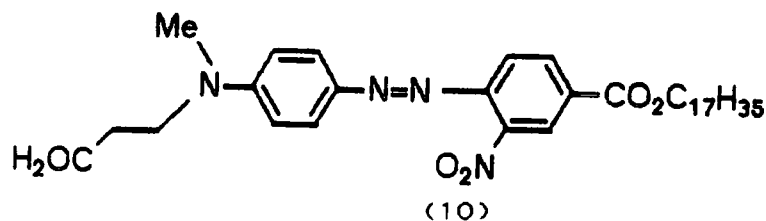
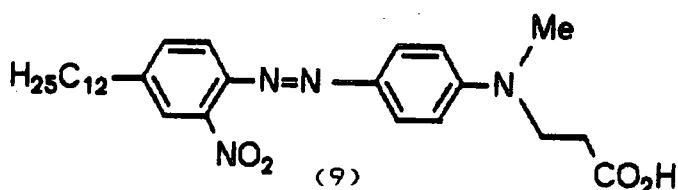


(8) R = C₆H₁₃, C₁₀H₂₁, C₁₄H₂₉ and C₁₈H₃₇.

The LB film forming properties of dyes (8) were studied. The C₆ and C₁₀ derivatives gave unstable monolayers. From the pressure-area isotherm for the C₁₈ derivative, the area per molecule (at $\Pi=0$) was found to be 50Å² which is larger than the cross-sectional area of a pair of alkyl chains, indicating that the chromophores are tilted at an angle away from the substrate normal.

Optical second harmonic generation studies gave disappointing results. For most of the monolayers tested, a high SHG signal was seen for the first pulse which reduced to between 10% and 1% of the initial value. The behaviour may be explained by laser damage which gives rise to thermally induced structural reorientation.

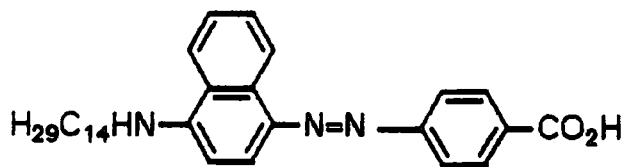
The SHG in alternate LB films of the diazostilbenes (9-11) was studied by Zyss *et al.*²⁴ Many workers have studied alternate layer LB structures.



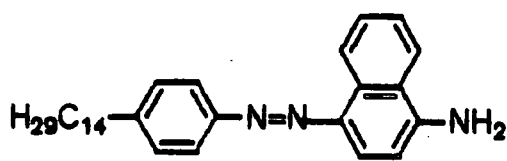
For example, the previously mentioned alternating layer films of ω -tricosenoic acid and merocyanine dye (4).¹⁸ These films contain so called "passive-active" layers. An alternative approach is the "active-active" layer where films of molecules with hydrophobic groups bonded to the donor group are deposited onto an initially deposited layer consisting of

molecules with hydrophobic groups bonded to the acceptor part. The film structure is Y type and the non-linear susceptibility results from the addition of the individual non-linearities of each species. The dyes (10) and (11) were successfully deposited in this mode. SHG was observed for various numbers of alternate Y type layers of (10) and (11). The results obtained show that the active-active structures exhibit χ_2 values far superior to the active-passive and Z type films.

Langmuir Blodgett films of the amphiphilic azo dyes (12) and (13) have been studied.²⁵ Both materials show strong SHG with second order hyperpolarisabilities (β) in the range $3-7 \times 10^{-49} \text{ C}^3\text{m}^3\text{J}^{-2}$.



(12)

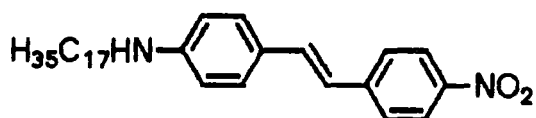


(13)

These values are comparable to that reported for other azo dyes.²⁶ Multilayers of (12) and (13), unfortunately have, a Y type structure and multilayer deposition was found to be poor, as judged from transfer ratios and the patchy appearance of the films. However, despite the Y type structure of films of (12), an increase in SHG was observed for increasing number of layers. This was explained in terms of incomplete cancellation by alternate layers. Molecule

(13) has an amino group to act as the electron donor but no obvious acceptor substituent and consequently shows weaker SHG. It is possible that the azo linkage is acting as the acceptor group. Films of (13) deposited from a subphase with an increased acidity (pH = 2.25) was found to increase the SHG by as much as a factor of 5. This may be explained by protonation of the amino group which moves the absorption band of the molecule closer to the SHG frequency, leading to an increase in SHG by resonance enhancement.

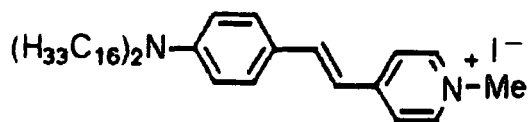
Petty et al studied the LB film forming properties and optical SHG of 4-n-heptadecylamino-4'-nitrostilbene (14). 27. 28



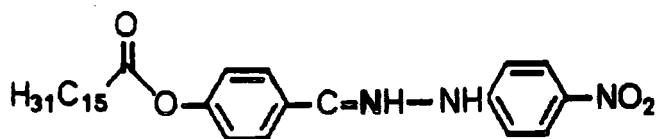
(14)

However, later studies showed that the initially prepared (14) consisted of an equimolar mixture of (14) and stearic acid. Pure (14) could not be deposited onto hydrophilic or hydrophobic substrates. However, the impure (14) forms stable LB multilayers on both hydrophilic and hydrophobic glass. The films have a Y type structure and monolayer SHG was observed. Optical SHG has also been observed from multilayer structures consisting of alternating layers of (14) and cadmium eicosonate. An active-active alternating structure has been produced with the hemicyanine dye (5).

The dye molecules (15) and (16) have been used in a study of the effect of amphiphile mixing on SHG and chromophore orientation in Langmuir Blodgett films.²⁹



(15)

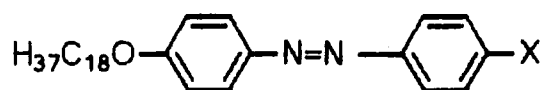


(16)

Several groups have studied the effect of neighbouring molecules on the non-linearity of a molecule with large hyperpolarisability in an LB monolayer.³⁰ SHG enhancement in hemicyanine monolayers on dilution with cadmium arachidate was reported by Girling *et al.*³¹ Schildkrant *et al.* reported a similar enhancement.³² Lupo *et al.* studied the effect of dilution on spectra, non-linearity and chromophore orientation of the hemicyanine amphiphile (15) and the phenylhydrazone ester (16).³³ The hemicyanine LB films diluted with increasing percentages of palmitic acid were observed to show no bulk enhancement, but a small increase in the effective non-linearity at low diluent concentrations, in contrast to other reports. The phenylhydrazone ester (16), which is known to have a high optical non-linearity, showed an abnormal SHG curve: no fringes were seen which indicated a lack of homogeneity. Diluting the films with up to 40% of palmitic acid resulted in "normal" curve behaviour. The

effect may be explained in terms of chromophore reorientation by the diluent.

Nakamura et. al have studied the effect of molecular mixing on the optical SHG of Langmuir Blodgett films of the amphiphiles (17) and (18).³⁴



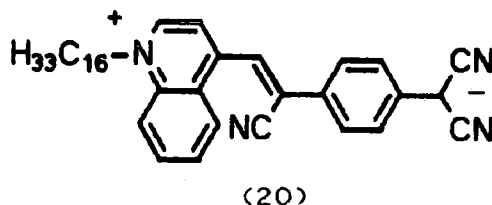
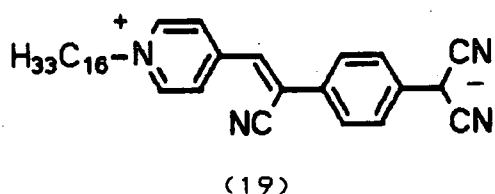
(17) X = NO₂

(18) X = CO₂H

The chromophore (17), with a nitro group as the electron acceptor, possesses a large polarity; dipole-dipole interactions between molecules of (17) within the LB monolayer will be expected to prevent a parallel stacking structure (H aggregate). When the chromophore (17) is mixed with the chromophore (18) one expects a mixed monolayer. The smaller polarity of chromophore (18) should reduce dipole-dipole interactions between molecules of (17) and thus vertical orientation of the chromophores becomes possible. This should lead to more efficient SHG in the mixed monolayer. Surface pressure - surface area isotherms of pure (17) and (18) and mixtures were obtained. The amphiphile (18) formed a stable monolayer with an area per molecule of 30Å². Amphiphile (17), however, did not give a stable monolayer; the area per molecule was 10Å² suggesting the formation of crystalline domains. SHG measurements on mixed monolayers containing varying concentrations of (17) were carried out. The SHG of monolayer (17) was very small. The result is consistent with the poor asymmetric orientation of

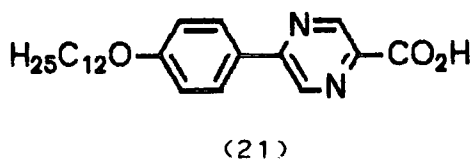
the chromophores. The SHG of the chromophore (18) was, in contrast, moderately large. The SHG was found to be greatly enhanced for mixed monolayers. The authors suggest that is consistent with the predominant orientation of polar amphiphiles (17) normal to the film plane as a result of mixing with chromophore (18).

The zwitterionic amphiphiles (19) and (20) have been studied for optical SHG in mixed Langmuir Blodgett mono/multilayers.³⁵



The mixed LB film structures are Z type. The non-centrosymmetric alignment is confirmed by the quadratic dependence of the SHG with the number of layers.

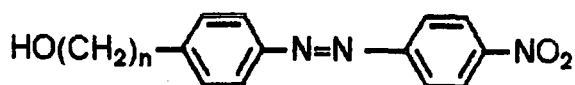
The amphiphilic phenylpyrazine derivative (21) has recently been studied by a Japanese group.³⁶



The derivative forms thick non-centrosymmetric LB films. Up to 200 bilayers of the material have been deposited by the LB technique. This corresponds to a thickness of more than 1µm and is a useful thickness for non-linear waveguides. The LB

multilayers are transparent from the visible to the near infrared region, making them applicable to a wide range of wavelengths. X-ray diffraction studies proved that the amphiphiles are oriented normal to the substrate surface in the LB film. A long spacing of 5nm was calculated from the diffraction peaks. This value is just smaller than the sum of the molecular lengths of (21) (2.83 nm) and arachidic acid (2.90 nm). Optical studies show that the SH intensity has a quadratic dependence on film thickness from 1 to 200 bilayers.

The optical SHG of azobenzene dyes (22) and (23) were investigated by an American group.³⁷



(22) n = 6

(23) n = 22

Langmuir Blodgett studies show that neither (22) nor (23) forms high quality monolayers on water. However, stable films may be obtained when (22) and (23) are mixed with stearic acid prior to spreading on the subphase. Y type (centrosymmetric) Langmuir Blodgett deposition studies of stearic acid:(22)[4:1] and stearic acid:(23)[2:1] were successful: the films may be transferred onto glass or quartz slides. Attempted Z type deposition gave cloudy films. For

non-centrosymmetric LB multilayer films of stearic acid: (23)[2:1] with stearic acid alternating layers the second order signal was found to be quadratically dependent on the number of LB layers.

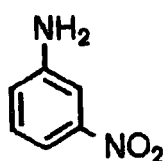
In conclusion, Langmuir Blodgett films of donor- π -acceptor amphiphiles are promising materials for the fabrication of non-linear optical devices. Amphiphiles which will deposit multilayer structures up to μm thickness offer potential for waveguiding devices. The ease of thin film processability is the great advantage of the LB technique. Further research into improving thermal and mechanical stability should further improve this class of material.

1.8 Organic Crystals For Non-Linear Optics

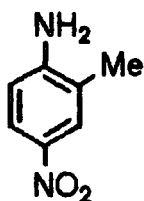
The initial interest in the search for materials with large NLO properties concentrated on inorganic materials (e.g LiNbO_3 , KDP etc.).⁹⁰ Alongside the development of thin film NLO materials, organic crystals have been extensively studied. In organic crystals, the bulk second order hyperpolarisability is preserved if the material has a non-centrosymmetric crystal structure. A comparison of χ_2 for inorganic crystals and organic crystals is depicted in Figure 1.9. From the comparison it can be seen that some organic materials have second order bulk susceptibilities greater than the best inorganic materials. Furthermore, the organics have greater chemical stability and are more useful

in that they have increased transparency and resistance to laser damage.

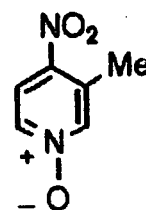
A range of nitroanilines (e.g 24-30) exhibit large second order non-linearities. 4-Nitroaniline and 2-nitroaniline crystallise centrosymmetrically thus χ_2 is not preserved.³⁹ However, 2-methyl-4-nitroaniline (MNA) (25) crystallises non-centrosymmetrically.⁴⁰ The material exhibits strong SHG with $\chi_2 = 6 \times 10^{-7}$ esu. This value is approximately 5×10^2 larger than that for potassium dihydrogen phosphate (KDP).



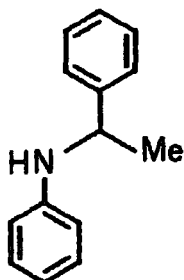
(24)



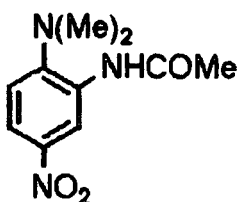
(25)



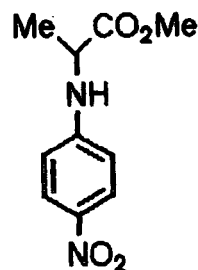
(26)



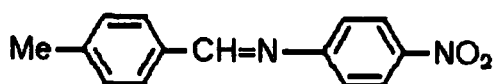
(27)



(28)



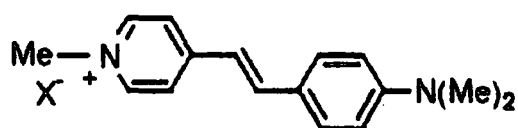
(29)



(30)

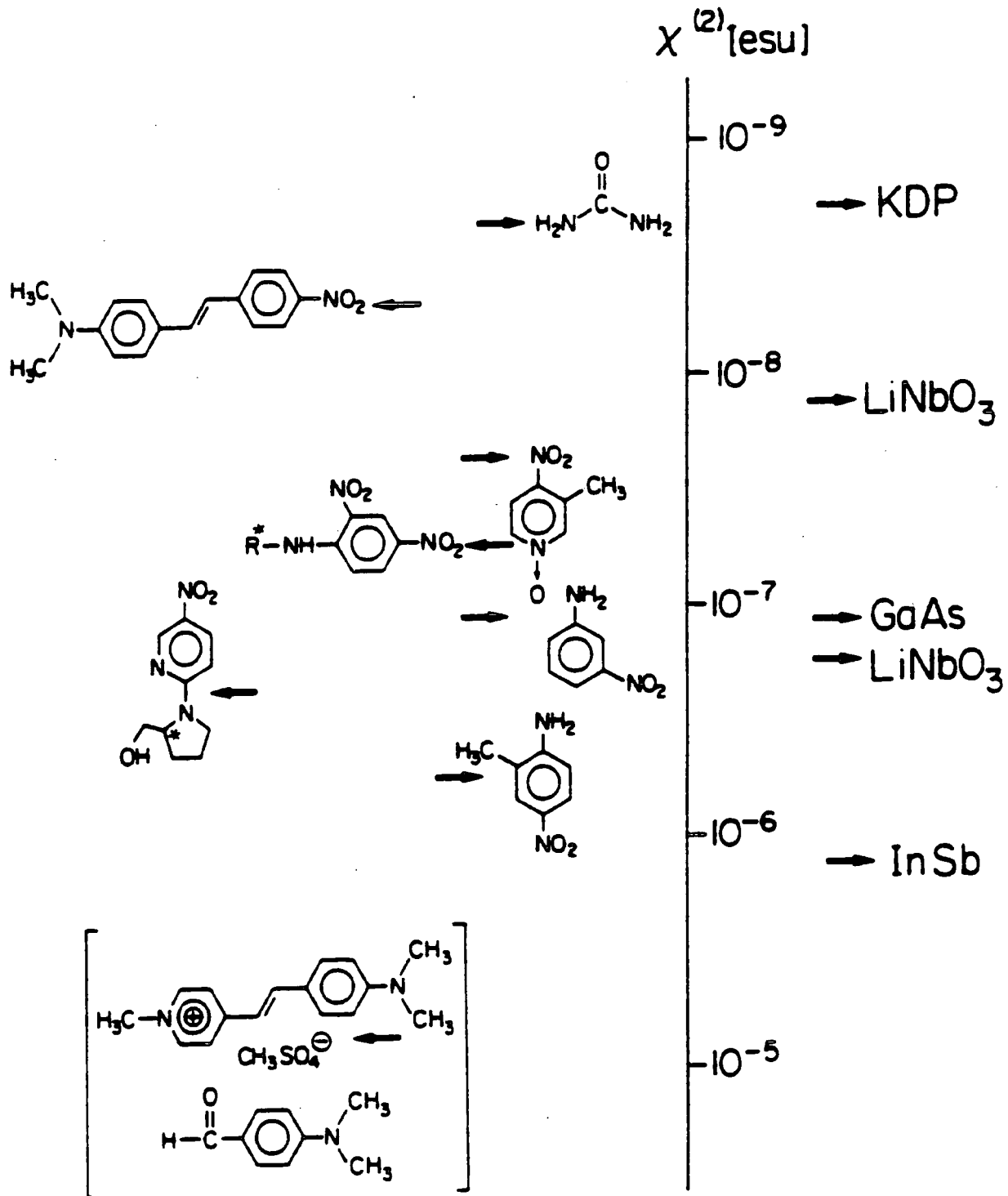
Meredith et.al studied the second order optical properties of a range of trans-stilbene salts (31-38) (Table 1.4).⁴¹ The methylsulphate salt (38) was found to have a second order powder efficiency an order of magnitude greater than MNA. It is the highest known value of χ_2 reported to date for a crystal. The non-linearity was found to be dependent on the anion: the iodide salt (34) showed no non-linearity, whereas the tetrafluoroborate salt (36) showed good SHG.

Table 1.4 : Second Order Optical properties of salts (31-38) relative to m-nitroaniline (determined by the Kurtz powder technique).



Crystalline powder	Relative harmonic intensity
m-Nitroaniline	1
(31) X=I ⁻	0
(32) X=IO ₃ ⁻	0.01
(33) X=NO ₃ ⁻	0.5
(34) X=C ₆ H ₅ CH=CHCO ₂ ⁻	1.5
(35) X=ClO ₄ ⁻	5
(36) X=BF ₄ ⁻	10
(37) X=ReO ₄ ⁻	18
(38) X=MeSO ₄ ⁻	30

Figure 1.9 : Comparison of χ_2 for organic and inorganic crystals. ¹



1.9 Polymers For Non-Linear Optics

Polymers are the subject of intense research because of the ability to tailor molecular structures which have inherently fast response times and large second and third order susceptibilities.⁴² Polymers provide synthetic and processing options that are not available with semiconductor and single crystal materials, as well as excellent mechanical properties, environmental resistance and high laser damage thresholds. Currently there are three main areas of investigation; polymeric solid solutions, main chain polymers and side chain polymers.

1.9.1 Polymeric Solid Solutions

In order to cover large areas with optically non-linear films of sufficient thickness for monomode waveguiding, non-linear polymers can be deposited via spincoating or dipping techniques. Thicknesses ranging from 0 - 20 microns can be obtained. One approach is to dissolve a polymer host, together with optically non-linear guest molecules, in a suitable solvent, followed by deposition onto a substrate. During the spinning or dipping step the solvent evaporates leaving behind a smooth film. The thickness of the film depends on the concentration of the solution and on the type of substrate.

However, after the deposition the system is most probably centrosymmetric. By applying a strong electric

field the permanent dipoles of the optically non-linear molecules in the polymer matrix are oriented by the field, thus breaking the symmetry and yielding a non-centrosymmetric material. Electric field poling of the initially isotropic system yields optically non-linear materials. In order to allow the NLO moieties to rearrange themselves in the polymer host during the poling step, the polymer has to be heated to above its glass transition temperature (T_g), where the polymer exhibits a strongly reduced viscosity. By successive cooling to below the T_g , while keeping the poling field on, the obtained polar order can be frozen in.

Polymeric solid solutions have several disadvantages. The amount of optically non-linear guest molecules that can be dissolved in a polymer host is restricted to a maximum of ca. 10% (by weight). At elevated temperatures orientational relaxation and segregation of the rather mobile guest molecules can occur, causing the sample to become electro-optically inactive again, and highly scattering due to crystalline growth.

1.9.2 Main Chain Polymers

In order to increase the concentration of active molecules in a polymer matrix and decrease the possibility of segregation and orientational relaxation after poling, the NLO moieties are built into the polymer backbone to obtain a main chain polymer. The disadvantage of this type of polymer is that large molecular fragments must change their

orientations in order to achieve a non-centrosymmetric system during the poling step.

1.9.3 Side Chain Polymers

By attaching optically active molecules as side chains to the polymer backbone, the concentration of these molecules in the polymeric system can be increased. Moreover, the side groups are again not free to migrate, thus preventing segregation and orientational relaxation after electric field poling. However, contrary to the main chain polymers only side groups need to be poled.

The advantage of the side chain polymer approach is that large areas can be covered and poled. The polymers are compatible with many type of substrate. The polymeric properties can be tailored by changing the structure of the backbone, the active group or the connecting spacer. Further low temperature deposition and shaping techniques are possible.

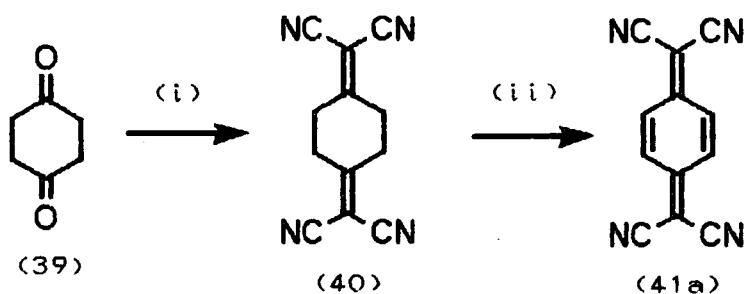
CHAPTER TWO

NEW DERIVATIVES OF 7, 7, 8, 8-TETRACYANO-P-
QUINODIMETHANE, N, N' -DICYANOQUINONEDIIMINE AND
N 7, 7-TRICYANOQUINOMETHANEIMINE SYSTEMS

2.1 Introduction

The synthesis of 7,7,8,8-tetracyano-p-quinodimethane (TCNQ) derivatives is important in the development of the understanding of the unusual electronic properties of organic materials with TCNQ as a component.⁴³ However, the potential of many TCNQ derivatives remains unexplored as their synthesis is not straightforward. Our interest was in the incorporation of substituted TCNQs into zwitterionic donor- π -acceptor structures.

Initial synthesis of TCNQ derivatives involved Knoevenagel condensations of malononitrile with 1,4-cyclohexanedione (39) to give 1,4-bis(dicyanomethylene)-cyclohexane (40) (Scheme 2.1).⁴⁴

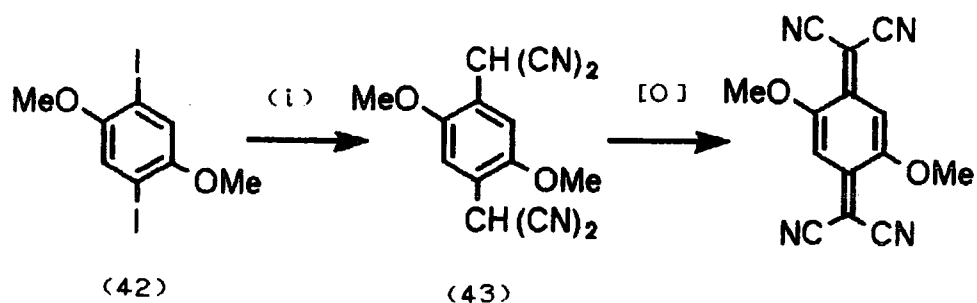


Scheme 2.1: (i) CH₂(CN)₂, β -alanine; (ii) Br₂, pyridine.

Oxidation of (40) in the presence of pyridine and bromine gave TCNQ (41a) in 80% yield. This method has been used to prepare methyl-TCNQ and 2,5-dimethyl-TCNQ.⁴⁵

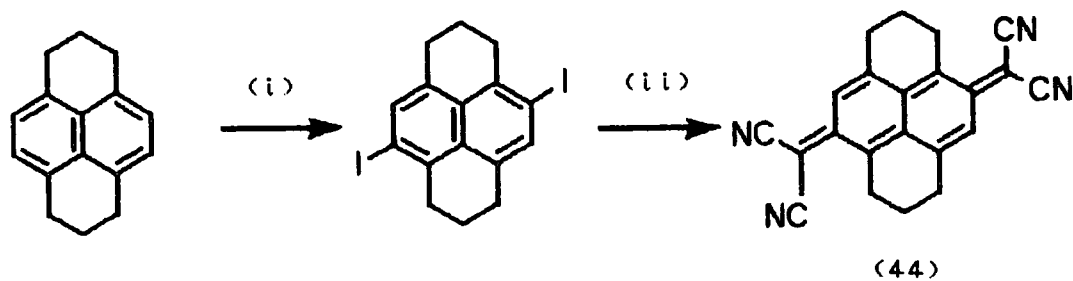
Palladium catalysed nucleophilic aromatic substitution reactions have proved useful in the synthesis of TCNQ

derivatives. Takahashi et al prepared a range of phenylene dimalononitrile derivatives eg. (43) from diiodoarenes (e.g 42) and malononitrile anion in the presence of tetrakis(triphenylphosphine)palladium (0) (Scheme 2.2).^{46, 47.}



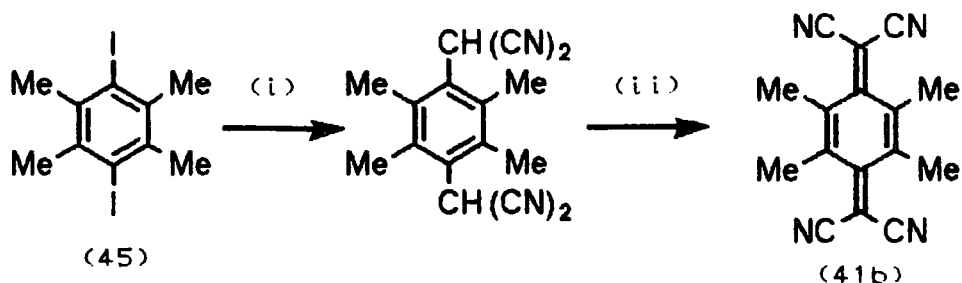
Scheme 2.2 : (i) CH₂(CN)₂, NaH, Pd(PPh₃)₄, THF.

Derivatives (43) are readily oxidised to the TCNQ derivatives in the presence of Br₂/pyridine. The procedure is quite general and has been used to prepare the new TCNQ derivative (44) (Scheme 2.3).⁴⁸



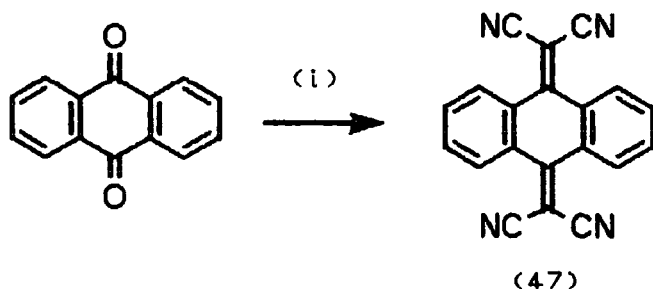
Scheme 2.3 : (i) HIO₄-I₂; (ii) CH₂(CN)₂, PdCl₂(Ph₃P)₂, oxidation, NaH.

By a similar strategy Staab *et al* prepared tetramethyl-TCNQ (41b) via the diodoarene (45) by a copper catalysed procedure (Scheme 2.4).⁴⁹



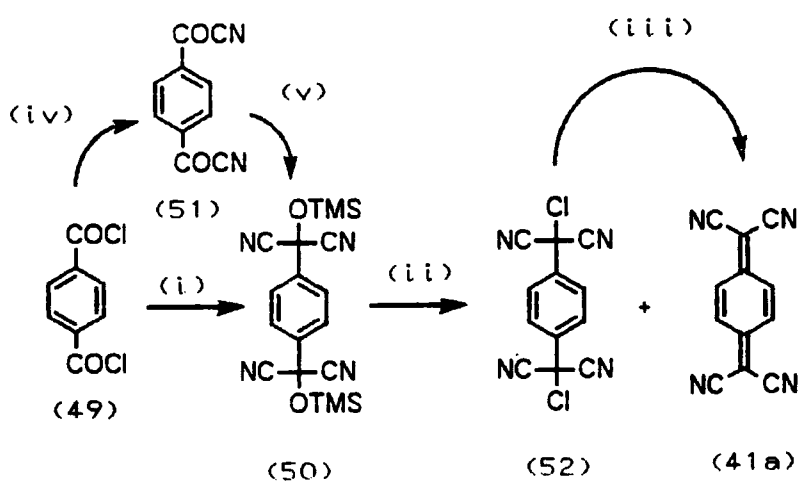
Scheme 2.4: (i) $\text{CH}_2(\text{CN})_2$, NaOMe, CuI, HMPT, 2h, 100°C;
(ii) Br_2 .

TCNQ derivatives may be prepared by TiCl_4 catalysed Knoevenagel condensations of 1,4-benzoquinones with malononitrile/pyridine.⁵⁰ The procedure is capricious and only seems applicable to tetrasubstituted derivatives e.g the preparation of 11,11,12,12-tetracyanoanthraquinodimethane (TCNAQ 47) from 9,10-anthraquinone (Scheme 2.5).⁵¹ Tetramethyl-TCNQ (41b) has been prepared by this procedure.⁵²



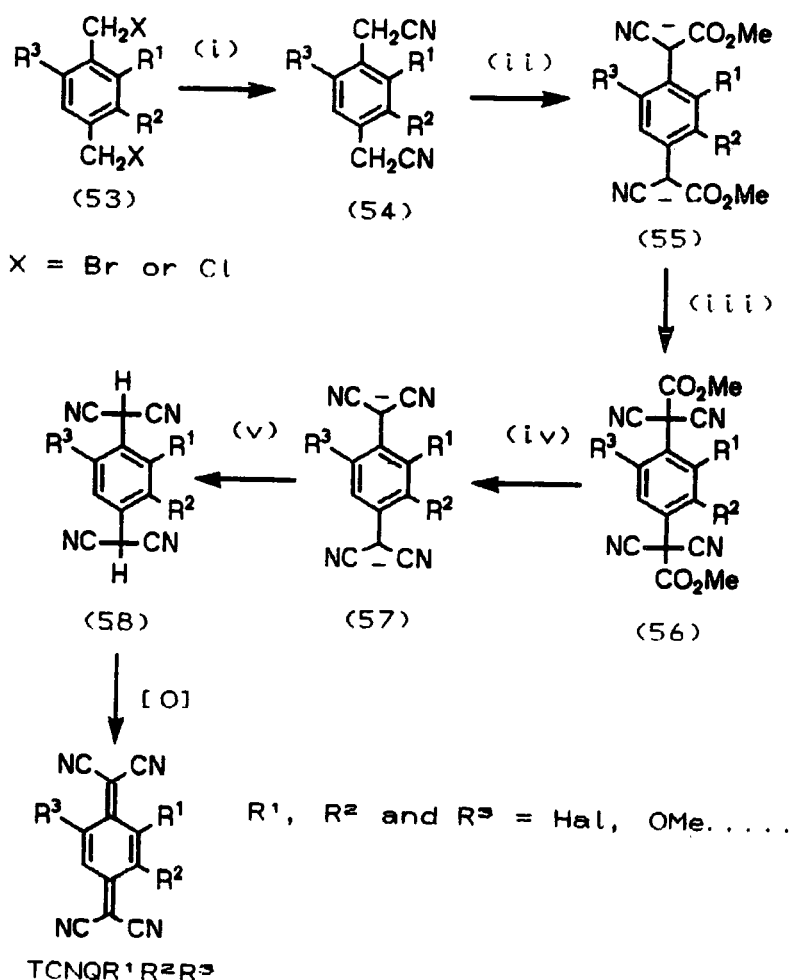
Scheme 2.5: (i) $\text{CH}_2(\text{CN})_2$, TiCl_4 , pyridine.

Alternatively benzene-1,4-dicarbonylchlorides can be converted to TCNQ (41a) via a two-step procedure employing the cyanating agent cyanotrimethylsilane, TMSCN (48).⁵³ Treatment of terephthaloylchloride (49) with reagent (48) and pyridine gives 1,4-bis(dicyanotrimethylsiloxyethyl)benzene (50). Compound (50) may also be prepared from terephthaloylcyanide (51) (prepared from terephthaloylchloride and copper(I)cyanide). Treatment of siloxy derivative (50) with phosphorus oxychloride-pyridine gives TCNQ (41a) plus the dichloride (52) which can be converted into TCNQ (41a) by sodium borohydride. 2,5-dimethyl-TCNQ, bromo-TCNQ and tetramethyl-TCNQ have been prepared by this procedure (Scheme 2.6).⁵³



Scheme 2.6 : (i) TMSCN (48), pyridine; (ii) POCl₃, pyridine; (iii) NaBH₄; (iv) Cu(I)CN; (v) TMSCN (48), pyridine.

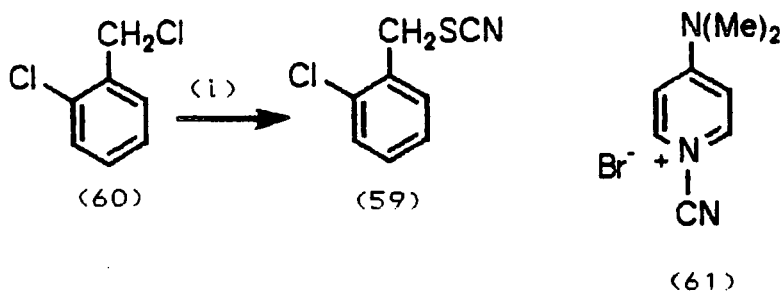
Wheland and Martin have reported a synthetic route to TCNQ derivatives starting from the corresponding p-xylylenedihalide (53).⁵⁴ The synthetic steps are shown in Scheme 2.7.



Scheme 2.7 : (i) NaCN ; (ii) NaOMe/(MeO)₂CO ; (iii) CNCl ; (iv) KOH ; (v) HCl.

Reaction of dihalide (53) with sodium cyanide gave the dinitrile (54). Treatment of (54) with sodium methoxide and dimethylcarbonate in benzene establishes an equilibrium with the dianion (55). Cyanogen chloride was added to the mixture to afford the diester (56) which on base hydrolysis and decarboxylation gives the dianion (57). Acidification with hydrochloric acid gives the dihydro-TCNQ (58) which on oxidation yields the TCNQ derivative. This method is very versatile and it has been used to produce twenty one TCNQ derivatives. The disadvantages of this route are the number of steps involved and the need to use the highly toxic and expensive gas cyanogen chloride. The requirement for efficient alternative methodology has been recognised.

Our investigations have concentrated on alternative routes to prepare the key intermediate (58). A source of electrophilic cyanide, other than cyanogen chloride, was clearly required. Staab et al reported that the reagent 2-chlorobenzylthiocyanate (59) was a convenient alternative to cyanogen chloride for the preparation of tetramethyl-TCNQ.⁴⁹ After initial investigations by Dr M Hasan in our laboratory, we have investigated in detail the scope of reagent (59) for the preparation of TCNQ derivatives. Reagent (59) is a shelf stable, non-toxic liquid which can be readily prepared from 2-chlorobenzylchloride (60) and potassium thiocyanate in large amounts (e.g 50g batches) (Scheme 2.8).



Scheme 2.8 : (i) KSCN

Currently there is great interest in sources of positive cyanide, e.g. 1-cyano-4-(dimethylamino)pyridinium bromide (CAP) (61) has been used to prepare 2-cyanoimidazoles.⁵⁵ Thiocyanates have rarely been used in this context.

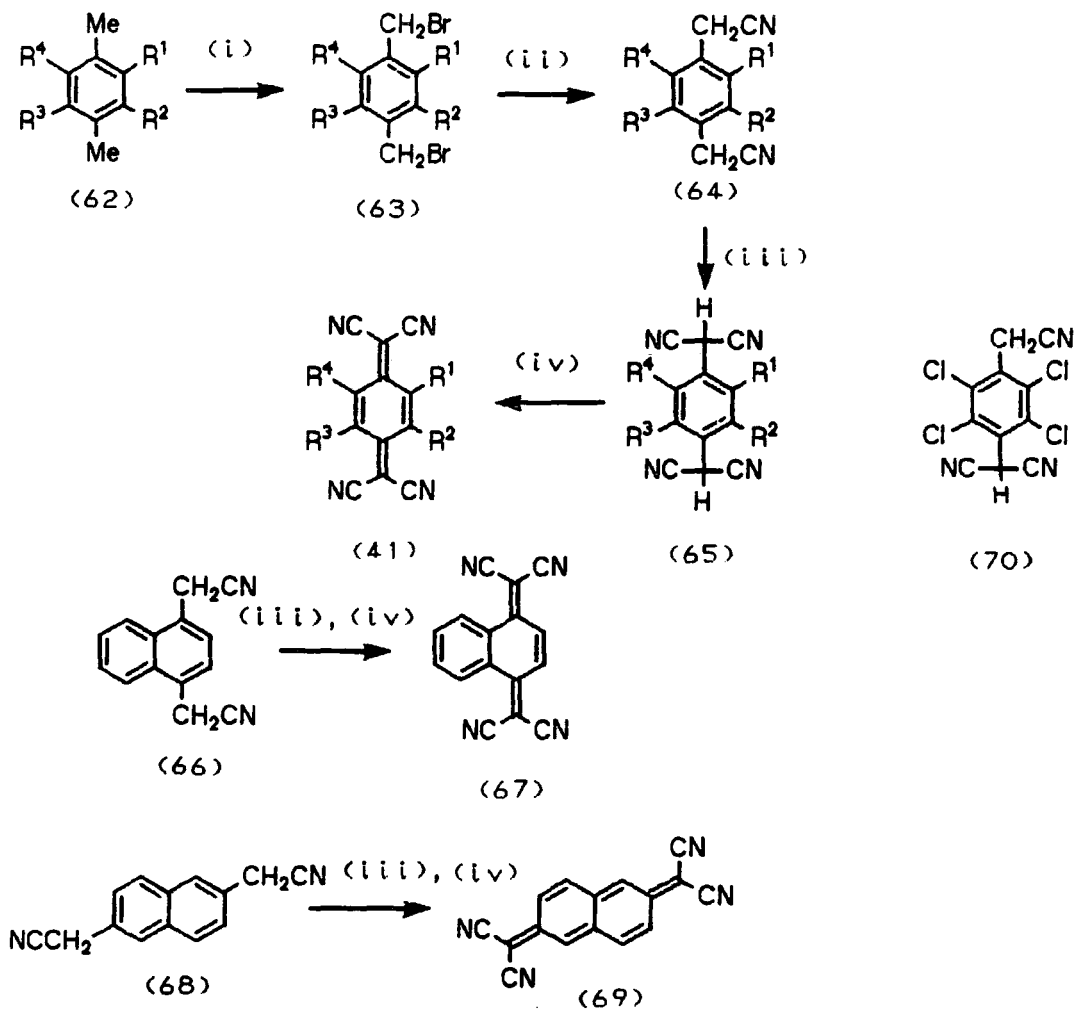
2.2 Synthetic Studies

The general synthetic strategy used for the synthesis of TCNQ derivatives (41c-41f), (67) and (69) is shown in Scheme 2.9. The method involved bromination of substituted p-xylene derivatives (62) with N-bromosuccinimide and reaction with sodium cyanide to give 1,4-di(cyanomethyl) derivatives e.g. (64). Di(cyanomethyl) arenes (64c-64e), (64g), (66) and (68) are all known compounds. Derivatives (64c), (64d) and (64g) were prepared from the corresponding dihalo compounds (63c), (63d) and (63g) as described previously. Compound (64f) was prepared from (63f) by the standard procedure. 2,6-Di(cyanomethyl)naphthalene (68) could not be obtained pure: a small amount of 2-bromomethyl-

6-cyanomethylnaphthalene (ca. 10-15% as judged by ¹H n.m.r and elemental analysis) was always present as a contaminant. The dinitriles (64) were deprotonated using four equivalents of lithium diisopropylamide (LDA); subsequent reaction with four equivalents of thiocyanate reagent (59) introduced two more cyano groups to yield dihydro-TCNQ derivatives (65). The dihydro-TCNQ derivatives (65) can be isolated but it is simpler to oxidise crude dihydro-TCNQ derivatives (65) with bromine to TCNQ derivatives without prior isolation. By this method TCNQ derivatives (41c-41f) and (67) were prepared in 35-45% yield from dinitrile starting materials. Yields of the TNAP derivative (69) were lower [ca.20%] partly because the dinitrile (68) could not be obtained pure. Compound (41f) is notable as it is a new TCNQ derivative containing a functionalised carbon substituent of which there are few examples.

Attempts to prepare the unknown tetrachloro-TCNQ (41g) by this procedure were unsuccessful. Only three cyano groups could be introduced into the system to yield the compound (70) (Scheme 2.9); none of the desired tetracyano compounds (41g) or (65g) could be obtained. However, the results obtained for compounds (41c-41f) have established that the reagent (59) is versatile in that both electron-donating and electron-withdrawing substituents on the benzene ring of compounds (64) can be tolerated.

Scheme 2.9 : (i) NBS, AIBN ; (ii) NaCN ; (iii) LDA, reagent (59), HCl ; (iv) Br₂.



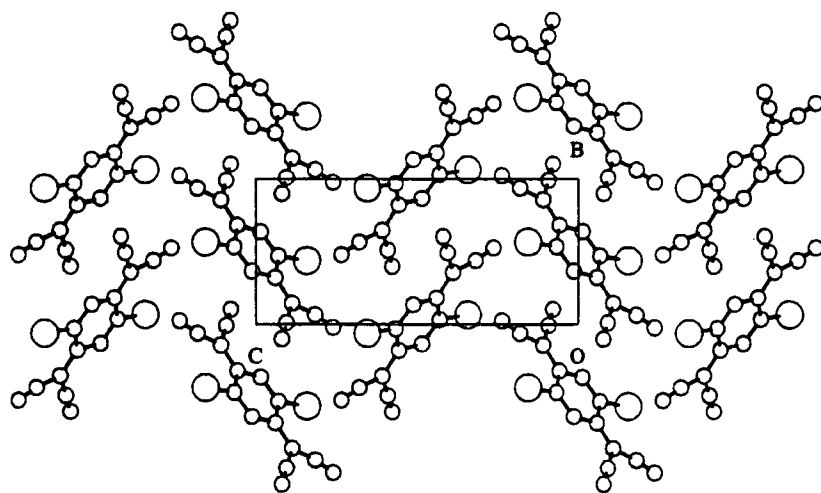
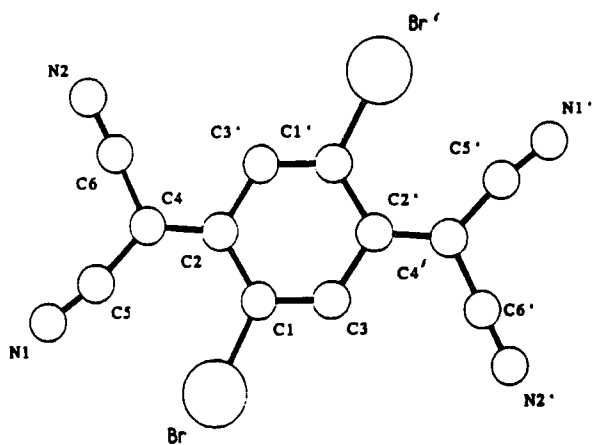
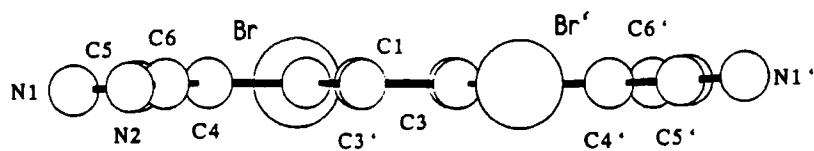
	R ¹	R ²	R ³	R ⁴
(a)	H	H	H	H
(b)	Me	Me	Me	Me
(c)	Cl	H	Cl	H
(d)	Br	H	Br	H
(e)	OMe	H	OMe	H
(f)	CO ₂ Me	H	H	H
(g)	Cl	Cl	Cl	Cl

2.3 X-Ray Crystal Structure Of 2,5-Dibromo-TCNQ (41d)

The hitherto difficult preparation of this TCNQ derivative has resulted in few reports of charge transfer complexes or anion radical salts of this acceptor.^{56, 57} The structure of the neutral molecule (41d) has not been reported. Of interest are the possible interstack interactions between the polarisable bromine atoms (Cf. chalcogen-chalcogen interactions which are important in stabilising the metallic state in organo-sulphur and -selenium donor systems⁵⁸).

The X-ray crystal structure of (41d) is shown in Figures (2.1-2.3). The molecule is essentially planar with C_{2v} symmetry (Figure 2.1). The $C_{(2)}-C_{(4)}$ bond bends in the plane of the ring away from the adjacent bromine atoms, presumably for steric reasons, such that the bond angle $C_{(4)}-C_{(2)}-C_{(3)}$ is $118.6(4)^\circ$ while $C_{(4)}-C_{(2)}-C_{(1)}$ is opened to $125.4(4)^\circ$. Consistent with this, one CN group of the dicyanomethylene unit is also bent away from the bromine atom with bond angles $C_{(6)}-C_{(4)}-C_{(2)} = 120.0(4)^\circ$ and $C_{(5)}-C_{(4)}-C_{(2)} = 128.8(4)^\circ$. The CN group adjacent to the bromine atom deviates significantly from linearity: the angle $C_{(4)}-C_{(6)}-N_{(2)} = 177.9(5)^\circ$. The molecules of compound (45d) pack in a herringbone fashion in the unit cell with close intermolecular N...Br contacts as shown (Figure 2.3), but there are no close Br...Br contacts.

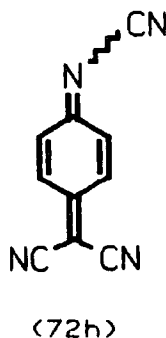
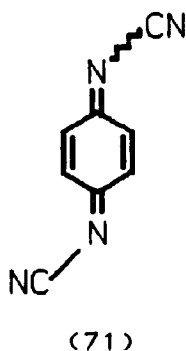
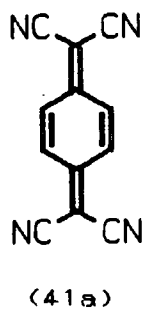
Figures 2.1-2.3: X-Ray Crystal Structure of
2,5-Dibromo-TCNQ (41d)



2.4 The Synthesis, Electrochemistry And X-Ray Crystal Structure Of Some New N, 7, 7-Tricyanoquinomethaneimines

2.5 Introduction

7, 7, 8, 8-Tetracyano-p-quinodimethane (TCNQ) (41a) is an electron acceptor of major importance as a component of materials that display unusual physical properties, e.g non-linear optical properties,³⁵ high electrical conductivity³⁷, ferromagnetism⁶⁰ and possibly molecular rectification⁶¹. Derivatives and analogues of the acceptor are of great interest.⁶² N, N'-Dicyanoquinonediimine (DCNQI) (71) derivatives are a new class of acceptors discovered by Hunig.⁶³ The synthesis of acceptors (71) is easily achieved by cyanoimination of quinones with bis(trimethylsilyl)carbodiimide (BTC). TCNQ derivatives are commonly prepared from the appropriate quinone and malononitrile in the presence of titanium tetrachloride and pyridine (Lehnert's Reagent). The method has been used to prepare a range of TCNQ derivatives most of which are tetrasubstituted (e.g tetramethyl-TCNQ (41b)).



Bryce and Davies recently reported the first acceptors in the N,7,7-tricyanoquinomethaneimine (72h) series; these can be considered as hybrids of the TCNQ (41a) and DCNQI (71) systems.⁶⁴ We have now extended these initial studies to include the synthesis of several new derivatives and studied their electrochemistry. X-ray crystal structures of the tetramethyl derivative (72m) and trimethyl derivative (72n) have been obtained. Variable temperature ¹H n.m.r spectra of derivatives (72n) and (72p) have been studied. Derivatives of system (72h) could not, however, be incorporated into D-Π-A zwitterions, analogous to (41a), by cyanide displacement.

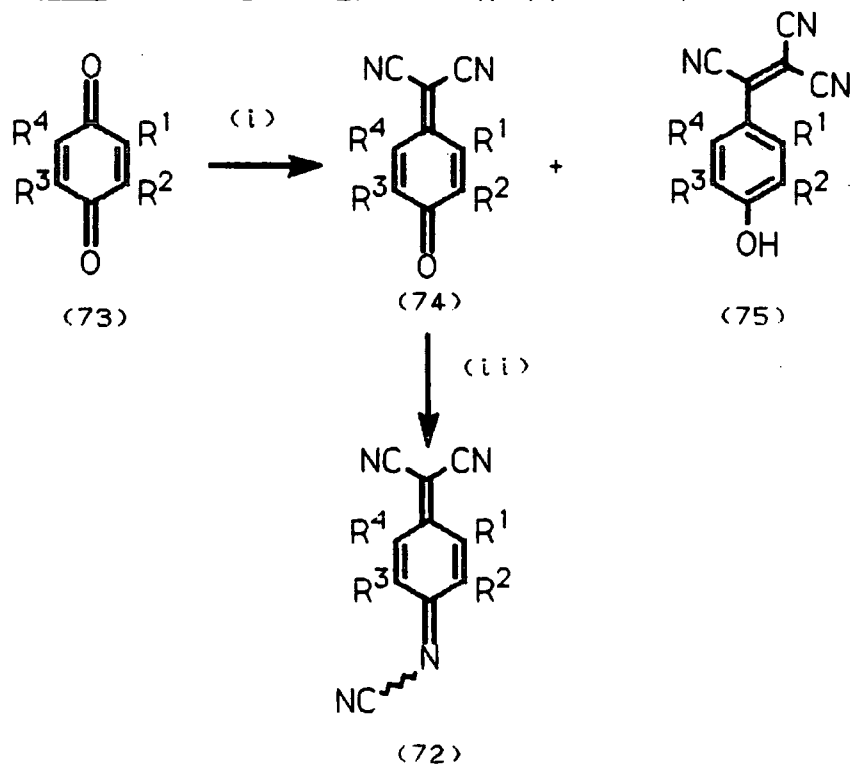
2.6 Synthesis of N,7,7-tricyanoquinomethaneimines (72h - 72r)

Some of the reactions which are reported to yield TCNQ (41a) derivatives were found to follow a different course in our laboratory. Cowan et al showed that treatment of duroquinone with malononitrile and Lehnert's reagent yields tetramethyl-TCNQ (41b) in ca. 55 % yield.⁵² In our hands, when this reaction was performed on 1-3 mmol of quinone, under a variety of conditions including those described by Cowan et al, no tetramethyl-TCNQ was obtained. The mono(dicyanomethylated) product (74m) was isolated (max yield 26%) and a phenolic product (75m) (15 % - 30 % yield) (Scheme 2.10).

After extensive investigation of various reaction conditions, we have found that tetramethyl-TCNQ (41b) is formed, under Cowan's conditions, only when the reaction is carried out on a larger scale (i.e. >1.0g, ≈ 6 mmol of

duroquinone 73m). A highly exothermic reaction occurs upon adding titanium tetrachloride to the reaction mixture under these conditions. The phenolic product (75m) and tetramethyl-TCNQ (41b) were obtained; no quinomethide (74m) was formed.

Scheme 2.10: (i) $\text{CH}_2(\text{CN})_2$, TiCl_4 , pyridine; (ii) TiCl_4 , BTC.



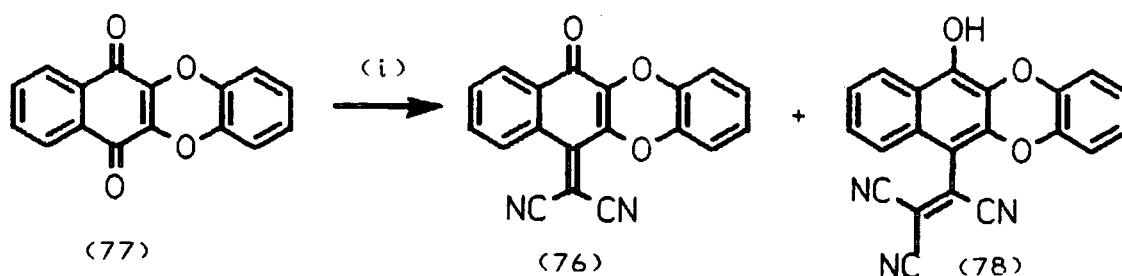
	R ¹	R ²	R ³	R ⁴
(h)	H	H	H	H
(k)	-CH=CH-	-CH=CH-	-CH=CH-	-CH=CH-
(m)	Me	Me	Me	Me
(n)	H	Me	Me	Me
(p)	H	Me	Me	H
(q)	-S-(CH ₂) ₂ -S-		-S-(CH ₂) ₂ -S-	
(r)	-CH=CH-CH=CH-		-S-(CH ₂) ₂ -S-	
(s)	Me	Me	H	H
(t)	Cl	Cl	Cl	Cl

A range of quinomethides (74h-74r) (typically 25-40 % yields) and phenolic products (75h-75r) were obtained from p-benzoquinones (73h-73r). When the reactions of quinones (73n) and (73p) were conducted on > 6 mmol scale (an attempt to prepare the unknown 2,3,5-trimethyl-TCNQ and 2,6-dimethyl-TCNQ) only quinomethides (74n), (74p) and phenolic products (75n) and (75p) were obtained. Quinones (73s) and (73t) gave complex mixtures which resisted purification. Attempts to prepare TCNQ (41a) and TCNAQ (47) from p-benzoquinone and anthraquinone by the published procedures were unsuccessful. Reactions of quinomethides (74h), (74m) and (74n) with malononitrile and Lehnert's reagent, hopefully to introduce a dicyanomethylene group, gave only the phenolic products (75h), (75m) and (75n) and there was no evidence for the formation of the corresponding TCNQ derivative.

Recently, other workers have reported the failure of Lehnert's reagent for the synthesis of TCNQ derivatives. Becker et al obtained only mono(dicyanomethylated) product (76) along with the phenolic product (78), from the tetracyclic quinone system (77) (Scheme 2.11).⁴⁵

It has been suggested that the heterocyclic oxygens in (76) might deactivate the carbonyl group to attack by the malononitrile anion and prevent the formation of the TCNQ. Within our series of quinomethide derivatives (74h-74r) this

electronic effect may operate in compounds (74q) and (74r) but it cannot explain our results with (74h-74p).

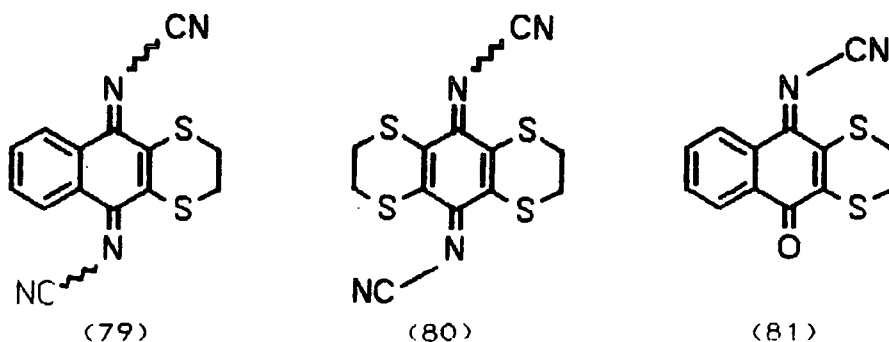


Scheme 2.11 : (i) $\text{CH}_2(\text{CN})_2$, pyridine, TiCl_4 .

One possible explanation of our results is steric crowding in the quinomethides (74). The only TCNQ derivative we have obtained is tetramethyl-TCNQ (41b). The intermediate quinomethide (74m) will be more sterically strained than the other quinomethides, with the exception of (74k) (which is known to be non planar from X-ray analysis⁶⁶). The distorted conformation of (74m) probably makes the O atoms of the carbonyl group more accessible to complexation by titanium tetrachloride.

Quinomethides (74h-74r) reacted with bis(trimethylsilyl) carbodiimide in the presence of titanium tetrachloride to give N,7,7-tricyanoquinomethaneimines (72h-72r) in 65-80% yield. Japanese workers reported compounds (72h) and (72k) prepared by this route at the same time as the initial

report from our laboratory of this reaction. They reported that compound (72h) was unstable and oligomerises in polar solvents (THF, MeCN) after 24h.⁶⁷ However, we have found that quinomethaneimine (72h) is stable for several days in acetonitrile solution from which it can be recovered unchanged in quantitative yield. Reaction of p-benzoquinone derivatives (73q) and (73r) with BTC and titanium tetrachloride gave as major products the DCNQI derivatives (79) and (80), respectively; compound (81) was obtained as a minor product.



2.7 Electrochemical Studies

The electrochemical redox properties of acceptors (72h-72r) were studied by cyclic voltammetry and the data is shown in Table 2.1. For the parent *N*,7,7-tricyanoquinomethaneimine (72h) the first and second half-wave reduction potentials are, predictably, close to the values for TCNQ (41) and DCNQI (71) (Figure 2.4). For *N*,7,7-tricyanoquinomethaneimines (72m), (72n) and (72p), there is a predictable lowering in electron affinity with methyl substitution. Sulphur substitution increases the acceptor ability; compound (72q) is the strongest acceptor in

the series and compound (71r) is among the strongest DCNQI acceptors known (Figure 2.5). This trend is consistent with the known electron withdrawing property of S atoms bonded to double bonds.

Table 2.1 : First and second half-wave reduction potentials of N,7,7-tricyanoquinomethaneimines (72h-72r), TCNQ (41a) and tetramethyl-TCNQ (41b). a. This work; versus Ag/AgCl, electrolyte 2×10^{-2} M $Bu_4N^+ClO_4^-$; Pt working electrode, scan rate 100 mV sec^{-1} using a BAS Electrochemical Analyser. n.o - not observed.

Compound	Solvent	$E^{1,1/2}/V$	$E^{2,1/2}/V$	$\Delta E/V$
72h	MeCN	+0.16	-0.42	0.58
72k	CH_2Cl_2	-0.43	n.o	
72m	MeCN	-0.03	-0.23	0.20
72n	MeCN	+0.07	-0.41	0.48
72p	MeCN	+0.11	-0.43	0.54
72q	CH_2Cl_2	+0.28	-0.13	0.41
72r	CH_2Cl_2	+0.17	-0.22	0.39
41a	CH_2Cl_2	+0.11	-0.31	0.42
41c	CH_2Cl_2		-0.25 (2e)	0.00

The value of ΔE is related to the Coloumbic repulsions resulting from the addition of two electrons to an acceptor.

Within compounds (72h-72r) the tetramethyl compound (72m) has a markedly lower value of ΔE (0.20V) compared to other derivatives. This value of ΔE is intermediate between that for tetramethyl-TCNQ ($\Delta E = 0.00V$) and tetramethyl-DCNQI ($\Delta E = 0.44V$). This may be explained on steric grounds: tetramethyl-TCNQ has a severely distorted ring skeleton as revealed by a single crystal X-ray structure. Other tetrasubstituted TCNQ's have a non planar structure (e.g TCNAQ, analogues of TCNAQ, tetracyanobianthraquinodimethane) while, in contrast, tetrasubstituted DCNQI derivatives, e.g (71b), are essentially planar. Planarity is maintained in the DCNQI derivatives as the NCN group, being smaller than the $C(CN)_2$ group, can bend in the plane of these derivatives. In contrast, the $C(CN)_2$ groups are forced out of the plane and the tetrasubstituted TCNQ ring distorts into a boat conformation.

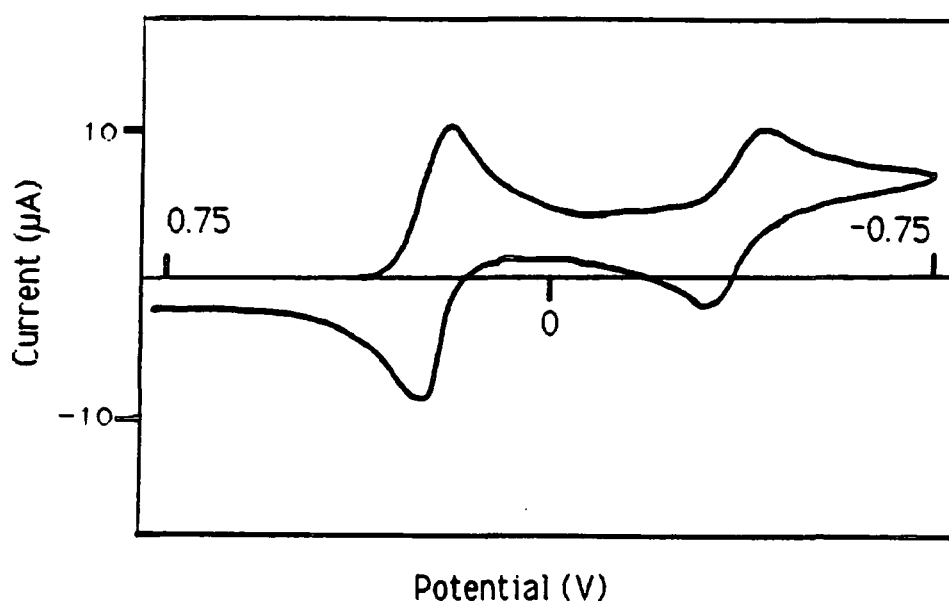


Figure 2.4 : Cyclic Voltammogram of (72h).

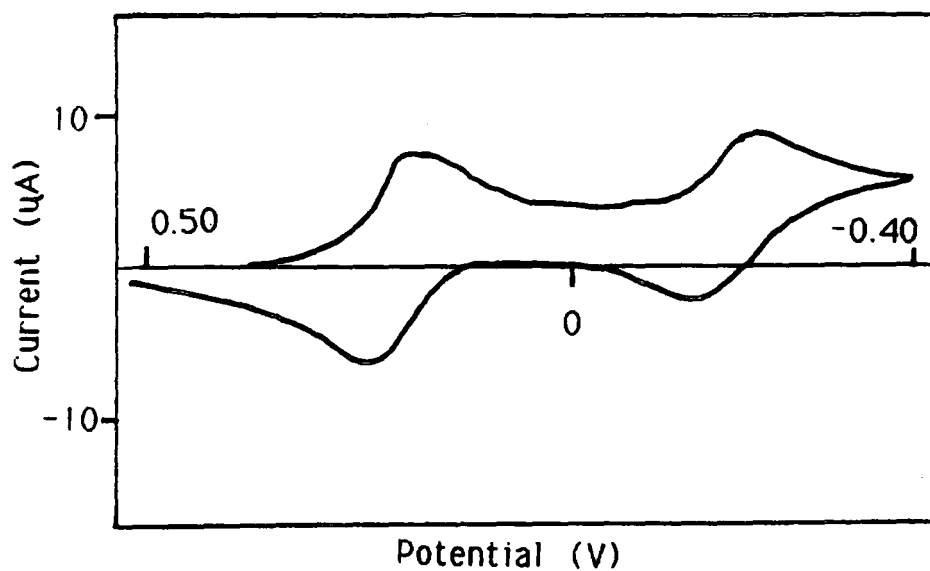


Figure 2.5 : Cyclic Voltammogram of (72q)

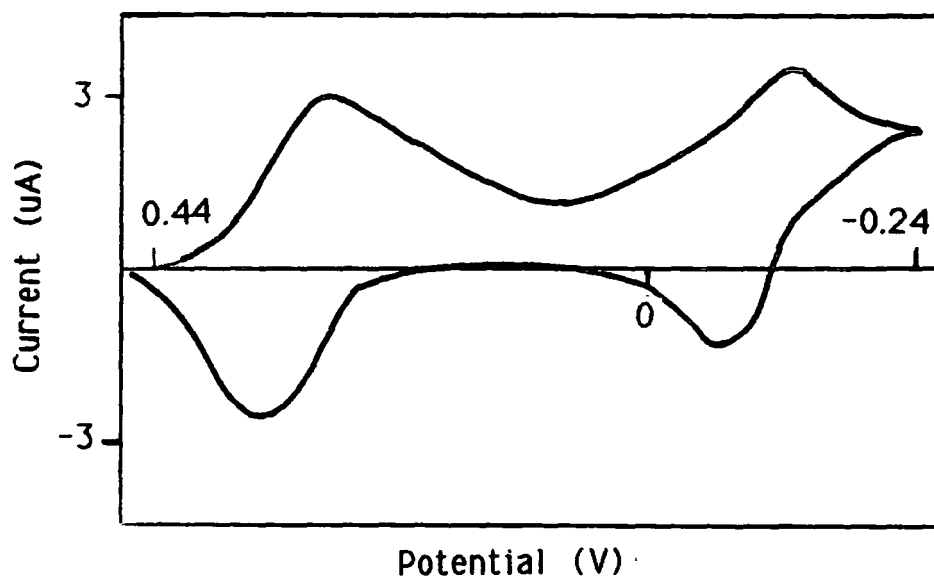


Figure 2.6 : Cyclic Voltammogram of (71r)

2.8 X-Ray Crystal Structures Of Compounds (72m) and (72n)

The ring of tetramethyl derivative (72m) is distorted into a boat conformation (See Figure 2.7). The following three planes were defined as follows: plane 1 by atoms C(4), C(5) and C(13); plane 2 by atoms C(7), C(9) and C(11); plane 3 by atoms C(5), C(7) and C(11). The angle between plane 1 and plane 3 is 29.81° , while that between plane 2 and plane 3 is 21.83° . Therefore the ring is more distorted about the bulky $C(CN)_2$ group than the NCN group. In contrast, the trimethyl derivative (72n) is essentially planar (Figure 2.8).

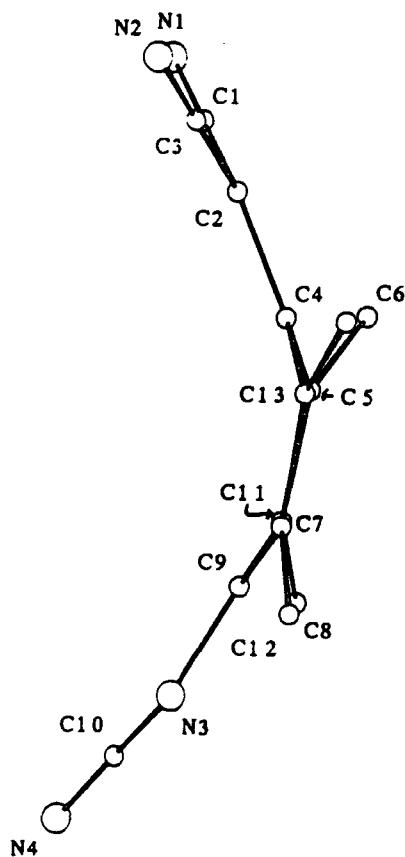


Figure 2.7: X-Ray structure of (72m)

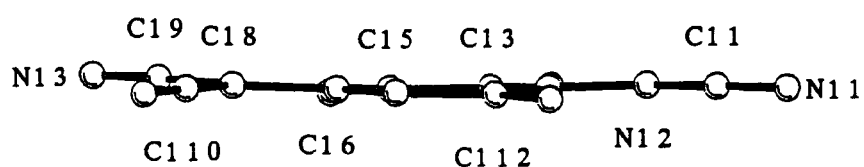


Figure 2.8 : X-Ray structure of (72n)

2.9 Variable Temperature Proton N.M.R Spectra Of (72n) and (72p)

The proton n.m.r spectra of compounds (72n) and (72p) are of interest. The spectrum of (72p) at 20°C consists of a broad singlet at 2.50 ppm and a singlet at 7.37 ppm. On cooling to 0°C the spectrum consists of two doublets.

(Figure 2.9). The proton n.m.r spectrum of (72n) at 10°C consists of a narrow singlet at 2.59 ppm and broad singlets at 7.36 and 2.32 ppm. On warming to 30°C the spectrum changes to four narrow singlets centred at 7.36, 2.59, 2.56 and 2.35 ppm. The observed splitting is caused by flipping of the cyano group attached to nitrogen. Similar variable temperature proton n.m.r results were obtained by Hunig *et al* for symmetrical/unsymmetrical *N, N'*-Dicyanoquinonediimine (DCNQI) (71) derivatives.⁶⁰

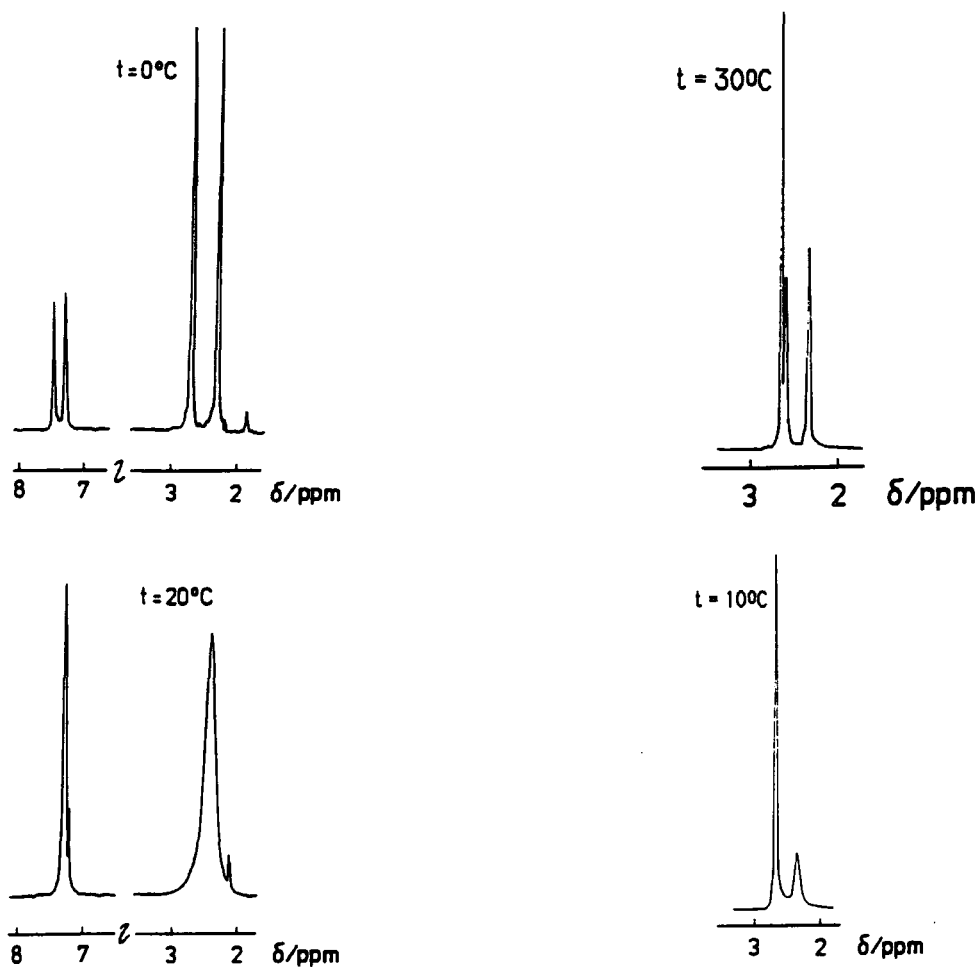


Figure 2.9 : Variable temperature proton n.m.r spectra of *N, 7, 7*-tricyanoquinomethaneimine derivatives (72n) and (72p).

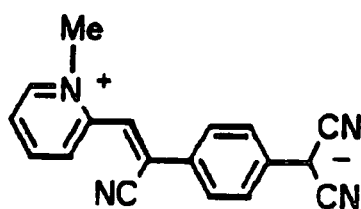
CHAPTER THREE

SYNTHESIS, LB DEPOSITION AND NLO PROPERTIES

OF R-Q3CNO CHROMOPHORES

3.1 Introduction

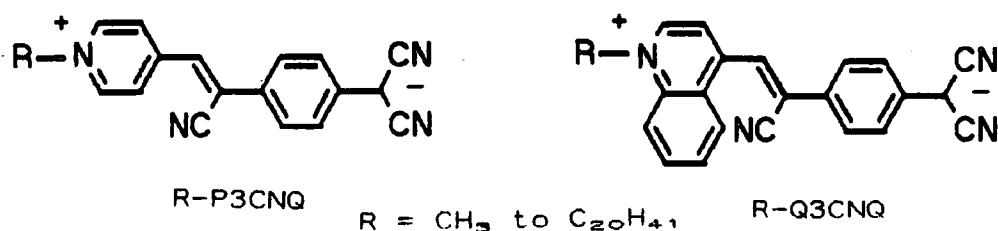
As described in Chapter 1 there is currently great interest in molecules which consist of donor and acceptor moieties linked via a π electron bridge because of their non-linear optical applications. Special attention is focused on second order non-linear effects such as Second Harmonic Generation (SHG) or frequency doubling. The magnitude of the second harmonic response is governed by the bulk second order hyperpolarisability (χ_2), and is maximised when non centrosymmetric alignment of the molecules allows maximum contribution of the second order molecular hyperpolarisabilities (β) to χ_2 . Non centrosymmetric alignment of amphiphilic D- π -A molecules can be achieved by LB deposition.⁶⁹ At Cranfield the interest in NLO materials stemmed from the synthesis of Z- β -(1-methyl-2-pyridinium)- α -cyano-4-styryldicyanomethanide (82) (P3CNQ).



(82)

The zwitterionic ground state is confirmed by X-ray crystallography.⁷⁰ The molecular geometry of P3CNQ is shown in Figure 3.1. The bond lengths in the pyridinium ring and the tricyanoquinodimethanide unit are benzenoid and not

Parr-Pople method.⁹ This high value can be contrasted with $0.45 \times 10^{-30} \text{ cm}^5 \text{esu}^{-1}$ for urea⁷¹, $200 \times 10^{-30} \text{ cm}^5 \text{esu}^{-1}$ for hemicyanine (5)²⁰ and $1000 \times 10^{-30} \text{ cm}^5 \text{esu}^{-1}$ for the unstable merocyanine dye (4)¹⁸. The non-linear potential of amphiphilic derivatives of P3CNQ was quickly established. Z- β -1-(1-Alkyl-4-pyridinium)- α -cyano-4-styryldicyanomethanide (R-P3CNQ) derivatives were prepared. The R-Q3CNQ zwitterions forms stable Z type films which exhibit SHG. Attention turned next towards the related quinolinium derivatives R-Q3CNQ.

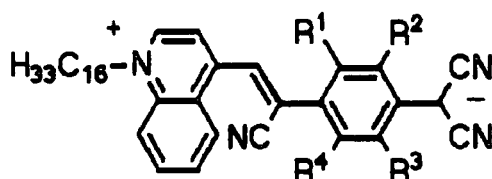


We have made an extensive study of the LB film forming and non-linear optical properties of these and related derivatives and it is this work that is presented here.

3.2 Synthesis Of R-Q3CNQ Derivatives

The R-Q3CNQ zwitterions were prepared from the reaction of a lepidinium halide with either LiTCNQ or neutral 7,7,8,8-tetracyano-p-quinodimethane (TCNQ) and piperidine. The other N-alkyl derivatives were synthesised similarly and substituted 2,5-dibromo (83), 2,5-dichloro (84), 2,3,5,6-tetrafluoro (85) and 2,3-benzo (86) analogues were obtained

from substituted TCNQs by the published procedure.⁷² The UV-VIS solution spectra of unsubstituted R-Q3CNQ are chain length independent. The absorption spectrum of C₃₃H₁₇-Q3CNQ (Figure 3.3) consists of a broad-top transition at 710 ± 5 nm with maxima at ca. 348 and 378 nm. The broad-top transition is solvatochromic and is shifted with decreasing solvent polarity, from 710 ± 5 nm in acetone (μ = 2.88 D). A transition from an ionic ground state to a neutral excited state is consistent with this behaviour. The IR spectra indicate a zwitterionic ground state. A comparison of the stretching frequencies of the R-Q3CNQ homologues (a doublet at 2180 and 2150 cm⁻¹) with those of TCNQ⁰ and TCNQ⁻ indicate a zwitterionic structure.



	R ¹	R ²	R ³	R ⁴
(20)	H	H	H	H
(83)	Br	H	Br	H
(84)	Cl	H	Cl	H
(85)	F	F	F	F
(86)	H	H	-CH=CH-CH=CH-	

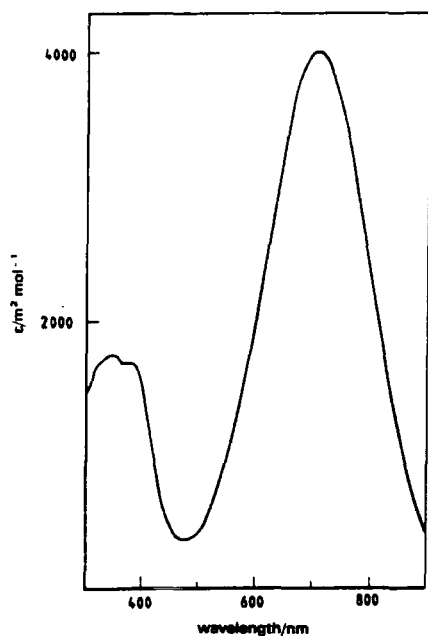


Figure 3.3 : Absorption Spectrum of (a) C₁₆H₃₃-Q3CNQ

3.3 Langmuir Blodgett Films of R-Q3CNQ

An investigation into the LB film forming properties of alkyl homologues of R-Q3CNQ (for R = CH₃ to C₂₀H₄₁) using a two compartment Nima technology trough was carried out. The materials were deposited in Z type mode at a surface layer pressure of 25 mNm⁻¹. LB films of R-Q3CNQ (R > C₆H₁₃) were obtained, from the molecular areas, given in Table 3.1, a transition in alignment occurs at R = C₁₅H₃₁. The molecular area (at Π = 0) where the surface pressure increases is 100 - 120 Å² for R > C₁₅H₃₁, and 50 - 70 Å² for R ≤ C₁₄H₂₉; this indicates a different tilt angle at Π = 0 in the monolayer (Figure 3.4). The calculated cross-sectional Van der Waals area (30 Å²) and face area (114 Å²) of the

chromophore indicate that for $R \geq C_{15}H_{31}$, the chromophore face lies flat on the water subphase.

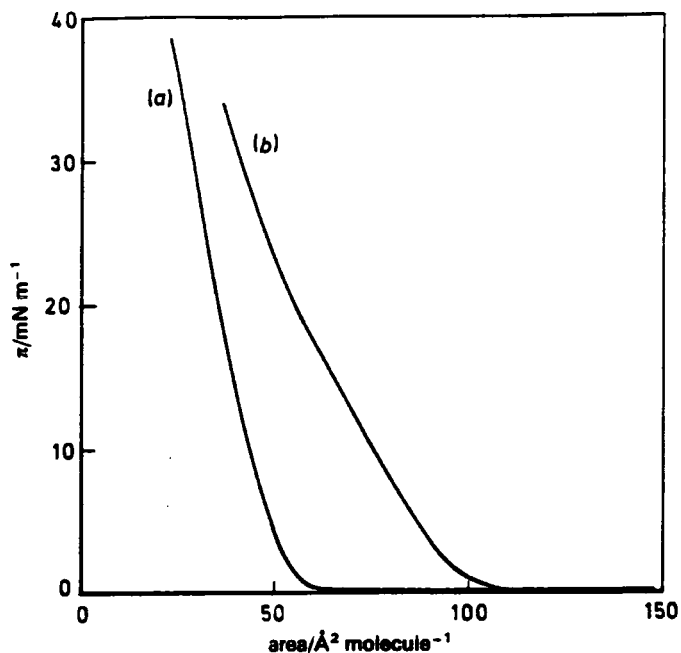


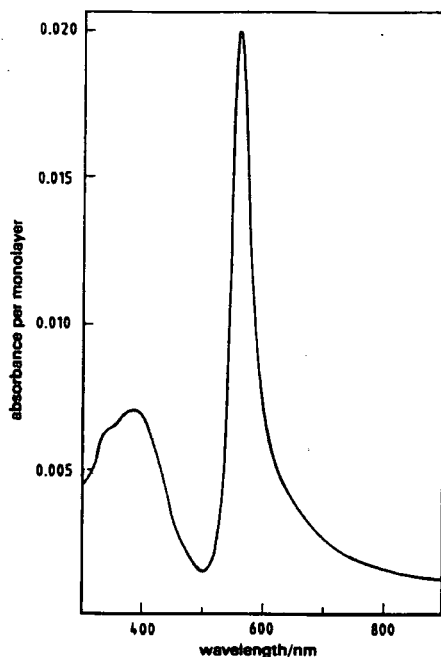
Figure 3.4 : Surface Pressure (Π) vs. Surface Area Isotherms of (a) C_9H_{17} -Q3CNQ; (b) $C_{16}H_{33}$ -Q3CNQ (20)

3.4 Charge Transfer Spectra

The LB film spectra are shown in Figure 3.3 and the spectroscopic data in Table 3.1. The general profile of the LB spectra is essentially the same as that of the solution spectra except that the position and the width of the CT band is altered. In acetonitrile the CT band is at 710 ± 5 nm for all the homologues. The position of the CT band of the LB spectra is dependant on the chain length e.g. for LB films of C_6H_{13} -Q3CNQ to $C_{14}H_{29}$ -Q3CNQ the band is shifted to 614 ± 4 nm

(HWHM = 37 ± 2 nm) and for $C_{15}H_{31}$ -Q3CNQ to $C_{20}H_{41}$ -Q3CNQ it occurs at 565 ± 4 nm (HWHM = 22 ± 1 nm).

Figure 3.5 : UV-VIS LB spectra of $C_{16}H_{33}$ -Q3CNQ



This shift may be attributed to a change in molecular alignment resulting in a change from an intermolecular CT band (614 ± 4 nm) to an intramolecular transition (565 ± 4 nm). This change can be explained if one considers the molecular areas at $\Pi = 25$ mNm⁻¹. The areas per molecule of $28 - 30 \text{ \AA}^2$ for C_6H_{13} -Q3CNQ to $C_{14}H_{27}$ -Q3CNQ are in close agreement with the cross-sectional Van der Waals area of 30 \AA^2 of the widest part of the chromophore, i.e. the quinolinium donor. Therefore, the alignment is nearly perpendicular to

Table 3.1 : Molecular areas and spectroscopic data (wavelength, absorbance and half widths at half maximum) of the R-Q3CNQ LB films.

alkyl group (R)	area/ \AA^2 at 25m Nm ⁻¹	λ_{max} (nm)	absorbance per layer	HWHM (nm)
n-Hexyl	29	610	0.014	37
n-Heptyl	28	614	0.017	39
n-Octyl	32	616	0.020	37
n-Nonyl	30	617	0.018	35
n-Decyl	34	616	0.017	39
n-Undecyl	30	616	0.018	38
n-Dodecyl	30	613	0.018	37
n-Tridecyl	31	615	0.022	36
n-Tetradecyl	28	614	0.020	37
n-Pentadecyl	40	561	0.016	22
n-Hexadecyl	47	565	0.020	22
n-Octadecyl	50	565	0.020	23
n-Eicosyl	48	568	0.020	21

the substrate and the band at 614 nm must be intermolecular as the intramolecular transition moment and electric vector are orthogonal. For $C_{15}H_{11}-Q3CNQ$ to $C_{20}H_{11}-Q3CNQ$, the area per molecule at $\Pi = 25 \text{ mNm}^{-1}$ suggests that the chromophores are tilted towards the plane of the substrate. The transition at 565 nm probably corresponds, therefore, to an intramolecular transition.

Both CT bands are in evidence for LB spectra of $C_{15}H_{11}-Q3CNQ$. When deposited at $\Pi = 40 \text{ mNm}^{-1}$, the main absorption band occurs at 614 nm, while at $\Pi = 25 \text{ mNm}^{-1}$ at 561 nm, with a broad shoulder above 600 nm. The two pyridinium analogues (see Table 3.2) have intermolecular and intramolecular CT bands observed in both LB and single crystal spectra.

Table 3.2 : Wavelengths of intramolecular and intermolecular charge transfer bands of quinolinium and pyridinium zwitterions.

Zwitterion	Intramolecular CT band/nm	Intermolecular CT band/nm
$CH_3-\alpha P3CNQ$	538	806
$C_6H_{11}-P3CNQ$	495 ± 4	634 ± 4
R-Q3CNQ	565 ± 4	614 ± 4

3.5 Analogues of C₁₄H₉N₃-Q3CNQ (20)

The spectral data for C₁₄H₉N₃-Q3CNQ (20) and four substituted analogues are summarised in Table 3.3. The zwitterions are listed in order of increasing transition energy. Mulliken CT theory states that HOMO-LUMO transition energy is given by equation (3.1).⁷⁹

$$E_{ct} = (E_{i,D} - E_{ea,A} - E_c) + 2t^2 / (E_{i,D} - E_{ea,A} - E_c) \dots (3.1)$$

$E_{i,D}$ = ionisation energy of the donor part of the molecule.

$E_{ea,A}$ = electron affinity of the acceptor part of the molecule.

E_c = Coloumb energy.

t = transfer integral.

The approximation that the second term is small compared to the first, applies unless $E_{i,D}$ and $E_{ea,A}$ are closely matched. Applying the approximation to equation (3.1) gives: -

$$E_{ct} = E_{i,D} - E_{ea,A} - E_c$$

For R-Q3CNQ and derivatives substituted only at the acceptor end, $E_{i,D}$ and E_c can be assumed constant, and E_{ct} depends only on the electron affinity of the acceptor part. Values of $E_{ea,A}$ for the phenyldicyanomethanide group are not available but $E_{ea,A}$ may be roughly approximated to the half-

wave reduction potentials of TCNQ and its derivatives. The effect of substituents on the position of the CT band is a hypsochromic shift with increasing half-wave reduction potential. For example, $\lambda_{\max}(\text{LB film}) = 623 \text{ nm}$ for the benzo analogue(86), 565 nm for unsubstituted derivative (20), 545 nm for dichloro, dibromo analogues (84) and (83), and 480 nm for the tetrafluoro analogue (85). Substitution may be used, therefore, to alter the wavelength of the CT band away from the position of the second harmonic in a controlled way.

3.6 Non-Linear Optical Properties

The quinolinium zwitterion (20) should possess a high second order coefficient on a theoretical basis by analogy with the pyridinium zwitterion R-P3CNQ. SHG studies were carried out on LB films of $\text{C}_{16}\text{H}_{33}\text{-Q3CNQ}$ (20) using the apparatus schematically shown in Figure 3.6. The films were irradiated with light from a Q switched Nd:YAG laser (1.064 μm ; pulse width 10 ns; repetition rate 2Hz) with the p-polarised beam incident to the substrate at 45°. SHG from a Y cut quartz plate reference and LB film were monitored simultaneously using fast rise-time photomultiplier tubes (Phillips XP2020) and a dual channel Hewlett-Packard 54111D digitising oscilloscope.

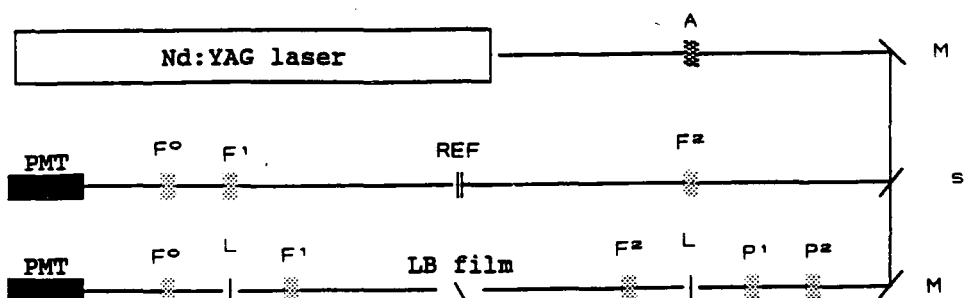
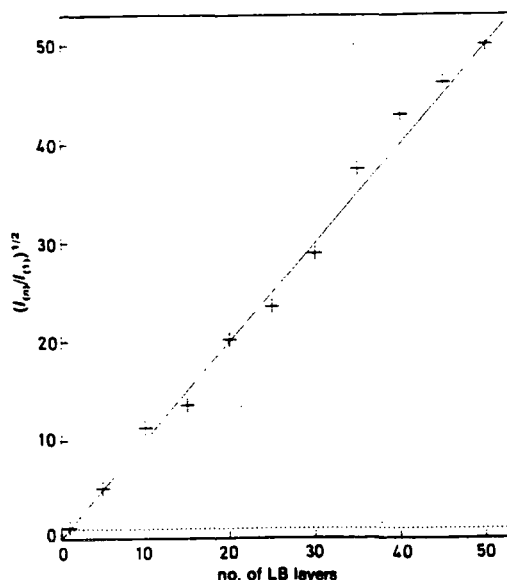


Figure 3.6 : Schematic diagram of the SHG apparatus: A, attenuator; M, mirror; s, beam splitter; F², visible blocking filter; REF, Y-cut quartz plate; F¹, infrared blocking filter; F⁰, 532 nm narrow bandpass filter; PMT, photomultiplier tube; P¹, halfwave plate; P², Glan Thompson filter; L, lens.

Table 3.3 : Wavelengths of solution and LB film CT bands for C₁₆H₃₃-Q3CNQ (20) analogues together with the half-wave reduction potential of the TCNQ from which they were prepared.

Zwitterion	CT band (CH ₃ CN) λ _{max} /nm(eV)	CT band (LB film) λ _{max} /nm(eV)	E _{1/2} /V
C ₁₆ H ₃₃ -Q3CNQ (benz)	742 (1.67)	623 (1.99)	-0.09
C ₁₆ H ₃₃ -Q3CNQ	712 (1.75)	565 (2.20)	+0.17
C ₁₆ H ₃₃ -Q3CNQ(Cl ₂)	602 (2.06)	545 (2.28)	+0.41
C ₁₆ H ₃₃ -Q3CNQ(Br ₂)	602 (2.06)	545 (2.28)	+0.41
C ₁₆ H ₃₃ -Q3CNQ(F ₄)	565 (2.20)	480 (2.59)	+0.53

Figure 3.7 : Square root of the normalised second harmonic intensity of $C_{16}H_{33}$ -Q3CNQ (20) vs. number of LB layers



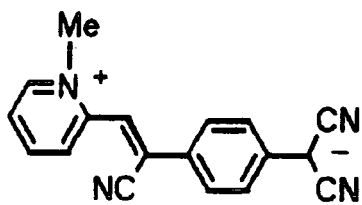
The intensity of the second harmonic for the $C_{16}H_{33}$ -Q3CNQ (20) LB film is compared with that of hemicyanine (5) which is known to have a high β , in Figure 3.7. The $C_{16}H_{33}$ -Q3CNQ (20) films have a non centrosymmetric Z type structure, in contrast to hemicyanine films which are Y-type (centrosymmetric). The bulk susceptibility of the bilayer (and all even numbers of layers) is zero. For $C_{16}H_{33}$ -Q3CNQ (20) the SH intensity was found to increase quadratically with the number of LB layers, consistent with theory; the data corroborate the Z-type structure. For Y-type hemicyanine films the incorporation of a spacer layer between the chromophores is necessary to achieve the non centrosymmetric alignment for SHG. Spacers are not required for $C_{16}H_{33}$ -Q3CNQ (20) because non centrosymmetric Z-type alignment can be achieved.

CHAPTER FOUR

SYNTHESIS, LB DEPOSITION AND NLO PROPERTIES
OF R-BT3CNQ AND R-T3CNQ CHROMOPHORES

4.1 Introduction

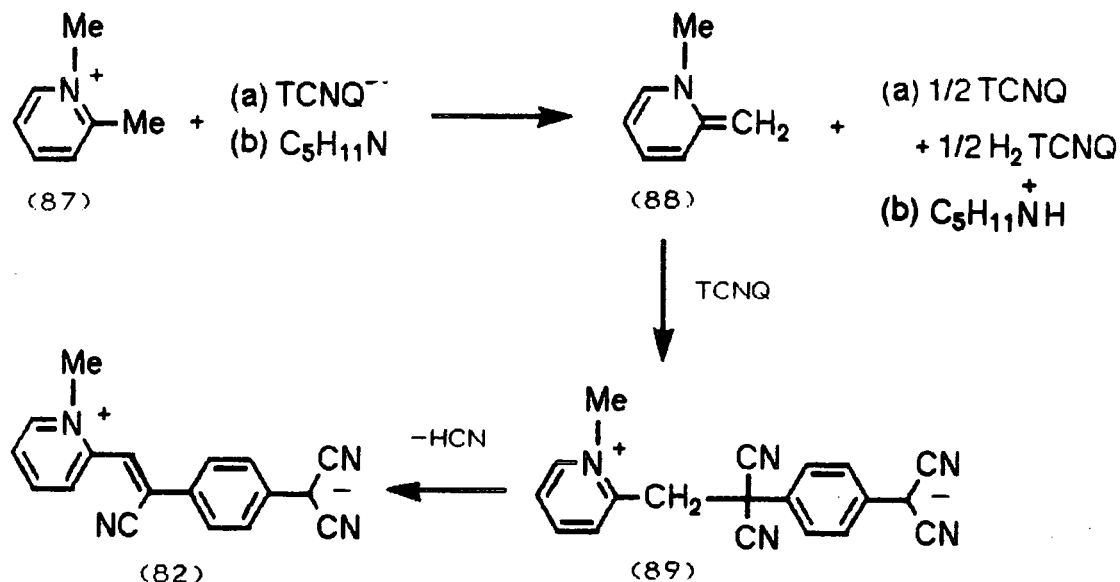
Currently the synthesis and second order non-linear optical properties of donor- π -acceptor chromophores is the focus of much attention. As mentioned previously the interest at Cranfield stemmed from the preparation of Z- β -(1-Methyl-2-pyridinium)- α -cyano-4-styryldicyanomethanide P3CNQ (82).



(82)

The reaction of donors (D) with acceptors (A) has led to the preparation of a vast number of charge transfer salts and complexes. P3CNQ (82) was prepared from the lithium salt of 7,7,8,8-tetracyano-p-quinodimethane (LiTCNQ) and 1,2-dimethylpyridinium iodide in acetonitrile.⁷⁴ The formation of P3CNQ was unexpected; in ethanol the expected product (a charge transfer salt of 1:1 stoichiometry) was formed.

Scheme 4.1: Possible mechanism for the formation of P3CNQ.

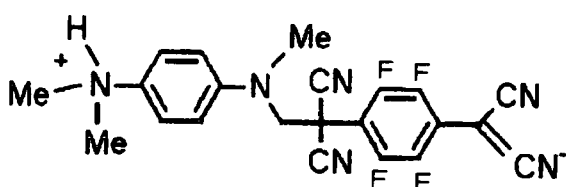


The intermolecular overlap of the P3CNQ molecules gives zero net dipole moment together with D⁺A⁻ stacking along the b axis.

The substitution of cyano groups of 7,7,8,8-tetracyano-p-quinodimethane by nucleophilic species has been described by workers at Du Pont.⁷⁵ Neutral TCNQ and piperidine can be used instead of LiTCNQ. A possible mechanism for the formation of P3CNQ is shown in Scheme 4.1. 1,2-Dimethylpyridinium iodide (87) is readily deprotonated in basic media to give the monomeric anhydro base (88). The anhydro base (88) reacts with neutral TCNQ to give the zwitterionic donor-sigma-acceptor intermediate (89), subsequent loss of HCN gives the product zwitterion P3CNQ (82). If the mechanism proceeds via a resonance stabilised

anhydro base (88) then 1,3-dimethylpyridinium iodide should not react in the same way as the intermediate anhydro base is not stabilised. Consistent with this proposal, the 1,3-derivative did not yield a zwitterion under identical reaction conditions. Furthermore, 1,4-dimethylpyridinium iodide does give a zwitterion from reaction with LiTCNQ or TCNQ/piperidine.

The preparation of a related zwitterionic donor-acceptor compound (90) from *N,N,N',N'*-tetramethyl-*p*-phenylene diamine (TMPD) and 7,7,8,8-tetracyanoperfluorop-*p*-quinodimethane (TCNQF₄) was reported by workers at Du Pont.⁷⁶ Reaction of donor TMPD and acceptor TCNQF₄ initially led to the formation of a charge transfer complex of 1:1 stoichiometry. Slow crystal growth of the complex led to isolation of crystals of (90): the single crystal X-ray study of which revealed a dimeric structure.



(90)

The amphiphilic derivatives of P3CNQ (e. g. C₁₆H₃₃-P3CNQ) have been the subject of intense study. The high second order theoretical coefficient of P3CNQ prompted the synthesis of Z-β-(1-hexadecyl-4-pyridinium)-α-cyano-4-styryldicyano-

methanide $C_{16}H_{33}-P3CNQ$ (19). $C_{16}H_{33}-P3CNQ$ was prepared from 1-hexadecyl-4-methylpyridinium bromide and LiTCNQ using the procedure described for P3CNQ.⁷⁴ $C_{16}H_{33}-P3CNQ$ forms a stable LB monolayer up to a surface pressure of 50 mNm^{-1} . From the surface pressure versus surface area isotherm the area per molecule (at $\Pi = 0$) was found to be 100\AA^2 . For $C_{16}H_{33}-P3CNQ$, the face area was calculated to be 100\AA^2 ; therefore, the hydrophilic chromophore must lie face down on the water subphase at $\Pi = 0$. $C_{16}H_{33}-P3CNQ$ forms Z type (non centrosymmetric) films on hydrophilically treated quartz slides. The charge transfer band of $C_{16}H_{33}-P3CNQ$ in acetonitrile occurs at 645nm. The band is blue shifted 150 nm to 495 nm and narrowed HWHM = 27 nm (HWHM = 76 nm - solution spectra) for the LB film.

LB films of $C_{16}H_{33}-P3CNQ$ are photochromic; they are bleached by radiation at wavelengths which overlap the charge transfer bands.⁷⁷ Ashwell et al assign the switching to intramolecular charge transfer from the negatively charged dicyanomethanide acceptor part to the donor (the pyridinium ring). The photochromic switching of $C_{16}H_{33}-P3CNQ$ in solution is shown in Figure 4.1. Photochromically switched solutions of $C_{16}H_{33}-P3CNQ$ slowly recolour through thermal photochromic reversion. Ashwell found that LB films of $C_{16}H_{33}-P3CNQ$ are readily bleached, and the bleached films show no signs of thermal reversion even after one year.

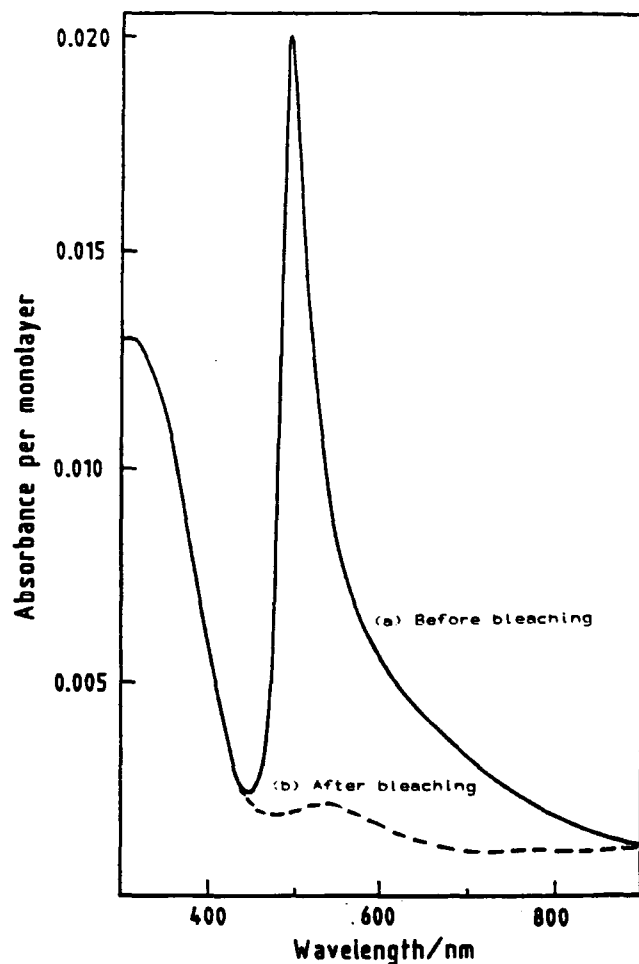
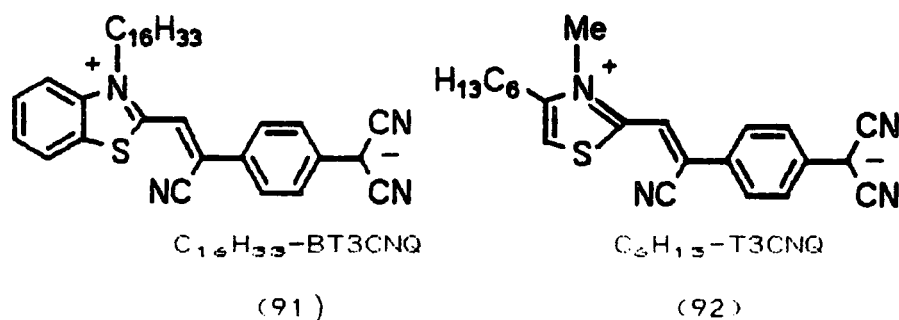


Figure 4.1 : Photochromic switching of C₁₆H₃₃-P3CNQ

LB films of C₁₆H₃₃-P3CNQ and the quinolinium derivative C₁₆H₃₃-Q3CNQ exhibit optical second harmonic generation. Ashwell et al have studied the quadratic non-linear optical properties of mixed films of C₁₆H₃₃-P3CNQ and C₁₆H₃₃-Q3CNQ.⁷⁸ The structure of the mixed films is Z type. This was confirmed by optical SHG measurements - the quadratic dependence of the optical second harmonic intensity with number of LB layers corroborates the non centrosymmetric structure. The charge transfer spectra of heteromolecular LB films show a single transition at a wavelength dependent on the mole fraction of C₁₆H₃₃-Q3CNQ. The charge transfer LB

spectra of heteromolecular films are not the combination of charge transfer LB spectra of $C_{16}H_{33}$ -P3CNQ and $C_{16}H_{33}$ -Q3CNQ. The presence of a single LB charge transfer band for heteromolecular LB films of $C_{16}H_{33}$ -P3CNQ and $C_{16}H_{33}$ -Q3CNQ indicates that mixed films are not phase separated but are an organic alloy.

The successful Z type LB deposition and efficient optical second harmonic generation of films of $C_{16}H_{33}$ -P3CNQ and $C_{16}H_{33}$ -Q3CNQ suggested that the amphiphilic benzothiazolium derivative $C_{16}H_{33}$ -BT3CNQ (91) should show interesting non-linear optical properties. The thiazolium derivative C_6H_{13} -T3CNQ (92) was also identified as a related target molecule, the synthesis of which would clearly be more demanding.

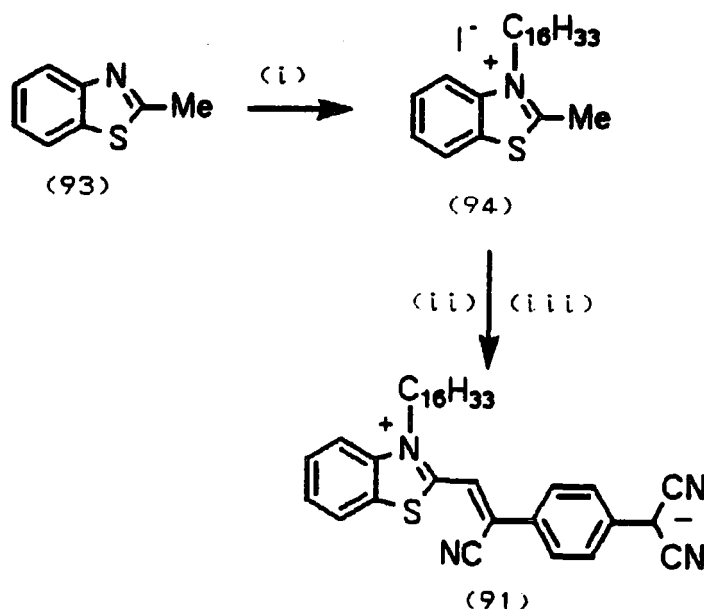


4.2 Synthetic Studies

(i) Z-β-(N-n-Hexadecyl-2-benzothiazolium)-α-cyano-
4-styryldicyanomethanide (91) ($C_{16}H_{33}$ -BT3CNQ)

$C_{16}H_{33}$ -BT3CNQ was prepared as outlined in Scheme 4.2. N-n-

Hexadecyl-2-methylbenzothiazolium iodide (94) was prepared by heating a mixture of 2-methylbenzothiazole (93) with one equivalent of n-hexadecyliodide at 90°C for 48h. Reaction of salt (94) with 7,7,8,8,-tetracyano-p-quinodimethane and N-methylpiperidine gave C₁₆H₃₃-BT3CNQ (91) in 63% yield as green microcrystals. The ionic ground state of C₁₆H₃₃-BT3CNQ is indicated by the IR spectra: a comparison of the cyanide stretching frequencies of C₁₆H₃₃-BT3CNQ (a doublet at 2180 and 2150 cm⁻¹) with those of TCNQ⁰ and TCNQ⁻¹ indicate a zwitterionic structure.

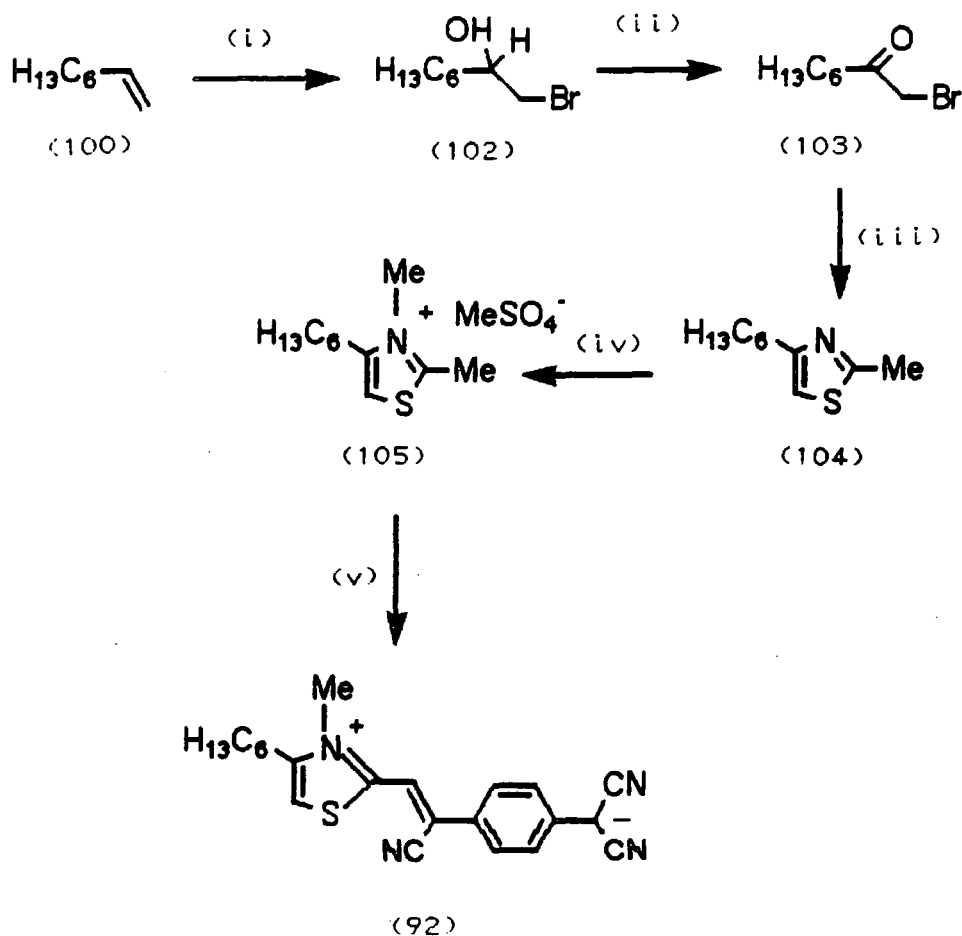


Scheme 4.2 : (i) C₁₆H₃₃I, 90°C; (ii) TCNQ;
 (iii) N-methylpiperidine.

(ii) A range of N-alkyl-BT3CNQ, -benzoxazole and benzoselenazole derivatives (95-99) were prepared and characterised. The spectroscopic and analytical data are summarised in the experimental section.

(iii) Z-β-(N-Methyl-4-hexyl-2-thiazolium)-α-cyano-
4-styryldicyanomethanide (92) (C₆H₁₃-T3CNQ)

The synthetic procedure used to prepare C₆H₁₃-T3CNQ is shown in Scheme 4.3 . Reaction of 1-octene (100) with N-bromosuccinimide in aqueous dimethylsulphoxide gave 1-bromo-2-octanol (102) in 80% yield. Oxidation of the alcohol (102) with acidified sodium dichromate solution gave 1-bromo-2-octanone (103) in 82% yield. 2-Methyl-4-hexylthiazole (104) was prepared from 1-bromo-2-octanone (103) and thioacetamide in refluxing ethanol by the method of Hantsch. A mixture of 2-methyl-4-hexylthiazole (104) and one molar equivalent of dimethylsulphate was heated at 90°C for 1h to afford 2,3-dimethyl-4-hexylthiazolium methylsulphate (105) as a purple oil. Reaction of salt (105) with the lithium salt of TCNQ in refluxing acetonitrile gave green microcrystals of C₆H₁₃-T3CNQ (92) in 72% yield.



Scheme 4.3: (i) NBS/DMSO/H₂O; (ii) K₂Cr₂O₇/H₂SO₄;
 (iii) MeCSNH₂; (iv) (MeO)₂SO₂/90°C;
 (v) LiTCNQ/N-methylpiperidine.

4.3 Langmuir Blodgett Deposition Of C₁₆H₃₃-BT3CNQ (91)

The film forming properties of C₁₆H₃₃-BT3CNQ were investigated using a two-compartment Nima Technology LB trough. Monolayers of (91) were spread from solutions of

$C_{16}H_{33}$ -BT3CNQ in aristar dichloromethane onto the pure water subphase (MilliQ, 18M Ω) of one compartment (A) which was isolated from the second compartment (B) by a surface barrier. $C_{16}H_{33}$ -BT3CNQ forms a stable monolayer; the surface pressure versus surface area isotherm is shown in Figure 4.2. At a surface pressure (Π) greater than 50 mNm $^{-1}$ the film collapses. LB films of $C_{16}H_{33}$ -BT3CNQ were transferred onto hydrophilically treated quartz slides at a surface pressure of 25 mNm $^{-1}$ at the rate of 0.15 mm Sec $^{-1}$.

4.4 LB UV-VIS Spectra And Optical Second Harmonic Generation

The UV-VIS LB spectrum of freshly deposited films of $C_{16}H_{33}$ -BT3CNQ show absorptions at 568 nm and at 652 nm (broad) with corresponding absorbances per monolayer of ca. 0.007 and 0.012. The absorbances at 568 nm and 652 nm are assigned to intramolecular (IRCT) and intermolecular (INCT) charge transfer bands, respectively, by comparison with the Kramers-Kronig transformed single-crystal absorption spectrum of the pyridinium analogue Z- β -(1-methyl-2-pyridinium)- α -cyano-4-styryldicyanomethanide (82). The structure of the deposited LB film of $C_{16}H_{33}$ -BT3CNQ is thermally unstable; after annealing at 50°C for \approx 4h there is a marked change in the UV-VIS spectra compared with the pristine film. The intramolecular charge transfer band fades while the intermolecular band is enhanced (absorbance per monolayer = 0.012) and sharpened (HWHM = 22 nm). The UV-VIS LB spectra of monolayers of pristine and annealed films of $C_{16}H_{33}$ -BT3CNQ

are shown in Figure 4.3 . As mentioned previously (Section 3.4), the quinolinium analogues R-Q3CNO show either an IRCT band ($R \geq C_{15}H_{31}$) or an INCT band ($C_6H_{13} \leq R \leq C_{14}H_{29}$) but not both. The UV-VIS LB spectra of R-Q3CNQ are dependant on molecular tilt and, therefore, for $C_{16}H_{33}$ -BT3CNQ the change upon heating may be attributed to a change in molecular orientation.

Langmuir Blodgett multilayers of $C_{16}H_{33}$ -BT3CNQ have a Y type structure (centrosymmetric) and optical second harmonic generation has been observed for odd numbers of layers. The intensity of the second harmonic varies with the number of laser pulses for an LB monolayer of $C_{16}H_{33}$ -BT3CNQ (Figure 4.4 . For freshly deposited films, the second harmonic intensity is negligible for the initial laser pulses, while for subsequent pulses the second harmonic intensity increases to 10-30% of the value for monolayer LB films of quinolinium zwitterions $C_{16}H_{33}$ -Q3CNQ and the hemicyanine dye (5). This variation in the second harmonic intensity may be explained by (i) a change in LB structure (the initial increase) and (ii) laser damage (the subsequent decrease). The pulses of IR radiation ($1.064\mu\text{m}$) probably cause a change in the film structure so that the second harmonic intensity is resonantly enhanced by the proximity of the increasing IRCT band at 564 nm.

Figure 4.2 : Surface pressure (Π) versus surface area isotherm for $C_{16}H_{33}$ -BT3CNQ.

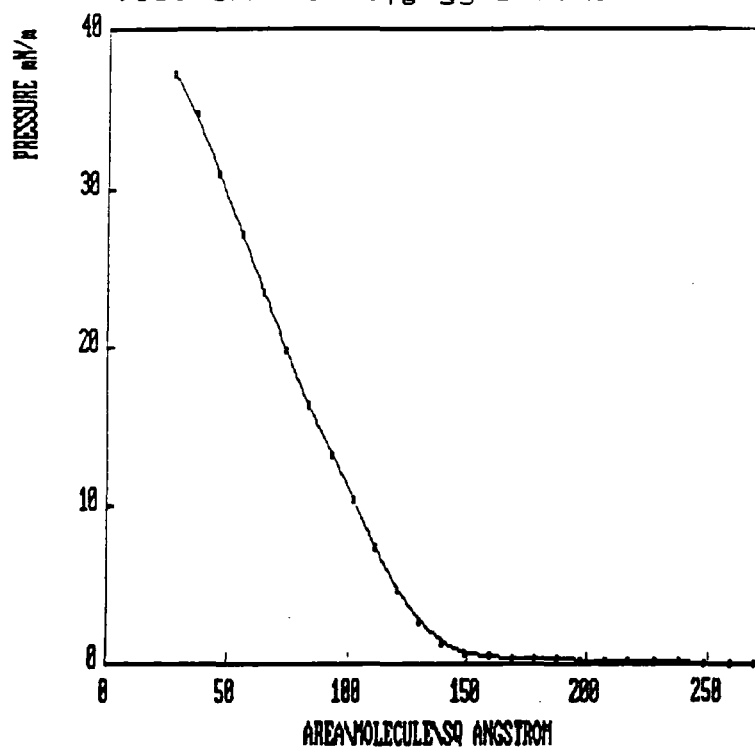


Figure 4.3 : UV-VIS LB spectra of monolayers of $C_{16}H_{33}$ -BT3CNQ.
(a) Ca. 5 min after deposition.
(b) After annealing at $50^{\circ}C$ for $\approx 4h$.

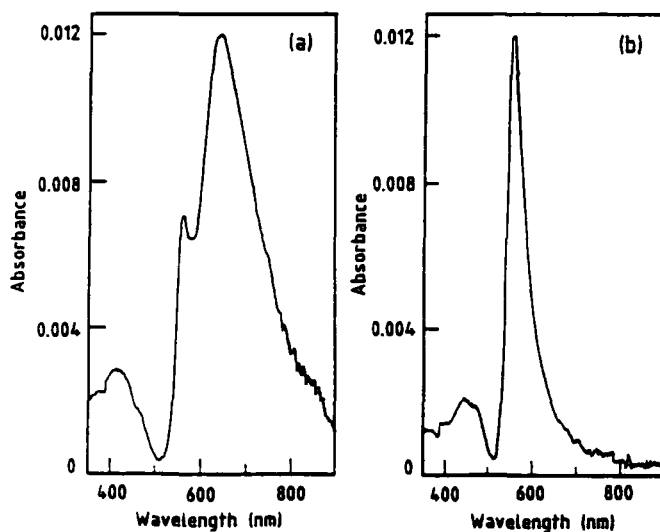
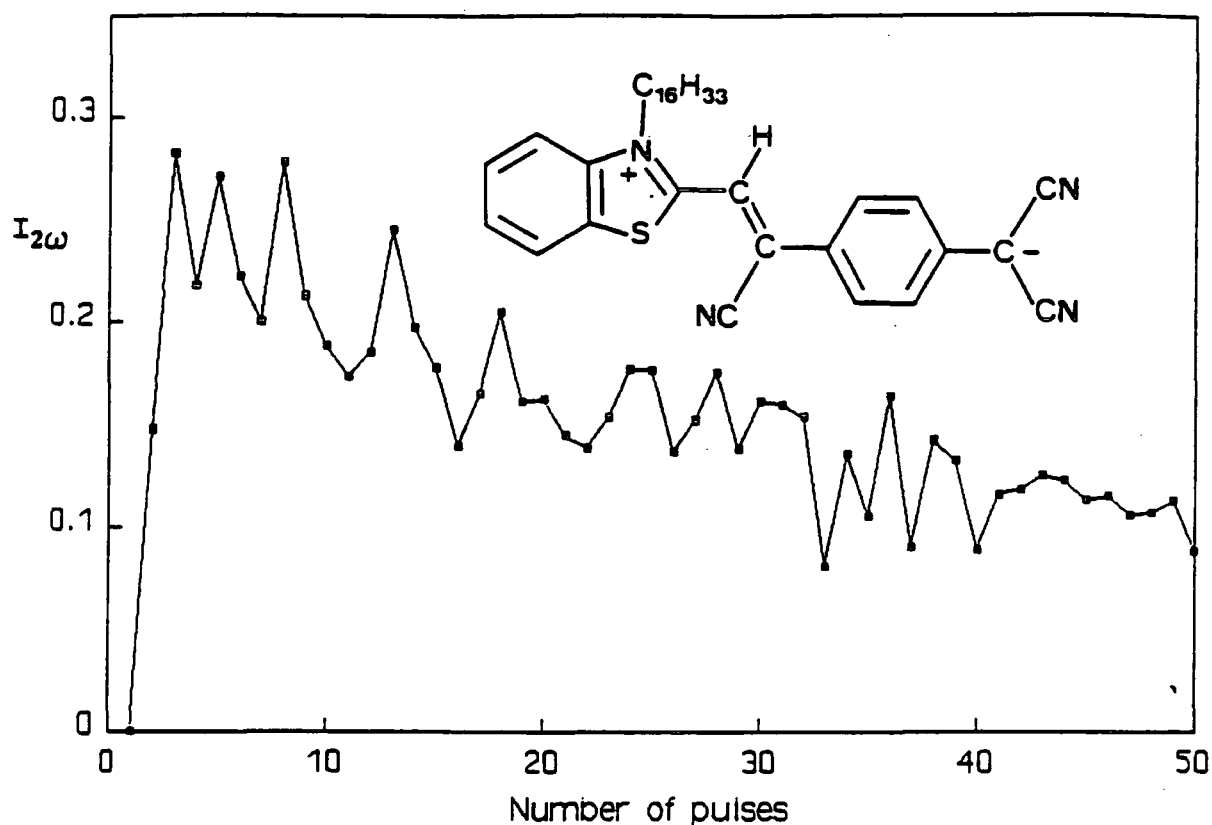


Figure 4.4 : Variation of the SH intensity with the Nd:YAG laser pulses. The signal intensity for the $C_{16}H_{33}$ -BT3CNQ film is relative to the intensity from a monolayer of hemicyanine (5).



4.5 Langmuir Blodgett Deposition Of $C_{16}H_{33}$ -T3CNQ (92)

Monolayers of $C_{16}H_{33}$ -T3CNQ were spread from solutions of $C_{16}H_{33}$ -T3CNQ in aristar chloroform onto the pure water subphase (MilliQ, 18 Ω) of compartment (A). The surface

pressure (Π) versus surface area isotherm was obtained on compressing the monolayer at $100 \text{ cm}^2 \text{ min}^{-1}$ (Figure 4.5). The compressed film is stable up to a surface pressure of $\approx 40 \text{ mNm}^{-1}$. At surface pressures above this the film begins to collapse. LB films of $\text{C}_6\text{H}_{13}\text{-T3CNQ}$ were transferred onto hydrophilically treated glass slides at a surface pressure of 30 mNm^{-1} . Transfer ratios were close to 100%.

4.6 LB UV-VIS Spectra And Optical Second Harmonic Generation

The UV-VIS LB spectrum of freshly deposited monolayers of $\text{C}_6\text{H}_{13}\text{-T3CNQ}$ shows an absorption at 482 nm with an absorbance per monolayer of 0.0446 (HWHM = 15 nm). The UV-VIS spectrum of a monolayer of $\text{C}_6\text{H}_{13}\text{-T3CNQ}$ is shown in Figure 4.6 . LB multilayers of $\text{C}_6\text{H}_{13}\text{-T3CNQ}$ can be successfully deposited onto hydrophilically treated glass slides. The UV-VIS LB spectrum of a 5 layer film of $\text{C}_6\text{H}_{13}\text{-T3CNQ}$ is shown in Figure 4.8 . The spectrum shows the expected absorbance increase of the band at 482 nm in accordance with the number of layers deposited.

Single pulse SHG measurements were performed using a Nd:YAG laser ($\lambda = 1.064 \mu\text{m}$; pulse width, 10 ns ; pulse energy, $< 1 \text{ mJ}$) with the beam at an angle of 45° to the film. SHG measurements were performed on monolayer and five layer films of $\text{C}_6\text{H}_{13}\text{-T3CNQ}$. No measurable second harmonic signal was obtained from a monolayer of $\text{C}_6\text{H}_{13}\text{-T3CNQ}$ even at high laser powers. Similarly, the five layer LB film of $\text{C}_6\text{H}_{13}\text{-T3CNQ}$ gave no observable second harmonic signal at low or high laser powers.

Figure 4.5 : Surface pressure (Π) versus area isotherm for $C_6H_{13}-T3CNQ$.

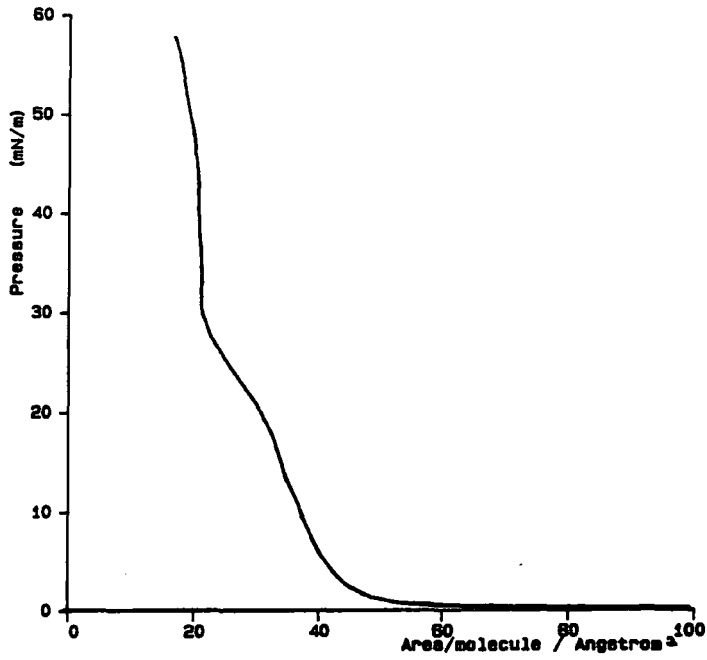
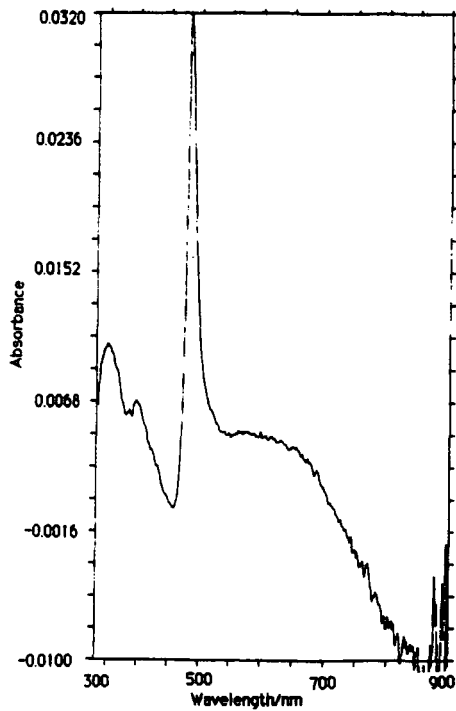
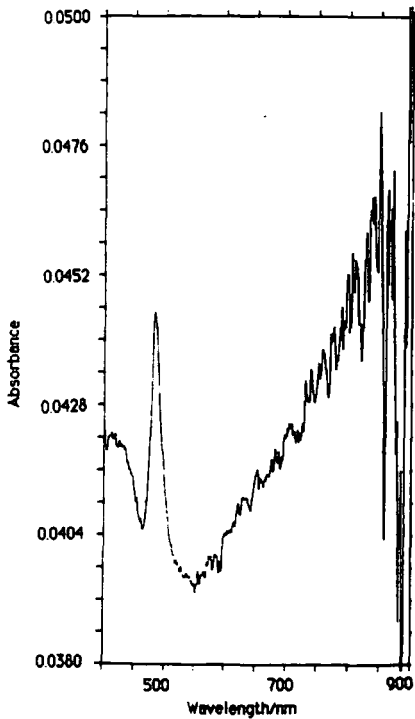


Figure 4.6 : (a) Monolayer UV-VIS LB spectrum of $C_6H_{13}-T3CNQ$.

(b) UV-VIS LB spectrum of 5 layers of $C_6H_{13}-T3CNQ$.

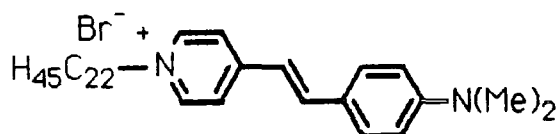


CHAPTER FIVE

SYNTHESIS, LB DEPOSITION AND NLO PROPERTIES
OF SOME NEW HEMICYANINE DERIVATIVES

5.1 Introduction

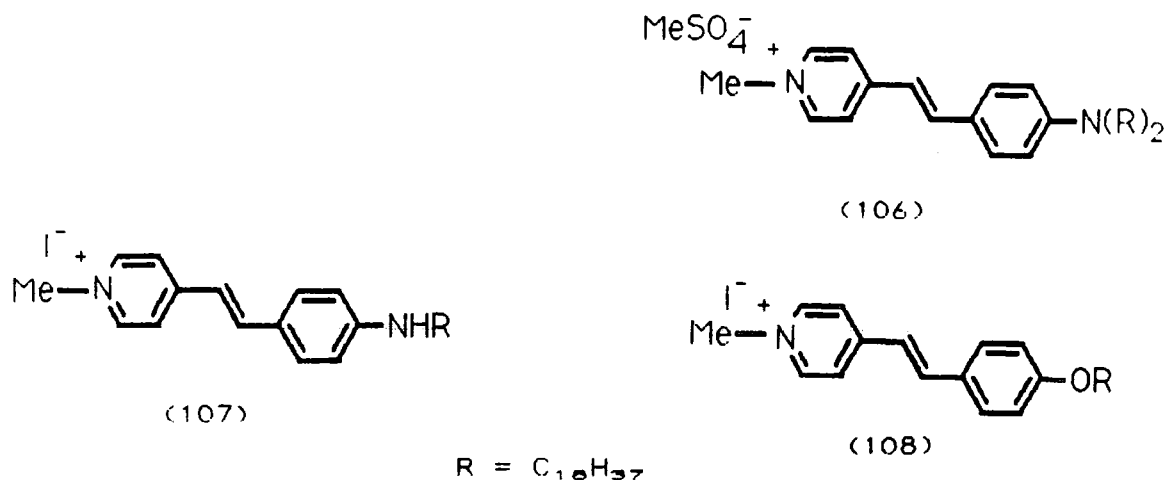
Accentric Langmuir Blodgett films represent promising approaches to high-efficiency SHG materials.⁷⁹ One of the earliest reports, by Girling *et al.*, of optical SHG from a Langmuir Blodgett multilayer concerned 1-docosyl-4-[2-(dimethylaminophenyl)ethenyl]pyridinium bromide (5).²⁹



(5)

This hemicyanine derivative (5) was deposited in monolayer and multilayer films and the second order optical properties investigated. Langmuir Blodgett multilayers of hemicyanine (5) have a Y type structure (centrosymmetric). Monolayers of derivative (5) exhibit SHG: the signal diminishes for the bilayer and all even number of layers. The incorporation of a spacer layer in the chromophore layers allows accentric alignment of the amphiphiles. The spacer molecule used for the hemicyanine derivative (5) was ω -tricosenoic acid. For LB multilayers of alternate layers of (5) and ω -tricosenoic acid, the observed second harmonic intensity was found to increase superlinearly and not quadratically with the number of layers.

The second harmonic non-linear optical properties of hemicyanine analogues, (106) and (107), have been studied.^{50, 51}



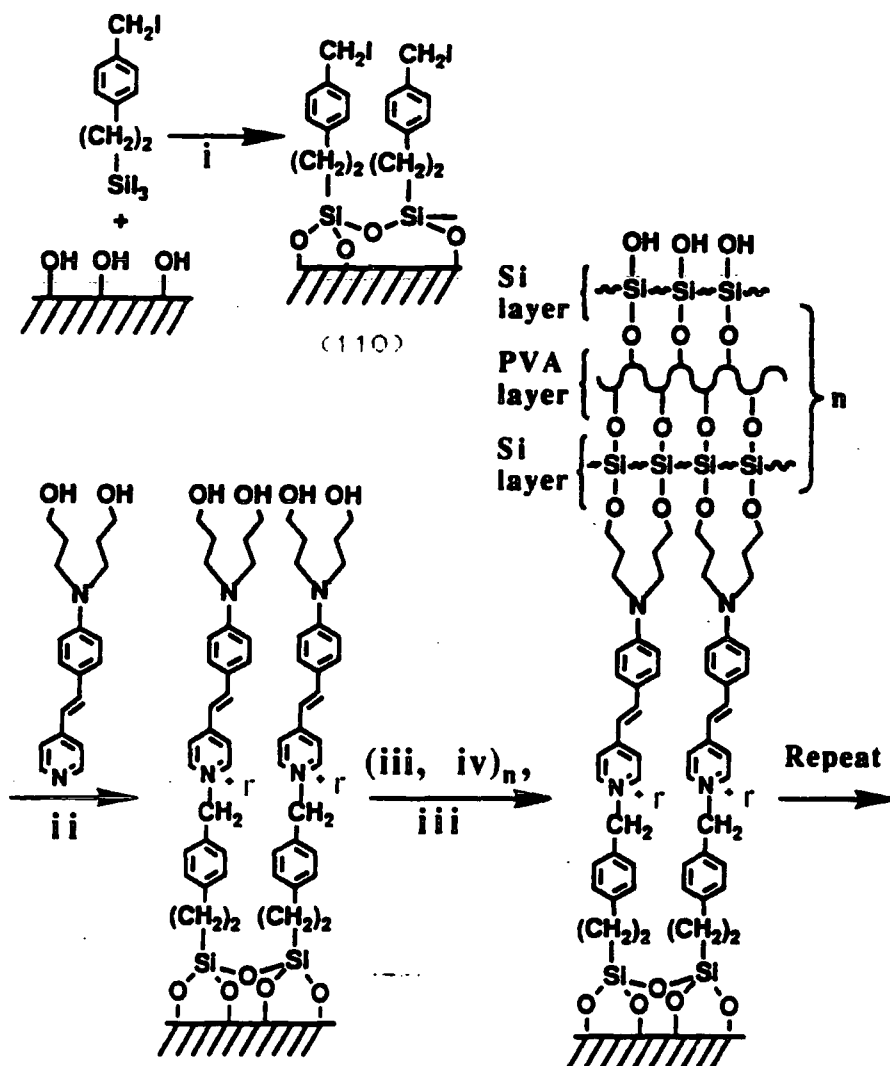
Monolayers of the hemicyanine dye (106) were deposited by the LB technique onto quartz slides. Optical second and third harmonic generation has been observed from the monolayers. The optical second order hyperpolarisability (β) was found to be 2.1×10^{-27} esu; for hemicyanine derivative (5) a value of 0.2×10^{-27} esu has been reported. The increase in β is assigned to the more charge-asymmetric configuration and hence stronger $\pi-\pi^*$ absorption band which is centred at 418 nm.

Monolayers of the hemicyanine derivative (107) deposited onto glass slides were found to exhibit strong SHG when irradiated by a Nd:YAG laser. An enhanced optical second harmonic signal for (107) was observed as compared to hemicyanine derivative (5). An SHG intensity of 110 ± 10 a.u. (arbitrary units) was observed for derivative (107) and

for the hemicyanine (5) an SHG intensity of 15 ± 5 a.u. The increase for the N-stilbazene (107) was unexpected. In the same report, the O-stilbazene derivative (108) was shown to form monolayers on glass which gave an SHG intensity of 12 ± 2 a.u, compared to 15 ± 5 a.u for hemicyanine derivative (5). The authors assign the SHG increase for the N-stilbazene (107) to resonant enhancement. LB multilayers of (107) and (108) have a Y type structure; no SHG signals from bilayers of these materials is consistent with this assignment.

Recently there have been reports of attempts to obtain non centrosymmetric thin films of hemicyanine derivatives.⁶² One novel approach to thin film production involves a self-assembly technique initially developed by Sagiv.⁶³ The synthetic strategy for the formation of self-assembled layers of the stilbazolium chromophore precursor (109) is shown in Scheme 5.1 . Reaction of hydroxyl groups on the silicate surface with triiodosilane gives the initial substrate-bound intermediate (110). Quaternisation enables the introduction of self-assembled chromophores with high second order coefficients (β). Finally, a multilayered polymer backbone consisting of two silicon layers and an internal PVA layer is introduced transverse to the chromophore stacking direction. The polymer layer is added to enhance structural stability.

Scheme 5.1 : The self-assembly of stilbazolium chromophores.



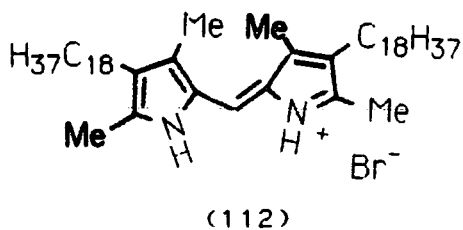
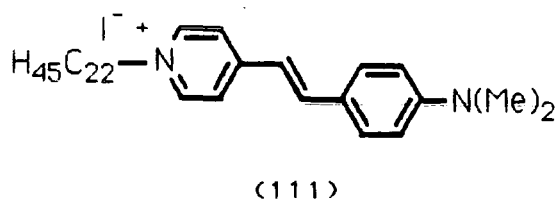
Conditions: (i) benzene, 25 °C; (ii) reflux in *n*-PrOH; (iii) $\text{Cl}_3\text{Si-O-SiCl}_2\text{OSiCl}_3$ in THF; (iv) poly(vinyl alcohol) in DMSO.

The resulting self-assembled layer has an architecture where the chromophores are aligned to form an H aggregate and anchored at the donor and acceptor ends. The self-assembled films were found to adhere strongly to glass and are insoluble in the majority of organic solvents.

Optical SHG measurements of multilayers of the self-assembled chromophores were carried out using a Nd:YAG laser. No in-plane anisotropy was observed from films rotated about the film normal. This indicates that the chromophores are aligned uniaxially about the substrate normal and that there is a high degree of order in the films. This is corroborated by the almost complete destructive interference of SHG from a sample with monolayers on each face of the glass substrate. From the SHG data an average orientation angle (ψ) between the chromophores and the substrate normal was found to be approximately $31-39^\circ$. The macroscopic second order coefficient ($\chi_{2z, z, z}$) was found to be 2×10^{-7} esu for the superlattice film. The optical SH intensity increased quadratically with the number of layers and is consistent with the non centrosymmetric alignment.

The use of spacer layers in LB multilayers of hemicyanines to increase the optical SHG efficiency has had only limited success. An exciting recent development is a report by Ashwell et al of the highest observed second harmonic intensity from a multilayer Langmuir Blodgett film.²⁴ They have studied the SHG properties of films of the hemicyanine dye (111) and the salt (112). The new

hemicyanine derivative (111) with the iodide counterion was found to give an optical SH intensity two to four times that of the hemicyanine standard (5) (bromide counterion).



The new amphiphilic spacer group (112) was found to give LB films with the hemicyanine dye (111) where the N-docosanyl chain of (111) interdigitates with N-octadecyl chains of the spacer group (112). The arrangement may be viewed as a "molecular zip". Low angle X-ray diffraction provides evidence of the interdigitation. A d spacing of 43\AA is 18\AA shorter than the calculated Van der Waals length of 61\AA . Optical SHG measurements on interleaved LB films were carried out. The second harmonic intensity [relative to hemicyanine (5)] was found to increase quadratically with the number of bilayers. A 200 layer film gave a second harmonic intensity 18,300 times the docosylhemicyanine value.

Recent work shows the continued importance of hemicyanines in non-linear optics; therefore new derivatives are attractive synthetic targets. The synthesis, LB

deposition and NLO properties of some hemicyanines containing the benzothiazolium group was, therefore, undertaken and the results are reported here.

5.2 Synthetic Studies

(1) C₁₈-Hemicyanines (113a-113d)

The hemicyanines were prepared as shown in Scheme (5.2). 4-Aminobenzonitrile (114) and 1-bromooctadecane in hexamethylphosphoramide at 120°C yielded 4-octadecyl aminobenzonitrile (115) as a white solid (84 %). Treatment of the nitrile (115) with 1.1M diisobutylaluminium hydride in toluene solution yielded 4-octadecylaminobenzaldehyde (116) in 76% yield.²⁵ Condensation of aldehyde (116) with N-alkyl-2-methyl iodide salts (117a-117e) in refluxing ethanol in the presence of a catalytic amount of piperidine gave new hemicyanine amphiphiles (113a-113d) in 80-87% yield.

(2) C₆-Hemicyanine (118)

The salt (105) was prepared as previously described; reaction with p-N,N-dimethylaminobenzaldehyde in the presence of piperidine gave 2-[2'-(4-dimethylaminophenyl)ethenyl]-4-n-hexylthiazolium methylsulphate (118) in 60% yield.

Scheme 5.2: (i) C₁₈H₃₇Br; (ii) DIBAL/toluene

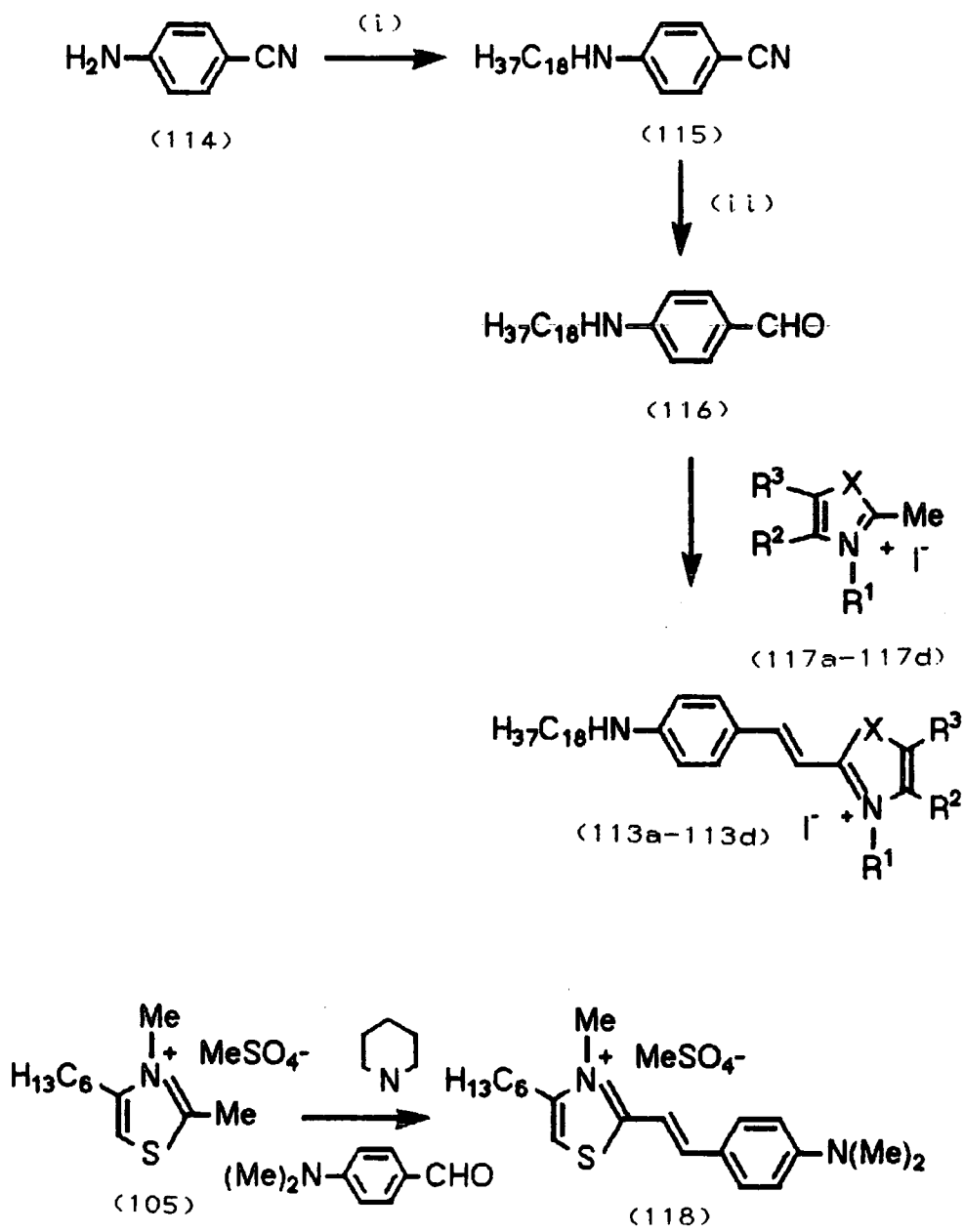


Table 5.1 : Hemicyanines prepared as outlined in
Scheme 5.2

Compound	R ¹	R ²	R ³	X	Yield(%)
(113a)	Me	-CH=CH-CH=CH-		S	84
(113b)	C ₁₆ H ₃₃	-CH=CH-CH=CH-		S	82
(113c)	Me	-CH=CH-CH=CH-		O	80
(113d)	Me	Me	H	S	87

5.3 Langmuir Blodgett Alignment Of C₆-Hemicyanine (118)

A Nima technology two compartment LB trough was used to investigate the film forming properties of the C₆-hemicyanine (118). A 1.0 mg ml⁻¹ solution of C₆-hemicyanine (118) in aristar dichloromethane was spread on the pure water subphase of compartment (A). The amphiphile did not form a stable monolayer; the material was soluble in the water subphase and therefore unsuitable for LB deposition. Hence monolayer SHG of C₆-hemicyanine (118) could not be studied.

5.4 Langmuir Blodgett Deposition of Hemicyanine (113a) and Hemicyanine (113b)

Ultrasound was used to enhance dissolution of hemicyanine (113a) and hemicyanine (113b) in aristar dichloromethane. Clear solutions were obtained by filtration. The solutions were spread on a pure water

subphase (MilliQ, 18M Ω) of compartment (A) which was isolated from the second compartment (B) by a surface barrier. The surface pressure versus surface area isotherm of hemicyanine (113a) is shown in Figure 5.1. The monolayer of hemicyanine (113a) is stable up to a surface pressure of 60 mNm⁻¹; above this pressure the film collapses. The surface pressure versus surface area isotherm of hemicyanine (113b) is shown in Figure 5.2. A plateau at 30 mNm⁻¹ is observed which is associated with a molecular reorganisation. On compression at surface pressures greater than 30 mNm⁻¹, there is a further rapid decrease in area per molecule until 50 mNm⁻¹ where film collapse is observed. The molecular area (at $\Pi = 0$) where the surface pressure increases is 200-210 Å² for the initially compressed film, whereas on recompression this value is reduced to 130-140 Å². It is possible that the molecular reorganisation may involve reorientation of one alkyl chain so that the monolayer is more densely packed.

Monolayers of hemicyanine (113a) and hemicyanine (113b) were transferred by withdrawal of the hydrophilic substrate through the subphase-LB film interface. Substrates were glass slides pre-treated by (i) acetone wash (ii) ultrasound in water (30 min.) (iii) ultrasound in 2-propanol (30 min.) (iv) immersion in 30% w/v hydrogen peroxide solution (24h.) (v) pure water wash (vi) dried by blowing with nitrogen. Monolayers of hemicyanine (113a) and hemicyanine (113b) were transferred at 30 mNm⁻¹. Transfer ratios were close to 100%.

Figure 5.1 : Surface pressure versus surface area isotherm for hemicyanine (113a).

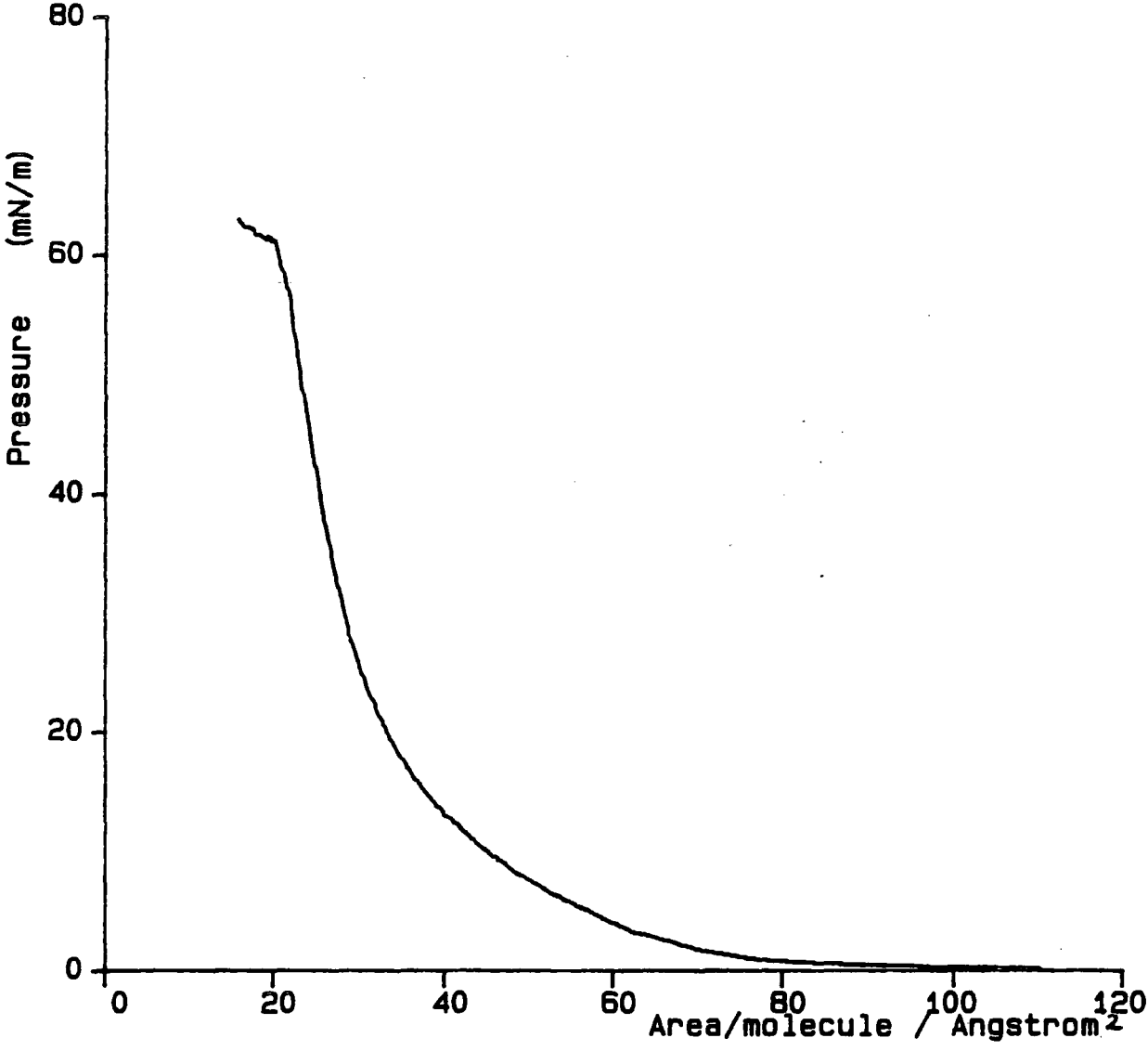


Figure 5.2 : Surface pressure versus surface area isotherm of hemicyanine (113b) (a) Initial compression (b) Recompression.

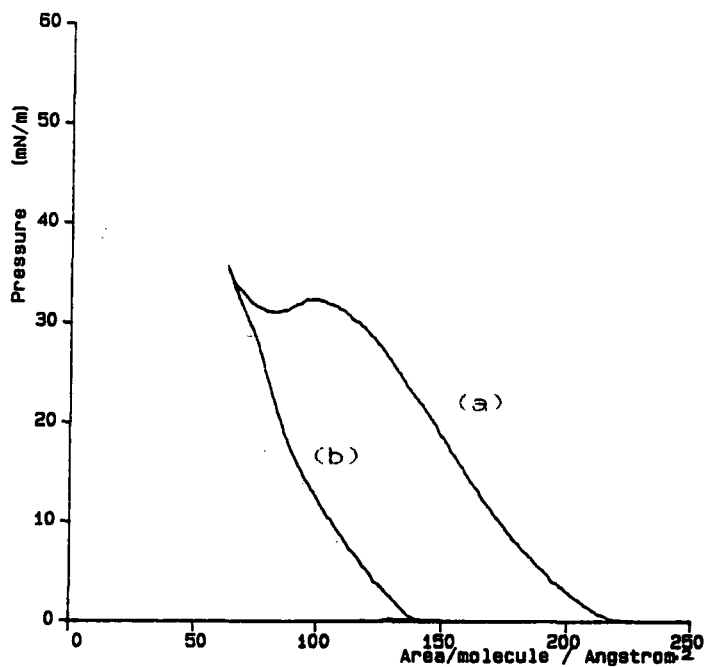


Figure 5.3: UV-VIS solution spectra in aristar dichloromethane (a) hemicyanine (113a). (b) hemicyanine (113b).

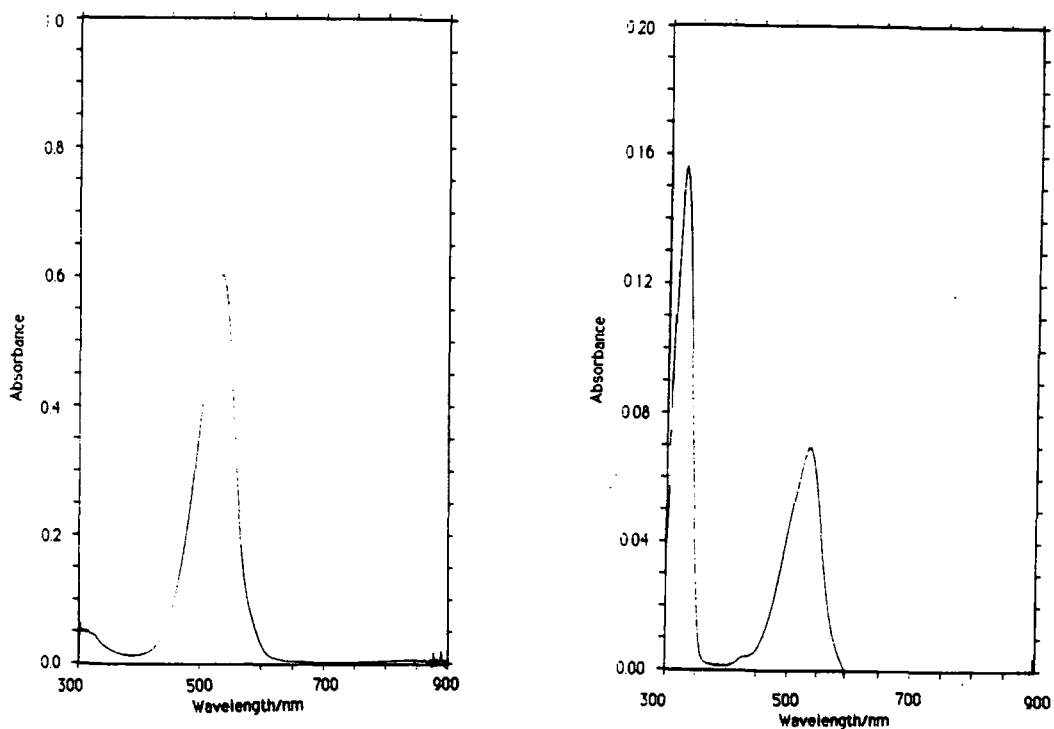
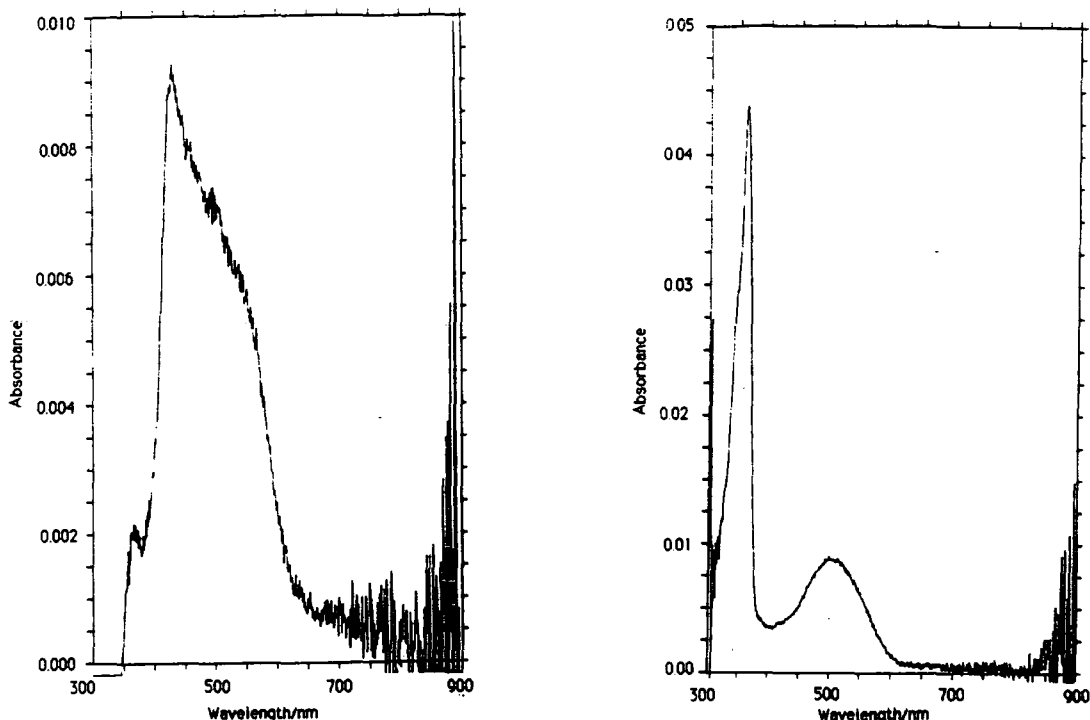


Figure 5.4: UV-VIS Langmuir Blodgett spectra of

(a) Monolayer hemicyanine (113a) deposited at $\Pi = 31 \text{ mN Mm}^{-1}$

(b) Monolayer hemicyanine (113b) deposited at $\Pi = 31 \text{ mN Mm}^{-1}$



5.5 UV-VIS Solution And LB Spectra

Monolayers of hemicyanine (113a) and hemicyanine (113b) were successfully transferred onto hydrophilically treated glass slides as judged by monolayer/multilayer UV-VIS spectra. The solution spectra of hemicyanine (113a) and hemicyanine (113b) in aristar dichloromethane are shown in Figure 5.3. A single band centred at 531 nm (HWHM = 70 nm) is present in solution spectra of both hemicyanine (113a) and hemicyanine (113b). An additional band centred at 326 nm (HWHM = 31 nm) was observed in the spectrum of hemicyanine (113b).

The UV-VIS LB monolayer spectrum of hemicyanine (113a)



is shown in Figure 5.4. In the LB spectrum the CT band is shifted to 430 nm ($\Delta\lambda = 101$ nm). For hemicyanine (113b) the LB UV-VIS spectrum contains bands at 480 nm (HWHM = 121 nm) and 361 nm (HWHM = 30 nm) and for this compound the shift in the CT band is reduced ($\Delta\lambda = 11$ nm), and the intensity is reduced compared to the band at 361 nm.

5.6 Optical Second Harmonic Generation

Single pulse SHG measurements were carried out using a Nd:YAG laser with the p-polarised beam incident to the substrate at 41°. Optical SHG measurements were performed on monolayers/multilayers of hemicyanine (113a) and hemicyanine (113b). The intensity of the second harmonic signal is compared to that from the hemicyanine dye (5). Monolayers of hemicyanine (113a) were found to give optical second harmonic intensities ca. 3.8 times that for monolayer hemicyanine (5). For monolayer hemicyanine (113b) the optical SH intensity was found to be ca. 2.3 times that for monolayer hemicyanine (5). Langmuir Blodgett multilayers of hemicyanine (113a) and hemicyanine (113b) have a Y type structure (centrosymmetric) and optical SHG has been observed for odd numbers of layers.

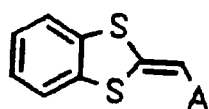
CHAPTER SIX

SYNTHESIS, LB DEPOSITION AND NLO PROPERTIES
OF CHROMOPHORES WITH THE 1,3-DITHIOLE DONOR GROUP

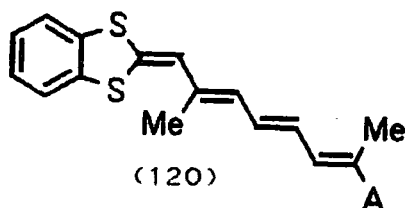
6.1 Introduction

The quadratic hyperpolarisability of amphiphilic D- π -A materials is currently of great interest.⁶⁶ The 1,3-dithiole heterocycle has received only little attention as a donor in D- π -A materials. This is surprising since this heterocycle has been the centre of much attention within the field of organic metals. The synthesis and electrochemistry of 1,3-dithiole donor derivatives is well developed and understood.⁶⁷

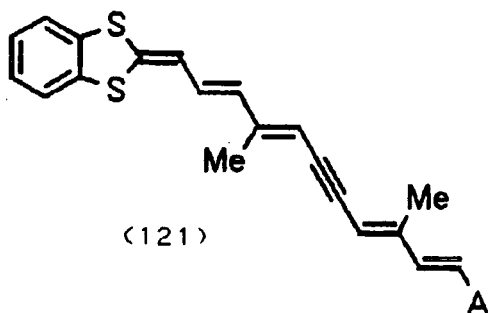
Lehn *et al* made a systematic study of the quadratic non-linearities of push pull polyenes.⁶⁸ They studied the NLO properties of polyenes with the benzodithiole donor group e.g. (119a-119f), (120a-120f), (121a-121f) and (122a-122f).



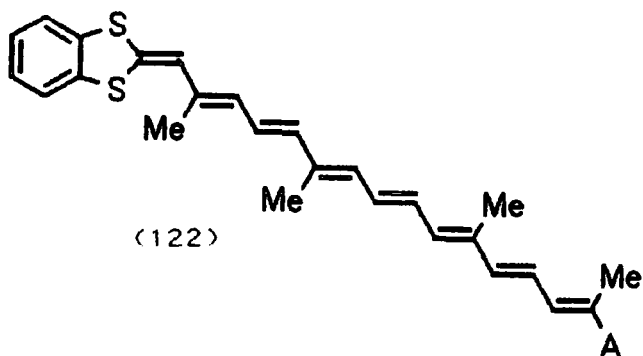
(119)



(120)

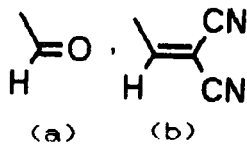


(121)



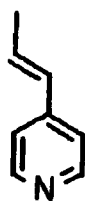
(122)

A =



(a)

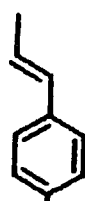
(b)



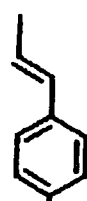
(c)



(d)



(e)



(f)

Their aim was to study two effects which are known to significantly enhance the molecular hyperpolarisability (8):

- an increase in the length of the conjugated system between the donor and acceptor groups.⁸⁹
- an increase in the charge-asymmetry between the ground and first excited states through altering the donor and acceptor groups.⁹⁰

Lehn et al studied the bulk second harmonic efficiencies of compounds (119-122), (a-f) by the Kurtz Powder Technique (described earlier pp 11). The results are shown in Table 6.1.

Table 6.1 : Relative powder efficiencies of compounds (119-122), (a-f). All measurements relative to SHG efficiency of powdered urea for irradiation at 1.06 μm (left) and 1.32 μm (right). f = two-photons fluorescence; ϵ = SHG efficiency between KDP (Potassium Dihydrogen Phosphate) and urea; - not measured.

	(119)		(120)		(121)		(122)	
(a)	-	0	f	0	f	0	0	0
(b)	-	0	ϵ	0	-	0	0	0
(c)	f	0	5	0	10	30	12	13
(d)	0	0	ϵ	0	ϵ	0	-	0
(e)	f	0	f	0	f	0		
(f)	1	13	0	0	0	0		

Their aim was to study two effects which are known to significantly enhance the molecular hyperpolarisability (β);

- an increase in the length of the conjugated system between the donor and acceptor groups.⁸⁹
- an increase in the charge-asymmetry between the ground and first excited states through altering the donor and acceptor groups.⁹⁰

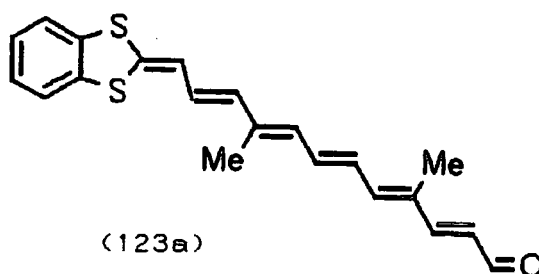
Lehn et al studied the bulk second harmonic efficiencies of compounds (119-122), (a-f), by the Kurtz Powder Technique (described earlier pp 11). The results are shown in Table 6.1.

	(119)		(120)		(121)		(122)	
(a)	-	0	f	0	f	0	0	0
(b)	-	0	ϵ	0	-	0	0	0
(c)	f	0	5	0	10	30	12	13
(d)	0	0	ϵ	0	ϵ	0	-	0
(e)	f	0	f	0	f	0		
(f)	1	13	0	0	0	0		

Table 6.1 : Relative powder efficiencies of compounds (119-122), (a-f). All measurements relative to SHG efficiency of powdered urea for irradiation at 1.06 μm (left) and 1.32 μm (right). f = two-photons fluorescence; ϵ = SHG efficiency between KDP (Potassium Dihydrogen Phosphate) and urea; - not measured.

One difficulty in interpreting powder SHG measurements is that the technique measures only a convolution of SHG signals and SHG annihilation effects on the bulk powder sample can effect the results.⁹¹ Taking these effects into consideration the results obtained indicate that the materials (119-122), (a-f) are good candidates for further optical studies e.g electric field induced second harmonic generation (EFISH) measurements and incorporating into organised assemblies. SHG signals more intense than that of urea were observed for compounds in the series b, c, d and f. The relative SHG powder efficiencies of series c are large and efficiency is dependant on the conjugation length between donor and acceptor.

An EFISH study of the push-pull carotenoids has recently been reported.⁹² The derivatives (119a-122a) were studied together with the previously unreported polyene (123a).



The molecular quadratic hyperpolarisabilities (β) determined by the EFISH experiments are given in Table 6.2.

For the series (119a-123a) a progressive red shift of the charge transfer band occurs on increasing the conjugation

length. An enhancement of the quadratic hyperpolarisability (β) occurs on lengthening the polyene chain.

Table 6.2 : Optical second order molecular hyperpolarisabilities determined at $1.32\mu\text{m}$ in chloroform. a. 10^{-40} esu.

Molecule	$\lambda_{\text{max}}/\text{nm}$	$\mu. \beta (2\omega)^1$	$\mu. \beta (0)^1$
(119a)	372	30	20
(120a)	456	1200	570
(121a)	466	2200	1000
(122a)	500	7250	2800
(123a)	485	2700	1100

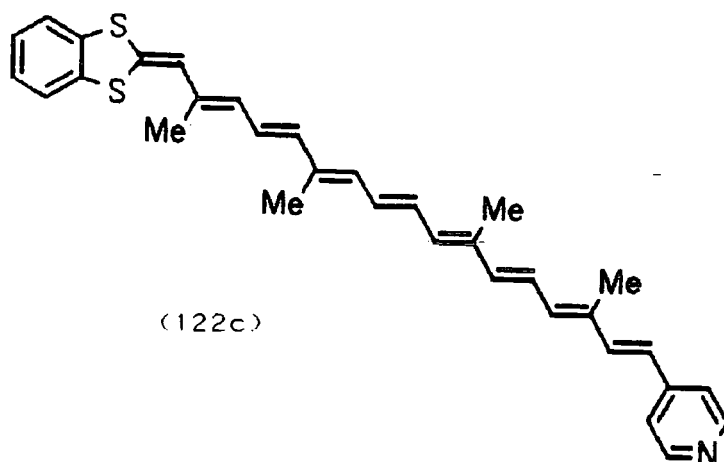
The off-resonance values of the second order molecular hyperpolarisability (β_0) are large, e.g for compound (122a) $\mu. \beta$ is equal to 7250×10^{-40} esu (Cf 4-nitroaniline $\mu. \beta = 293 \times 10^{-40}$ esu⁷³). The off-resonance second order molecular hyperpolarisability, β_0 , for derivatives (119a-123a) may be approximated by equation (6.1).

$$\beta_0 \propto n^2 \dots (6.1)$$

where n = number of double bonds in the polyene chain.

The approximate square dependence is in agreement with the reported experimental results for other polyene systems.⁷⁴

For series (119a-123a) the equation (6.1) is obeyed for $n < 10$. In a later report, Lehn et al studied Langmuir Blodgett films built from mixtures of the carotenoid benzodithia-9-polyene-pyridine (122c) and ω -tricosenoic acid.⁹⁵



The carotenoid (122c) does not give a stable monolayer on the water subphase of a Langmuir Blodgett trough. The pure film was found to collapse below 10 mNm^{-1} . The surface pressure area isotherm displayed a plateau at 18 mNm^{-1} associated with a molecular reorganisation. The films were found to collapse at a pressure higher than 45 mNm^{-1} .

The orientation of the polyene chain in the film of (122c) was studied by UV-VIS linear dichroism.⁹⁶ The results suggest that the carotenoid is oriented perpendicular to the substrate in LB films and therefore the films are promising candidates for optical SHG. The authors suggest that the low wavelength of the π - π^* transition is a result of the formation of an ordered parallel aggregation of molecules of (122c) (H aggregate) which are formed at a surface pressure

of 18 mNm^{-1} corresponding to the plateau on the Π -A isotherm.

The NLO properties of donor- π -acceptor compounds (124) and (125) have been studied by the EFISH technique²⁷. The derivatives were prepared by Wittig condensations of the reagent (126) with 4-tricyanovinylbenzaldehyde and 4-nitrobenzaldehyde. The results of the EFISH measurements are given in Table 6.3.

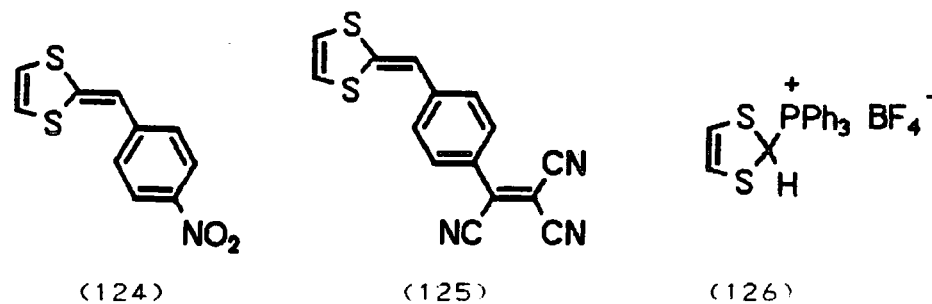


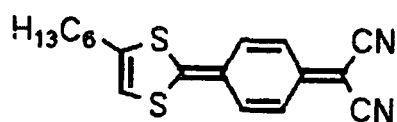
Table 6.3 : Quadratic non-linear optical susceptibilities (β , β_0), dipole moments and electronic transition energies (E) of push pull derivatives. 1. $10^{-30} \text{ cm}^3 \text{ esu}^{-1}$. 2. D. 3. eV. 4. determined at $1.58 \mu\text{m}$.

Compound	β'	β'	μ^2	E^0
(127)	21	12	7.1	3.07
(124)	52	25	6.9	2.71
(125) ⁴	$\beta \cdot \mu = 1200$			2.06

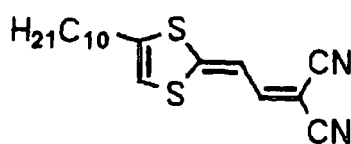
The EFISH measurements of $\beta \cdot \mu$ were obtained in Me_2SO solution. The value of β_0 , which can be used to compare the NLO properties between molecules, is independent of transition energy and, thus, the value is not greatly affected by resonance enhancement.

The nitrophenyl derivative (124) has a β value ($52 \times 10^{-30} \text{ cm}^5 \text{ esu}^{-1}$) of the order of the prototypical *p*-*N,N*-dimethylaminonitrobenzene (127) ($21 \times 10^{-30} \text{ cm}^5 \text{ esu}^{-1}$). The derivative (125) gives an intense second harmonic and a $\beta \cdot \mu$ value of $1200 \times 10^{-30} \text{ cm}^5 \text{ esu}^{-1}$ which is an order of magnitude higher than (127). The dipole moment of (125) was not measured due to its poor solubility and hence a value of β could not be obtained. It is clear that amphiphilic derivatives of (125) would be promising materials for optical second harmonic generation in Langmuir Blodgett films.

In this chapter the results of synthesis, Langmuir Blodgett alignment and optical SHG studies of the new amphiphilic donor- π -acceptor derivatives (128) and (129) are described.



(128)



(129)

The large second order molecular hyperpolarisability of derivative (125) and the benzodithiolenylidene derivatives (119), suggested that long chain chromophores with the 1,3-dithiolenylidene

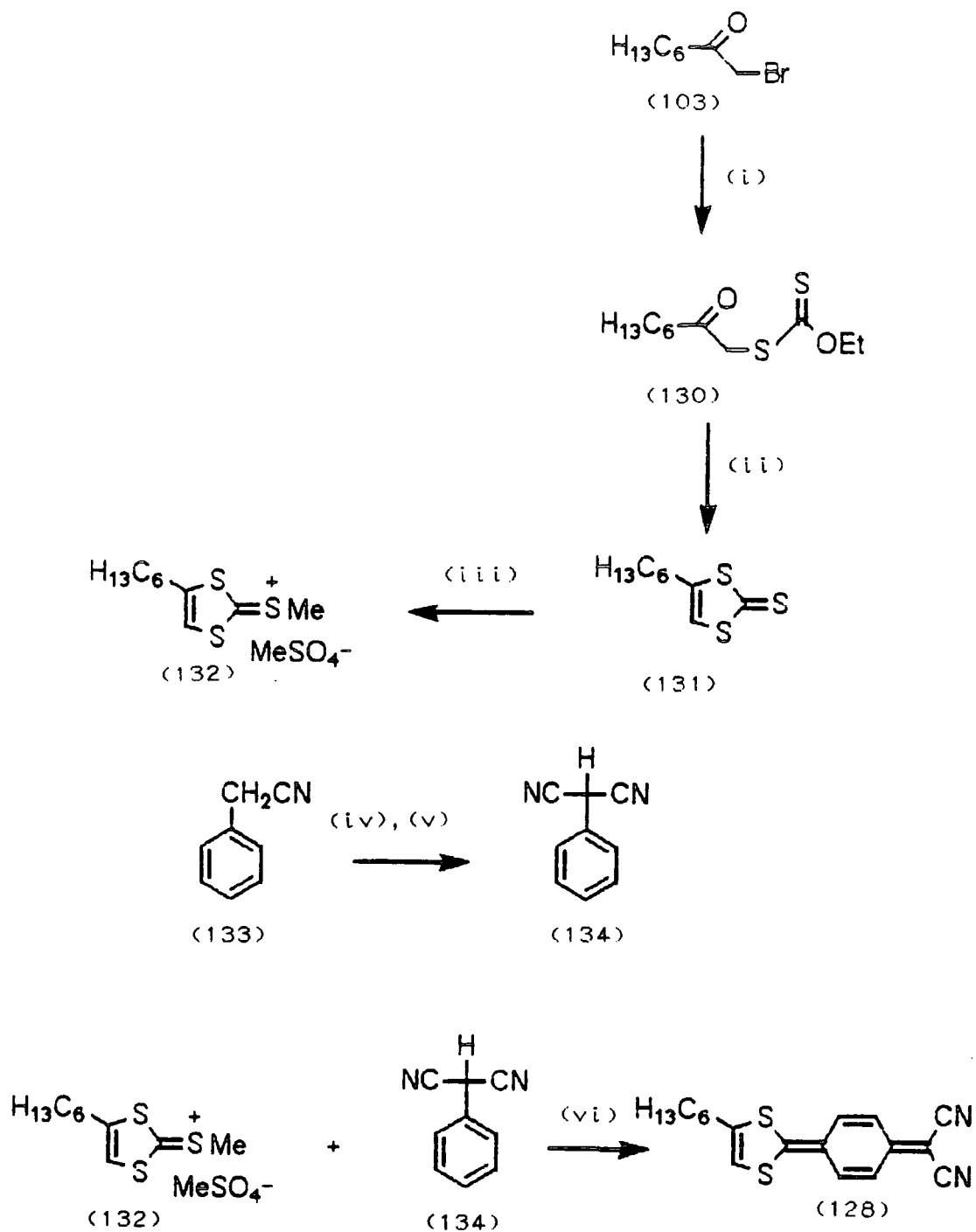
donor group linked to a dicyanomethylene acceptor group (e.g. (128) and (129)) may be promising NLO materials.

6.2 Synthesis

(i) 4-(n-Hexadecyl)-2-(4-dicyanomethylene-2,5-cyclohexadiene)-1,3-dithiole (128)

The synthetic route to (128) is shown in Scheme 6.1. 1-Bromo-2-octanone (103) was prepared as previously described. Reaction of (103) with potassium ethyl xanthate in refluxing ethanol gave O-ethyl-1-xanthioctan-2-one (130) in high yield. 4-Hexyl-1,3-dithiole-2-thione (131) was prepared from the dithiocarbonate derivative (130) and phosphorus pentasulfide in refluxing toluene. A solution of thione (131) and one equivalent of dimethylsulphate was heated at 90°C; this yielded 2-methylthio-4-n-hexyl-1,3-dithiolium methylsulphate (132) in 45% yield.

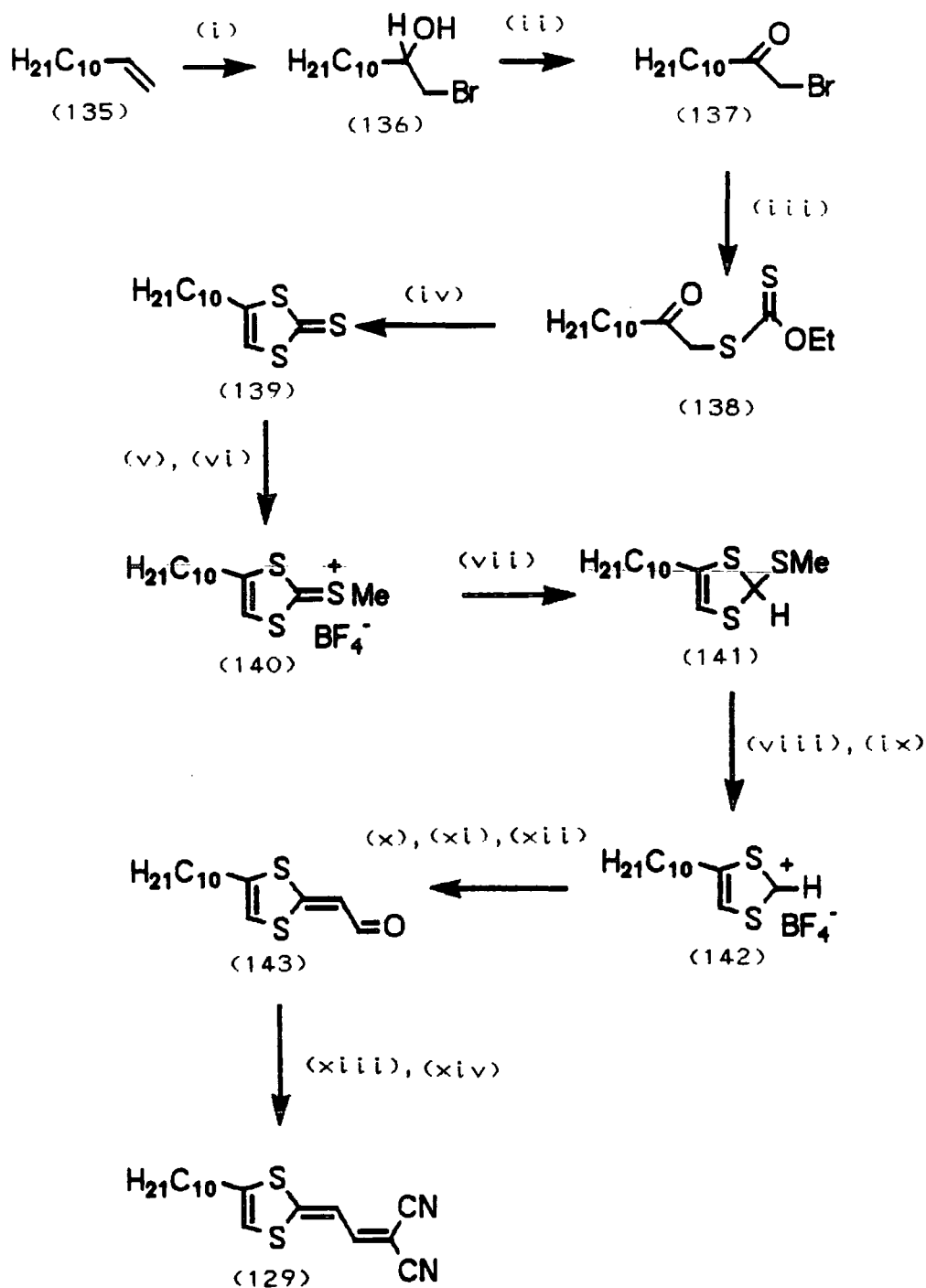
Phenylmalononitrile (134) was prepared by the route described by Cava *et al.*⁹⁶ Treatment of benzylnitrile (133) with one equivalent of LDA then 2-chlorobenzylthiocyanate gave compound (134) after an acidic work up. The push pull chromophore (128) was prepared in 85% yield by coupling 4-n-hexyl-1,3-dithiolium methylsulphate (132) with phenylmalononitrile (134).



Scheme 6.1 : (i) $\text{EtCOS}_2\text{-K}^+$, acetone, reflux; (ii) P_2S_5 , toluene, reflux; (iii) $(\text{MeO})_2\text{SO}_2$, 90°C ; (iv) LDA; (v) 2-chlorobenzylthiocyanate; (vi) pyridine/glacial acetic acid 3/1 (v/v)

(ii) 4-(n-Dodecyl)-2-(dicyanomethylenemethylene)
-1,3-dithiole (129)

The synthetic route to (129) is shown in Scheme 6.2. Salt (140) was prepared from 1-dodecene in 20% overall yield by an analogous route (Scheme 6.2) described above for the synthesis of the C₆ analogue. Salt (140) was then reduced with sodium borohydride in ethanol to give 2-methylthio-4-(n-dodecyl)-2H-1,3-dithiole (141). Treatment of (141) with acetic anhydride, followed by tetrafluoroboric acid diethyletherate, gave tetrafluoroborate salt (142) in 83% yield. Aldehyde (143) was prepared by an analogous route to that developed by Yoshida.⁹⁹ Treatment of salt (142) with tributylphosphine followed by aqueous glyoxal and triethylamine gave the aldehyde (143). Knoevenagel condensation of aldehyde (143) with malononitrile and piperidine gave the target dicyanomethylated push pull amphiphile (129) in 38 % yield.



Scheme 6.2: (i) NBS/DMSO/H₂O; (ii) Na₂Cr₂O₇/H₂SO₄; (iii) EtCOS₂⁻K⁺, acetone; (iv) P₂S₅, toluene; (v) (MeO)₂SO₂; (vi) HBF₄·Et₂O; (vii) NaBH₄, ethanol; (viii) Ac₂O; (ix) HBF₄·Et₂O; (x) PBu₃; (xi) 40 wt% aqueous glyoxal; (xii) triethylamine; (xiii) CH₂(CN)₂; (xiv) piperidine.

6.3 Langmuir Blodgett Films Of Chromophores (128) and (129)

A systematic investigation of the film forming properties of the 1,3-dithiole derivatives (128) and (129) was carried out using a two compartment Nima Technology LB trough. Solutions of the chromophores in anisole, dichloromethane or chloroform, were spread on the pure water subphase (MilliQ, 18M Ω) of one compartment (A) which was isolated from the second compartment (B) by a surface barrier.

A volume of 50 μ l of a 0.30 mgml⁻¹ solution of (128) was spread on the pure water subphase of compartment (A). The surface pressure versus surface area isotherm for (128) is shown in Figure 6.1. The amphiphile forms a stable monolayer which collapses at a low surface pressure (π 30 mNm⁻¹). Films of (129) were deposited onto hydrophilically treated glass slides at a surface pressure of 30 mNm⁻¹.

The UV-VIS solution spectrum of amphiphile (128), displays absorptions at 594 nm and 645 nm with half width at half maximum (HWHM) of 50 and 35 nm, respectively (Figure 6.3). The UV-VIS LB monolayer spectrum of (128) is markedly different to the solution spectrum. There is a diminution of peaks at 594 nm and 645 nm and the appearance of an absorption at 411 nm (HWHM = 10 nm). The UV-VIS solution spectrum of (129), with absorptions at 228, 347 and 542 nm, is shown in Figure 6.3. The monolayer LB UV-VIS spectrum is shown in Figure 6.4. Peaks present in the solution spectrum are absent in the LB spectra and an absorption at 287 nm

(HWHM = 20 nm) appeared. Therefore amphiphiles (128) and (129) have LB spectra where there is a window at the second harmonic (532 nm) and optical SHG measurements are, therefore, not affected by resonance enhancement.

6.4 Optical Second Harmonic Generation

SHG measurements were carried out using the apparatus previously described (Section 3.6). The mean second harmonic intensity is compared with the corresponding signal from an LB monolayer of the hemicyanine dye (5).

By comparison with other chromophores with the 1,3-dithiole donor group, which show large second order nonlinearities (e.g (119), (125)), the amphiphiles (128) and (129) should possess high second order coefficients. Remarkably, monolayers of (128) deposited at a surface pressure of 30 mNm⁻¹ show no optical SHG even at high laser powers. Similarly, monolayers of the amphiphile (129) which were deposited at 25 mNm⁻¹ did not give any observable second harmonic signal at low and high laser powers.

Figure 6.1 : Surface pressure (Π) versus surface area isotherm of (128).

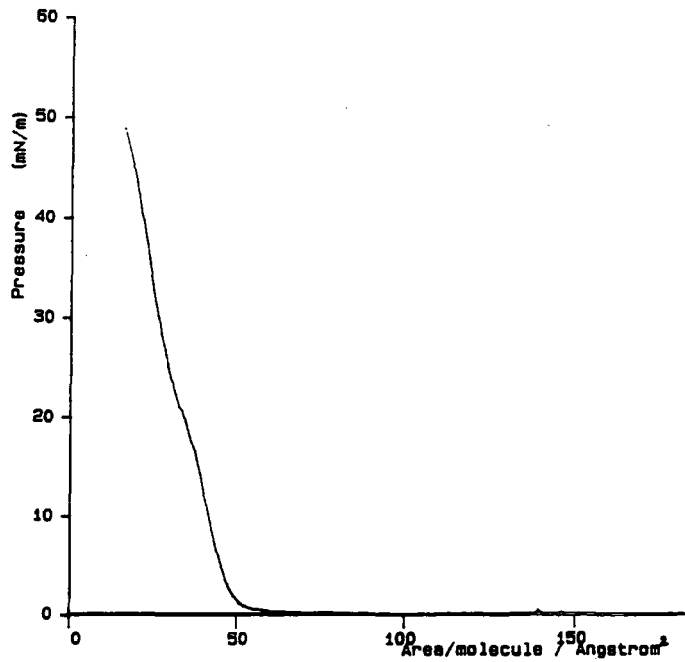


Figure 6.2 : Surface pressure (Π) versus surface area isotherm of (129).

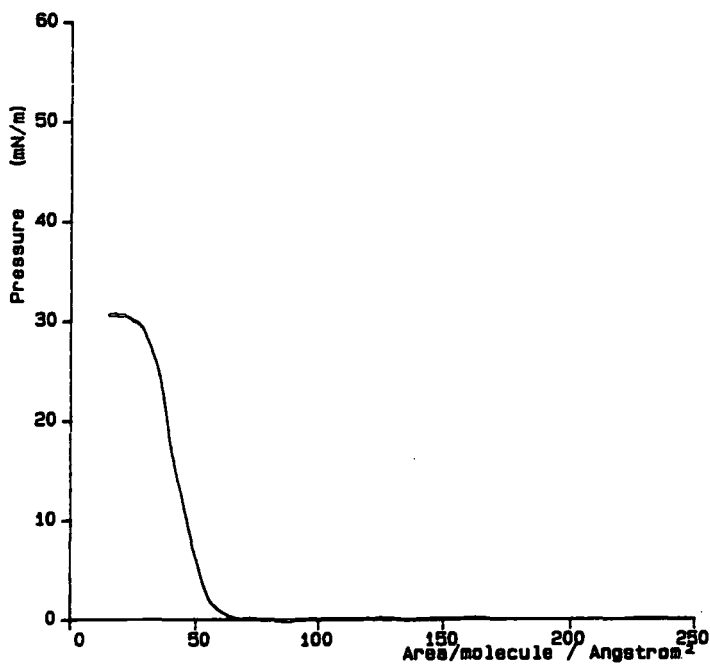


Figure 6.3 : UV-VIS solution spectra in aristar
dichloromethane (a) amphiphile (128).
(b) amphiphile (129).

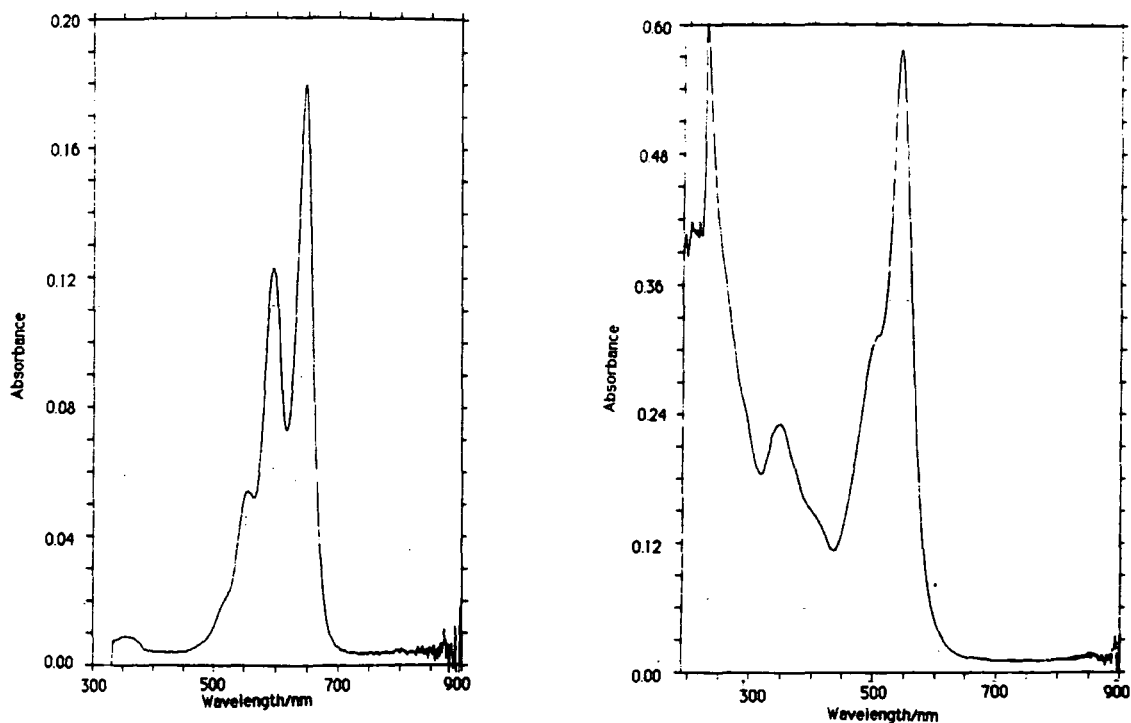
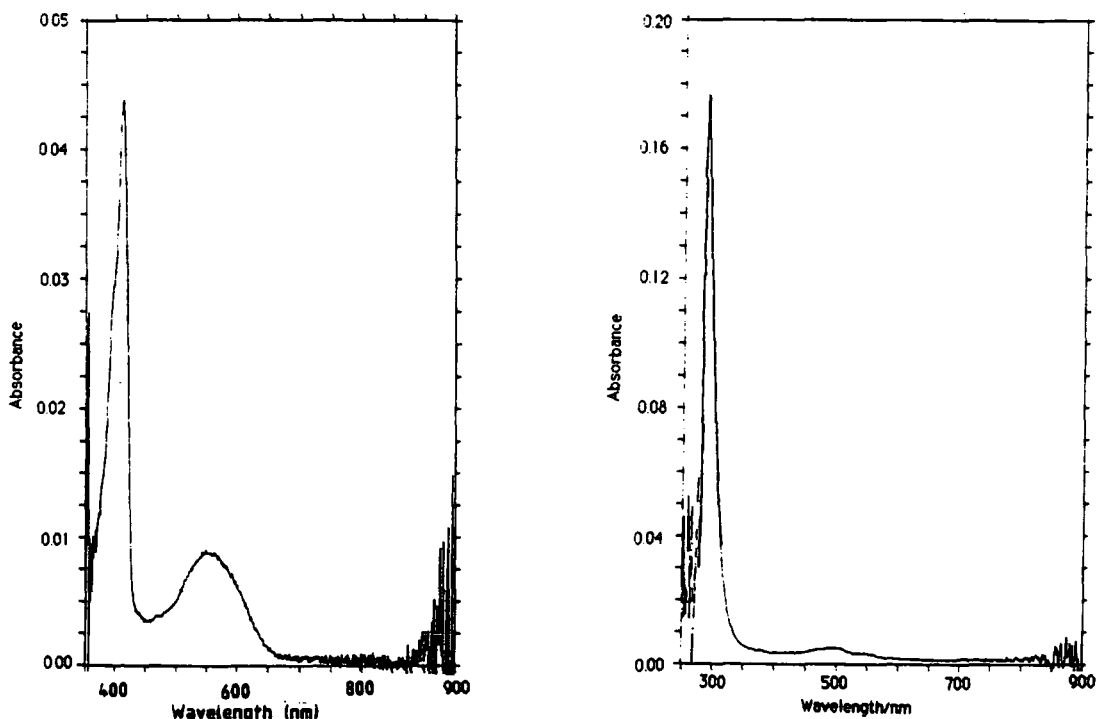


Figure 6.4 : UV-VIS Langmuir Blodgett spectra of
(a) Monolayer amphiphile (128) deposited at $\Pi = 25 \text{ mNm}^{-1}$
(b) Monolayer amphiphile (129) deposited at $\Pi = 30 \text{ mNm}^{-1}$



CHAPTER SEVEN

EXPERIMENTAL

7.1 GENERAL METHODS

Mass spectra were obtained on a VG 7070E instrument operating at 70eV. Infrared spectra were recorded on Perkin Elmer 577 and 457 spectrophotometers. Melting points were recorded on a Kofler hot-stage microscope apparatus and are uncorrected. Proton NMR were recorded on a Bruker AC250 instrument (250.133MHz) and a Perkin Elmer R-24B instrument (60MHz). Chemical shifts are relative to tetramethylsilane (TMS) and are given in ppm.

Cyclic Voltammograms (CV) were obtained on a BAS 100 electrochemical analyser. The CV cell consisted of Ag/AgCl reference electrode, platinum working electrode with tetrabutylammonium perchlorate (TBAP, $2 \times 10^{-2}M$) electrolyte in dichloromethane or acetonitrile.

7.2 EXPERIMENTAL TO CHAPTER 2

7.2.1 Methyl-2,5-di(bromomethyl)benzoate (63f)

Methyl-2,5-dimethylbenzoate (62f) (5.53g, 0.034mol), N-bromosuccinimide (13.5g, 0.075 mol) and azobisisobutyronitrile (0.3g) were mixed in dichloromethane (60ml) and refluxed for 2h. Standard aqueous work up afforded compound (63f) (7.2g, 66%) as a white solid. Mpt. 81-83°C (from methanol); EI m/e : 324 (M^+); Analysis found: C, 37.8; H, 3.1; Br, 49.9. Calculated for $C_{10}H_{10}Br_2O_2$: C, 37.3; H, 3.1; Br, 49.6%; IR ν_{max} (KBr): 1725, 1445, 1290, 1092, 997 and 920 cm^{-1} ; δH (250MHz, $CDCl_3$) 7.95 (s, 1H), 7.40 (s, 2H), 4.95 (s, 2H), 4.39 (s, 2H) and 3.95 (s, 3H) ppm.

7.2.2 Methyl-2,5-di(cyanomethyl)benzoate (64f)

Compound (63f) (4.6g, 0.014mol) and sodium cyanide (4.5g, 0.09mol) were suspended in a mixture of dioxane (30ml) and water (30ml) and stirred vigorously for 24h at 20°C. Solvent was partially removed *in vacuo* and the solid product collected by filtration, washed with water, dried and recrystallised from methanol to yield compound (64f) (2.6g, 84%) as a white solid. Mpt. 98-99°C; EI m/e : 214 (M^+); Analysis found: C, 67.5; H, 4.7; N, 13.0. Calculated for $C_{12}H_{10}N_2O_2$: C, 67.3; H, 4.7; N, 13.1%; IR ν_{max} (KBr): 2290, 1724,

1460, 1444, 1300, 1098, 1000 and 961 cm^{-1} ; δH (60MHz, CDCl_3): 7.95 (s, 1H), 7.55 (s, 2H), 4.08 (s, 2H), 3.90 (s, 3H) and 3.74 (s, 2H) ppm.

7.2.3 Preparation of TCNQ Derivatives Using 2-Chlorobenzylthiocyanate

7.2.3.1 General Procedure

The reactions were performed in dry benzene and under an atmosphere of nitrogen. A solution of di(cyanomethyl) compound (64) in benzene was added dropwise over 0.5h to a stirred solution of lithium diisopropylamide (LDA) (4 equivalents) in benzene at 0-5°C. A solution of 2-chlorobenzylthiocyanate (4 equivalents) in benzene was then added dropwise over 20min. The solution was stirred at 0-5°C for 4h, extracted with water and the aqueous extract acidified with concentrated hydrochloric acid. Bromine (ca. 4 equivalents) was added to the stirred aqueous suspension which was stirred until all the TCNQ had precipitated (typically 24-48h). The product was collected by filtration, dried and purified by silica column chromatography or recrystallisation. There was thus obtained:

7.2.3.2 *2,5-Dichloro-TCNQ* (41c) as yellow crystals (38% yield). Mpt. 305-307°C (dec.) (from acetonitrile) [lit. 305°C (dec.)].

7.2.3.3 *2,5-Dibromo-TCNQ (41d)* as orange crystals (40% yield). MPt. 315°C(dec.) (from acetonitrile) [lit⁵⁴ 316-318°C(dec.)].

7.2.3.4 *2,5-Dimethoxy-TCNQ (41e)* as a red powder (38% yield). MPt. 300-305°C(dec.) (from 1,1,2-trichloroethane) [lit⁵⁴ 300-305°C(dec.)].

7.2.3.5 *2-Methoxycarbonyl-TCNQ (41f)* as a yellow solid (35% yield). MPt. 224-226°C(dec.) (from acetonitrile); EI m/e : 262 (M^+); Analysis found: C, 64.2; H, 2.5; N, 21.3. Calculated for $C_{14}H_6N_4O_2$: C, 64.1; H, 2.3; N, 21.4%; IR ν_{max} (KBr): 2220, 1725, 1435, 1295, 1195 and 1084 cm^{-1} ; δ_H (60MHz, $CDCl_3$): 8.4-7.6(m, 3H) and 4.2(s, 3H) ppm.

7.2.3.6 *11,11,12,12-Tetracyano-1,4-naphthoquinodimethane (67)* as golden crystals (45% yield) (from dichloromethane/petroleum ether, after column chromatography on silica, eluant dichloromethane/cyclohexane 9:1 v/v). MPt. 216-218°C [lit¹⁰⁹ 244-245°C(dec.)].

7.2.3.7 *11,11,12,12-Tetracyano-2,7-naphthoquinodimethane (69)* as a purple powder (ca. 20% yield). MPt. >350°C (from acetonitrile) [lit¹¹⁰ >365°C].

7.2.3.8 *1-Cyanomethyl-4-(dicyanomethyl)tetrachlorobenzene (70)* as a white powder (14% yield). MPt. 236-238°C from

acetonitrile; EI m/z : 317 (M^+); Analysis found : C, 41.2; H, 0.8; N, 13.1; Cl, 43.9. Calculated for $C_{11}H_5N_3Cl_4$: C, 41.4; H, 0.9; N, 13.2; Cl, 44.5%; IR ν_{max} (KBr): 2940, 2240, 2220, 1580, 1460, 1340, 1210, 1020, 870 and 850cm^{-1} ; δH (250MHz, CDCl_3) 6.08 (s, 1H) and 4.18 (s, 2H) ppm.

7.2.4 Preparation of Mono(dicyanomethylated)-p-benzoquinones

7.2.4.1 General Procedure

To a solution of the substituted p-benzoquinone, in dichloromethane, was added titanium tetrachloride followed by a solution of pyridine and malononitrile in dichloromethane. The mixture was stirred, typically, at 25°C for 24h. The reaction mixture was poured onto water, the organic layer separated, dried (MgSO_4) and the solvent removed *in vacuo*. The crude residue was purified, where necessary, by silica column chromatography or fractional sublimation.

7.2.4.2 1-Oxo-4-dicyanomethylene-2,5-cyclohexadiene (74h)

The quinomethide (74h) was prepared from 1,4-cyclohexanedione monoethylene ketal by the method of Hyatt.¹⁰¹

7.2.4.3 *1-Oxo-2,3,5,6-tetramethyl-4-dicyanomethylene-2,5-cyclohexadiene (74m)*

To a solution of 2,3,5,6-tetramethyl-p-benzoquinone (73m) (400mg, 2.4mmol) in dichloromethane (25ml) was added titanium tetrachloride (1.16g, 6.1mmol) and then a solution of pyridine (948mg, 12mmol) and malononitrile (402mg, 6.1mmol) in dichloromethane (25ml) at 0-5°C. The mixture was stirred at 25°C for 24h. Column chromatography, eluant dichloromethane/hexane (7:3 v/v) gave compound (74m) (112mg, 22%). MPt. 124-128°C; EI m/e : 212 (M^+); Analysis found: C, 73.2; H, 5.5; N, 12.5. Calculated for $C_{13}H_{12}N_2O$: C, 73.5; H, 5.7; N, 13.2%; IR ν_{max} (KBr): 2220, 1635, 1580, 1510, 1460, 1440, 1385, 1370, 1355, 1330, 1310, 1265, 1220, 1160, 1130, 1100, 1030, 1010, 860, 775, 690 and 600 cm^{-1} ; δH (250MHz, $CDCl_3$): 2.44 (s, 6H) and 2.02 (s, 6H) ppm.

Followed by a second component, which was not obtained analytically pure, identified as compound (75m). EI m/e : 251 (M^+); IR ν_{max} (KBr): 3570, 2920, 2220, 1630, 1570, 1450, 1385, 1330, 1300, 1220, 1130, 1100 and 1030 cm^{-1} .

7.2.4.4 *1-Oxo-2,3,6-trimethyl-4-dicyanomethylene-2,5-cyclohexadiene (74n)*

To a solution of 2,3,6-trimethyl-p-benzoquinone¹⁰² (73n) (867mg, 5.8mmol) in dichloromethane (15ml) was added

titanium tetrachloride (1.2g, 6.4mmol) and then a solution of pyridine (1.0g, 12.7mmol) and malononitrile (420mg, 6.4mmol) in dichloromethane (25ml) at 0-5°C. The mixture was stirred for 24h at 25°C. Column chromatography, eluant toluene-hexane (1:1 v/v) gave compound (74n) (477mg, 41%). MPt. 102-106°C; EI m/e : 198 (M⁺); Analysis found: C, 72.5; H, 4.9; N, 14.0. Calculated for C₁₂H₁₀N₂O: C, 72.7; H, 5.1; N, 14.1%; IR ν_{max} (KBr): 2225, 1630, 1575, 1500, 1435, 1400, 1375, 1345, 1290, 1260, 1220, 1170, 1125, 1105, 1035, 930, 900, 875, 780, 670, 620, 580, 515 and 495 cm⁻¹; ; δ H(250MHz, CDCl₃): 7.46(s, 1H), 2.52(s, 3H) and 2.12(s, 6H)ppm.

Followed by a second component, which was not obtained analytically pure, identified as compound (75n). EI m/e : 237(M⁺); IR ν_{max} (KBr): 3550, 2970, 2920, 2850, 2240, 1600, 1570, 1550, 1480, 1380, 1330, 1320, 1270, 1240, 1210, 1100, 1030, 935, 895, 860, 805, 740, 700, 690, 550, 520 and 400 cm⁻¹; δ H(60MHz, CDCl₃): 7.06(s, 1H), 2.30(s, 6H) and 2.16(s, 3H)ppm.

7.2.4.5 1-Oxo-2,6-dimethyl-4-dicyanomethylene-2,5-cyclohexadiene (74p)

To a solution of 2,6-dimethyl-p-benzoquinone¹⁹⁹ (73p) (366mg, 2.7mmol) in dichloromethane (25ml) was added titanium tetrachloride (1.28g, 6.75mmol) and then a solution of pyridine (1.06g, 13.5mmol) and malononitrile (444mg, 6.75mmol)

in dichloromethane (25ml) at 0-5°C. The mixture was stirred at 25°C for 15h. Column chromatography, eluant dichloromethane, gave compound (74p) (122mg, 24%) as an orange solid. Mpt. 134-138°C; EI m/e : 184 (M^+); Analysis found: C, 71.7; H, 4.3; N, 15.3. Calculated for $C_{11}H_6N_2O$: C, 71.7; H, 4.3; N, 15.2%; IR ν_{max} (KBr): 2220, 1635, 1580, 1430, 1380, 1240, 1200, 1040, 1030, 950, 930, 910, 900 and 780 cm^{-1} ; δH (60MHz, $CDCl_3$): 7.26 (s, 2H) and 2.06 (s, 6H) ppm.

Followed by a second component, which was not obtained analytically pure, identified as compound (75p). EI m/e : 233 (M^+); IR ν_{max} (KBr): 3400, 2230, 1600, 1520, 1480, 1310, 1290, 1210, 1170, 935, 890 and 745 cm^{-1} ; δH (250MHz, $CDCl_3$): 7.80 (s, 2H) and 2.33 (s, 6H) ppm.

7.2.4.6 *Benzo[1,2-b,4,5-b']bis[1,4]dithiin-5-oxo-10-dicyanomethylene 2,3,7,8-tetrahydro (74q)*

To a solution of bis(ethylenedithio)-p-benzoquinone¹⁰⁴ (73q) (284mg, 1mmol) in dichloromethane (50ml) was added titanium tetrachloride (105mg, 2.5mmol) and then a solution of pyridine (393mg, 5mmol) and malononitrile (164mg, 2.5mmol) in dichloromethane (20ml). The mixture was heated at reflux for 24h. Column chromatography, eluent dichloromethane, gave compound (74q) (44mg, 34%) as a black solid. Mpt. 212-214°C; EI m/e : 336 (M^+); Analysis found: C, 46.2; H, 2.1; N, 8.1. Calculated

for $C_{13}H_8S_4N_2O$: C, 46.4; H, 2.4; N, 8.3%; IR ν_{max} (KBr): 2220, 1620, 1580, 1460, 1380, 1280, 1150, 1130 and 820cm^{-1} .

Followed by a second component, which was not obtained analytically pure, identified as (75q). EI m/e : 375(M^+); IR ν_{max} (KBr): 3420, 2930, 2230, 1605, 1570, 1465, 1310, 1220, 1210, 1140, 945 and 750cm^{-1} .

7.2.4.7 *Naphtho[2,3-b][1,4]dithiin-5-dicyanomethylene-10-one 2,3-tetrahydro (74r)*

To a solution of ethylenedithionaphthoquinone¹⁰⁹ (73r) (100mg, 0.4mmol) in dichloromethane (20ml) was added titanium tetrachloride (383mg, 2mmol) and then a solution of pyridine (157mg, 2mmol) and malononitrile (132mg, 2mmol) in dichloromethane (20ml). The mixture was stirred at 25°C for 24h. Fractional sublimation (220°C , 0.05mBar) yielded compound (74r) (52mg, 44%) as a black solid. M.Pt. $240-242^\circ\text{C}$; EI m/e : 296(M^+); Analysis found: C, 60.6; H, 2.7; N, 9.5. Calculated for $C_{15}H_8N_2S_2O$: C, 60.8; H, 2.7; N, 9.5%; IR ν_{max} (KBr): 2220, 1635, 1590, 1540, 1490, 1470, 1420, 1340, 1280, 1250, 1150, 1120, 880, 820, 780 and 720cm^{-1} .

A second sublimed component was obtained, which was not analytically pure, identified as compound (75r). EI m/e : 335(M^+); IR ν_{max} (KBr): 3400, 2940, 2235, 1600, 1540, 1470, 1220, 1180, 910 and 880cm^{-1} .

7.2.5 Preparation of N, 7, 7-Tricyanoquinomethaneimines.

7.2.5.1 General Procedure

To a solution of the substituted quinomethide in dichloromethane was added titanium tetrachloride and then bis(trimethylsilyl)carbodiimide. The reaction mixture was stirred typically for 72h at 25°C. The mixture was poured onto water, the organic layer separated, dried (MgSO₄) and the solvent removed *in vacuo*. The crude residue was purified, where necessary, by silica column chromatography or fractional sublimation.

7.2.5.2 *N*-Cyano-4-dicyanomethylene-cyclohexa-2,5-dienylideneamine (72h)

To a solution of quinomethide (74h) (100mg, 0.64mmol) in dry dichloromethane (20ml) was added titanium tetrachloride (613mg, 3.2mmol) and bis(trimethylsilyl) carbodiimide (599mg, 3.2mmol). The mixture was stirred at 25°C for 72h. Column chromatography, eluting with dichloromethane, yielded compound (72h) (49mg, 43%) as an orange solid. MPt. 176-178°C(dec.); EI m/e : 180(M⁺); Analysis found: C, 66.4; H, 2.2; N, 30.9. Calculated for C₁₀H₄N₄: C, 66.7; H, 2.2; N, 31.1%; IR ν_{max} (KBr): 2240, 2180, 1550, 1380, 1260, 1250, 1030 and 750 cm⁻¹; δ H(60MHz, CDCl₃): 7.68(d, 2H), 7.49(d, 1H) and 7.16(d, 1H)ppm.

7.2.5.3 *N*-Cyano-2,3,5,6-tetramethyl-4-dicyanomethylene-cyclohexa-2,5-dienylideneamine (72m)

To a solution of quinomethide (74m) (100mg, 0.47mmol) in dichloromethane (10ml) was added titanium tetrachloride (136mg, 0.71mmol) and bis(trimethylsilyl)carbodiimide (133mg, 0.71mmol). The mixture was stirred at 25°C for 60h. Column chromatography, eluting with dichloromethane, separated compound (72m) (80mg, 76%) as a yellow solid. MPt. 192°C; EI m/e : 222 (M^+); Analysis found: C, 71.1; H, 5.0; N, 23.5. Calculated for $C_{14}H_{12}N_4$: C, 71.2; H, 5.1; N, 23.7%; IR ν_{max} (KBr): 2220, 2160, 1560 and 1380 cm^{-1} ; δ H (250MHz, $CDCl_3$): 2.40 (br. s, 6H) and 2.21 (br. s, 6H) ppm.

7.2.5.4 *N*-Cyano-2,3,6-trimethyl-4-dicyanomethylene-cyclohexa-2,5-dienylideneamine (72n)

To a solution of quinomethide (74n) (257mg, 1.3mmol) in dry dichloromethane (12ml) was added titanium tetrachloride (308mg, 1.6mmol) and bis(trimethylsilyl)carbodiimide (297mg, 1.6mmol). The mixture was stirred at 25°C for 40h. Column chromatography, eluting with dichloromethane, gave compound (72n) (243mg, 84%). MPt. 136°C (dec.); EI m/e : 236 (M^+); Analysis found: C, 70.4; H, 4.1; N, 25.0. Calculated for $C_{13}H_{10}N_4$: C, 70.2; H, 4.5; N, 25.2%; IR ν_{max} (KBr): 2220, 2160, 2140, 1630, 1540, 1445, 1410, 1380, 1310, 1230, 1130, 1040,

1015, 935, 890, 755, 665 and 545 cm^{-1} ; δH (250MHz, CDCl_3): 7.45 (s, 1H), 2.58 (s, 6H) and 2.33 (s, 3H)ppm.

7.2.5.5 *N*-Cyano-2,6-dimethyl-4-dicyanomethylene-cyclohexa-2,5-dienylideneamine (72p)

To a solution of quinomethide (74p) (424mg, 2.3mmol) in dichloromethane (20ml) was added titanium tetrachloride (574mg, 2.9mmol) and bis(trimethylsilyl)carbodiimide (534mg, 2.9mmol). The mixture was stirred at 25°C for 60h. Column chromatography, eluting with dichloromethane, gave compound (72p) (320mg, 67%). MPt. 261–262°C (dec.); EI m/z : 208 (M^+); Analysis found: C, 69.1; H, 3.6; N, 26.6. Calculated for $\text{C}_{12}\text{H}_8\text{N}_4$: C, 69.2; H, 3.8; N, 26.9%; IR ν_{max} (Nujol): 2235, 2150, 1630, 1570, 1550, 1495, 1385, 1260, 1210, 1040, 970, 945, 915, 760, 725, 655, 550 and 465 cm^{-1} ; δH (250MHz, CDCl_3): 7.37 (br. s, 2H) and 2.50 (vbr s, 6H)ppm.

7.2.5.6 5-Dicyanomethylene-10-*N*-cyanoimine-2,3,7,8-tetrahydro-benzol[1,2-*b*, 4,5-*b'*]bis[1,4]dithiin (72q)

To a solution of quinomethide (74q) (100mg, 0.30mmol) in dichloromethane (40ml) was added titanium tetrachloride (287mg, 1.5mmol) and bis(trimethylsilyl)carbodiimide (281mg, 1.5mmol). The mixture was heated at reflux for 48h. Preparative t.l.c on a silica coated plate, using dichloromethane eluant, provided an analytically pure sample

of (72q) (67mg, 62%) as a black solid. Mpt. $>320^{\circ}\text{C}$; EI m/e : 360 (M^+); Analysis found: C, 46.5; H, 2.1; N, 15.3. Calculated for $\text{C}_{14}\text{H}_8\text{N}_4\text{S}_4$: C, 46.7; H, 2.2; N, 15.5%; IR ν_{max} (KBr): 2920, 2220, 2180, 1560, 1440, 1390, 1030, 750 and 680cm^{-1} .

7.2.5.7 *5-Dicyanomethylene-10-N-cyanoimine-2,3-tetrahydro-naphtho[2,3-b][1,4]dithiin (72r)*

To a solution of quinomethide (74r) (40mg, 0.14mmol) in dichloromethane (10ml) was added titanium tetrachloride (134mg, 0.7mmol) and bis(trimethylsilyl)carbodiimide (131mg, 0.7mmol). The mixture was stirred at 25°C for 24h. Preparative t.l.c on a silica coated plate, using dichloromethane eluant, gave compound (72r) (22mg, 68%) as a black solid. Mpt. $258-260^{\circ}\text{C}$; EI m/e : 320 (M^+); Analysis found: C, 59.6; H, 2.3; N, 17.2. Calculated for $\text{C}_{14}\text{H}_8\text{N}_4\text{S}_2$: C, 60.0; H, 2.5; N, 17.5%; IR ν_{max} (KBr): 2220, 2180, 1570, 1490, 1460, 1330, 1280, 1260, 1160, 750, 730 and 680cm^{-1} .

7.2.6 Preparation of N, N'-Dicyanoquinonediiimines

7.2.6.1 *N,N'*-Dicyano-5,10-diimine-2,3,7,8-tetrahydro-benzol[1,2-b,4,5-b']bis[1,4]dithiin (80)

To a solution of bis(ethylenedithio)-p-benzoquinone (73q) (150mg, 0.53mmol) in dichloromethane (50ml) was added titanium tetrachloride (498mg, 2.6mmol) and bis(trimethyl

silyl) carbodiimide (487mg, 2.6mmol). The mixture was heated at reflux for 96h, poured onto water, the organic layer separated, dried ($MgSO_4$) and the solvent removed *in vacuo*. Purification of the solid residue by silica column chromatography, eluant dichloromethane, gave compound (80) (62mg, 35%) as a black solid. MPt. $>320^\circ C$; EI m/z : 338 ($M^+ + 2H$); Analysis found: C, 41.9; H, 2.1; N, 16.6. Calculated for $C_{12}H_9N_4S_4$: C, 42.8; H, 2.4; N, 16.7%; IR ν_{max} (KBr): 2130, 1550, 1460, 1260, 1135, 1100 and $820cm^{-1}$.

7.2.6.2 5-Oxo-10-N-cyanoimine-2,3-tetrahydro-benzol[1,2-b,4,5-b']bis[1,4]dithiin (81) and N,N'-Dicyano-5,10-diimine-2,3-tetrahydro-benzol[1,2-b,4,5-b']bis[1,4]dithiin (79)

To a solution of ethylenedithionaphthoquinone (73r) (200mg, 0.8mmol) in dichloromethane (40ml) was added titanium tetrachloride (766mg, 4mmol) and bis(trimethylsilyl) carbodiimide (749mg, 4mmol). The mixture was stirred at $25^\circ C$ for 24h, poured onto water, the organic layer separated, dried ($MgSO_4$) and the solvent removed *in vacuo*. Purification of the solid residue by silica column chromatography, eluent dichloromethane, separated compound (81) (50mg, 23%). MPt. $172-174^\circ C$; EI m/z : 272 (M^+); Analysis found: C, 57.1; H, 2.7; N, 10.1. Calculated for $C_{13}H_9N_2S_2O$: C, 57.3; H, 3.0; N, 10.3%; IR ν_{max} (KBr): 2150, 1640, 1580, 1560, 1510, 1320, 1280, 1250, 1150, 880 and $690cm^{-1}$; δH (250MHz, $CDCl_3$): 8.98 (m, 1H), 8.10 (m, 1H), 7.70-7.67 (m, 2H), 3.27 (m, 4H) ppm followed by compound (79)

(161mg, 68%) . Mpt. 180–182°C (dec.). Analysis found: C, 56.5; H, 2.8; N, 18.3. Calculated $C_{14}H_{25}N_4S_2$: C, 56.7; H, 2.7; N, 18.9%; IR ν_{max} (KBr): 2150, 1550, 1510, 1470, 1330, 1310, 1260, 1170, 1140, 1130, 910, 770 and 670 cm^{-1} ; δH (250MHz, $CDCl_3$): 7.77–7.73 (m, 4H) and 3.28 (s, 4H) ppm.

7.4 EXPERIMENTAL TO CHAPTER 4

7.4.1 *N-n-Hexadecyl-2-methylbenzothiazolium iodide (94)*

To 2-methylbenzothiazole (93) (2.98g, 20mmol) was added n-hexadecyliodide (14.08g, 40mmol) and the mixture heated at 90°C for 48h. The mixture was cooled to 0°C and diethylether (400ml) was added. The precipitated white solid of (94) was collected, washed with diethylether, and dried *in vacuo* (2.0g, 20%). Mpt. 121–123°C (from methanol); EI m/z : 374 ($M^+ - I^-$); Analysis found: C, 57.4; H, 8.1; N, 3.5. Calculated for $C_{24}H_{40}INS$: C, 57.5; H, 8.0; N, 3.7%; IR ν_{max} (KBr): 2900, 2840, 1580, 1520, 1470, 1440, 1375, 1340, 1060, 1020, 780, 730 and 720 cm^{-1} .

7.4.2 *Z-β-(N-n-Hexadecyl-2-benzothiazolium)-α-cyano-4-styryl dicyanomethanide [C₁₄H₃₃-BT3CNQ] (91)*

To a solution of salt (94) (250mg, 0.50mmol) in acetonitrile (30ml) was added TCNQ (45) (102mg, 0.50mmol) and

N-methylpiperidine (50mg, 0.5mmol). The solution was heated at reflux for 24h. On cooling to 0°C the product was collected, washed with cold acetonitrile, and dried *in vacuo*. This yielded green microcrystals of C₁₆H₂₃-BT3CNQ (91) (171mg, 62%). Mpt. 186-188°C; Analysis found: C, 76.3; H, 7.4; N, 9.7; S, 5.8. Calculated for C₃₅H₄₂N₄S: C, 76.4; H, 7.6; N, 10.2; S, 5.8%; IR ν_{\max} (KBr): 2900, 2840, 2180, 2150, 1600, 1530, 1500, 1460, 1370, 1345, 1335, 1290, 1260, 1200, 840, 740 and 720cm⁻¹.

7.4.3 2-Methyl-4-n-hexylthiazole (104)

To a solution of 1-bromo-2-octanone (103) (1.5g, 7.3mmol) in ethanol (20ml) was added thioacetamide (0.55g, 7.3mmol) and the resulting solution heated at reflux for 24h. The solvent was removed *in vacuo* to give a clear yellow oil (104) (1.0g, 80%). EI m/z : 184 (M⁺+1); Analysis found: C, 65.5; H, 9.1; N, 7.5. Calculated for C₁₀H₁₇NS: C, 65.6; H, 9.3; N, 7.7%; IR ν_{\max} (neat): 2920, 2860, 1540, 1460, 1380, 1260, 1060, 870, and 690cm⁻¹.

7.4.4 2,3-Dimethyl-4-n-hexylthiazolium methylsulphate (105)

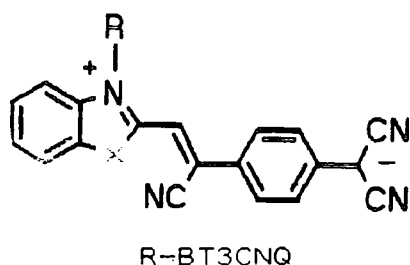
Dimethylsulphate (590mg, 5mmol) was added to 2-methyl-4-n-hexylthiazole (104) (1.0g, 5mmol) and the mixture heated at 120°C for 1h. The mixture was cooled to 0°C and

diethylether (60ml) added, the salt (105) separated as a purple oil (1.33g, 86%). EI m/e : 198 ($M^+ - MeI$); Analysis found: C, 46.4; H, 7.2; N, 4.4%. Calculated for $C_{12}H_{23}NO_4S_2$: C, 46.6; H, 7.4; N, 4.5%.

7.4.5 *Z*- β -(*N*-Methyl-4-hexylthiazolium)- α -cyano-4-styryl-dicyanomethanide [$C_{22}H_{22}N_4S$] (92)

To a solution of salt (105) (300mg, 1.08mmol) in dry acetonitrile (20ml) was added TCNQ (220mg, 1.08mmol) and *N*-methylpiperidine (107mg, 1.08mmol). The resulting solution was heated at reflux for 24h. On cooling to 0°C compound (92) was collected by filtration (250mg, 62%). MPt. 220°C (dec.) (from acetonitrile); Analysis found: C, 70.3; H, 5.8; N, 14.6. Calculated for $C_{22}H_{22}N_4S$: C, 70.5; H, 5.9; N, 14.9%; IR ν_{max} (KBr): 2940, 2860, 2190, 2160, 1610, 1550, 1500, 1360, 1350, 1330, 1280, 1250, 1225, 1200, 970, 830 and 770 cm^{-1} .

Table 7.1 : Spectroscopic and analytical data for R-BT3CNQ derivatives.



- (95) R = CH₃, X=S
 (96) R = CH₃, X=O
 (97) R = C₁₆H₃₃, X=O
 (98) R = CH₃, X=Se
 (99) R = CH₂Ph, X=S

Compound	Found (%)	Calc (%)	Yield (%)	Mpt. °C	λ_{max}^1 /nm
(95)	C, 70.6; H, 3.5; N, 16.5; S, 9.4.	C, 69.2; H, 3.4; N, 15.9; S, 9.5.	50	328 (dec.)	712.0
(96)	C, 73.9; H, 3.4; N, 17.1.	C, 74.0; H, 3.7; N, 17.3.	30	212-214	624.0 644.0
(97)	C, 78.2; H, 7.6; N, 10.1.	C, 78.7; H, 7.9; N, 10.5.	37	183-184	698.0 767.0
(98)	C, 62.4; H, 2.7; N, 15.7.	C, 62.0; H, 3.1; N, 14.5.	30	334 (dec.)	691.0 710.0
(99)	C, 74.9; H, 3.9; N, 13.5.	C, 75.0; H, 3.9; N, 13.5.	60	238-240	256.0 750.0

1. in DMSO.

7.5 EXPERIMENTAL TO CHAPTER 5

7.5.1 Preparation of Hemicyanines (113a-113d)

7.5.1.1 General Procedure

To a stirred solution of 4-(octadecylamino)benzaldehyde (116)²⁵ in ethanol was added the appropriate N-alkyl-2-methyl salt (117a-117d) and a catalytic amount of piperidine. The mixture was heated at reflux for 4h. On cooling to 0°C, the product was collected by filtration and then recrystallised from n-butanol or methanol and dried *in vacuo*.

7.5.1.2 2-[2-(4-Octadecylaminophenyl)ethenyl]-3-N-methylbenzothiazolium iodide (113a)

A mixture of aldehyde (116) (800mg, 2.1mmol), 2,3-dimethylbenzothiazolium iodide (117a) (1.16g, 2.1mmol) and piperidine (0.4ml) in ethanol (20ml) was heated at reflux for 4h. This yielded compound (113a) (2.2g, 84%) as a red solid. MPt. 176-178°C (from n-butanol); EI m/e : 374 ($M^+ - MeI$); Analysis found: C, 63.0; H, 8.0; N, 4.2. Calculated for $C_{34}H_{51}IN_2S$: C, 63.2; H, 8.3; N, 4.3%; IR ν_{max} (Nujol) 3360, 1590, 1540, 1390, 1160, 830 and 810 cm^{-1} ; UV λ_{max} (ethanol) 532.0nm.

7.5.1.3 *2-[2-(4-Octadecylaminophenyl)ethenyl]-3-N-n-hexadecylbenzothiazolium iodide (113b)*

A mixture of aldehyde (116) (500mg, 1.34mmol), *N-n*-hexadecyl-2-methylbenzothiazolium iodide (117b) (650mg, 1.34mmol) and piperidine (0.4ml) was heated at reflux for 4h. This yielded compound (113b) as a red solid (940mg, 82%). Mpt. 99-101°C (from methanol); Analysis found: C, 68.6; H, 9.4; N, 3.3. Calculated for $C_{49}H_{81}IN_2S$: C, 68.7; H, 9.5; N, 3.3%; IR ν_{max} (KBr): 3360, 2920, 2860, 1590, 1570, 1470, 1350, 1160, 830 and 810cm^{-1} ; UV λ_{max} (ethanol) 535.0, 337.0 and 204.0nm.

7.5.1.4 *2-[2-(4-Octadecylaminophenyl)ethenyl]-3-N-methylbenzoxazolium iodide (113c)*

A mixture of aldehyde (116) (410mg, 1.1mmol), 2,3-dimethylbenzoxazolium iodide (117c) (300mg, 1.1mmol) and piperidine (0.4ml) in ethanol (20ml) was heated at reflux for 4h. This yielded compound (113c) as a red solid (551mg, 80%). Mpt. 189-190°C (from *n*-butanol); Analysis found: C, 64.6; H, 7.9; N, 4.2. Calculated for $C_{34}H_{51}IN_2O$: C, 64.8; H, 8.1; N, 4.4%; IR ν_{max} (Nujol): 3360, 1590, 1545, 1490, 1460, 1310, 1140, 845 and 820cm^{-1} ; UV λ_{max} (ethanol) 533.0, 314.0 and 289.0nm.

7.5.1.5 2-[2-(4-Octadecylaminophenyl)ethenyl]-3-N-methyl-4-methyl-thiazolium iodide (113d)

A mixture of aldehyde (116) (500mg, 1.34mmol), 2,3,4-trimethylthiazolium iodide (117d) (342mg, 1.34mmol) and piperidine (0.4ml) in ethanol (20ml) was heated at reflux for 4h. This yielded compound (113d) as an orange solid (711mg, 87%). Mpt. 184-186°C (from n-butanol); EI m/z : 468 ($M^+ - MeI$); Analysis found: C, 60.8; H, 8.3; N, 4.5. Calculated for $C_{31}H_{51}IN_2S$: C, 70.0; H, 8.4; N, 4.6%; IR ν_{max} (Nujol): 3360, 1590, 1540, 1480, 1455, 1430, 1345, 1180, 830 and 810 cm^{-1} ; UV λ_{max} (ethanol) 485.0, 275.0 and 204.0nm.

7.5.1.6 2-[2-(4-Octadecylaminophenyl)ethenyl]-3-N-methyl-4-n-hexylthiazolium methylsulphate (118)

To a solution of 2,3-dimethyl-4-n-hexylthiazolium methylsulphate (105) (500mg, 1.6mmol) in ethanol (20ml) was added N,N'-dimethylaminobenzaldehyde (240mg, 1.6mmol) and piperidine (0.4ml). The solution was heated at reflux for 1h. The solvent was evaporated *in vacuo* to yield a red solid. Silica column chromatography (eluant acetone/diethylether, 5:1 v/v) separated compound (118) (406mg, 58%). Recrystallisation from methanol/diethylether (4:1 v/v) afforded an analytically pure sample. Mpt. 142-144°C; Analysis found: C, 57.2; H, 7.3; N, 6.2. Calculated for $C_{21}H_{32}N_2O_4S_2$: C, 57.3; H, 7.3; N, 6.4%; IR ν_{max} (KBr): 2920, 1570, 1530, 1440,

1380, 1330, 1290, 1260, 1170, 1060 and 810 cm^{-1} ; UV λ_{max} (ethanol) 481.0 and 204.0nm.

7.6 EXPERIMENTAL TO CHAPTER 6

7.6.1 *2-Methylthio-4-n-hexyl-1,3-dithiolium methylsulphate* (132).

To 4-n-hexyl-1,3-dithiole-2-thione (131) (500mg, 2.3mmol) was added dimethylsulphate (290mg, 2.3mmol) and the mixture heated at 90°C for 0.5h. On cooling to 0°C diethylether (200ml) was added. This yielded compound (132) as a purple oil (356mg, 45%). EI m/e : 238 ($\text{M}^+ + 2\text{H} - \text{MeSO}_4^-$); Analysis found: C, 38.3; H, 5.7. Calculated for $\text{C}_{11}\text{H}_{20}\text{O}_4\text{S}_4$: C, 38.4; H, 5.8%; δH (250MHz): 6.90 (s, 1H), 3.80 (s, 3H), 2.78 (t, 2H), 1.34 (m, 8H) and 0.98 (t, 3H) ppm.

7.6.2 *4-n-Hexyl-2-(4-dicyanomethylene-2,5-cyclohexadiene)-1,3-dithiole* (128)

To a solution of salt (132) (231mg, 0.70mmol) in pyridine/glacial acetic acid (20ml, 3:1 v/v) was added phenylmalononitrile (134) (100mg, 0.70mmol) and the solution heated at reflux for 24h. On cooling to 0°C the solution was poured onto water (200ml), diethylether added (100ml), the organic layer was separated, dried (MgSO_4) and the solvent removed *in vacuo* to yield compound (128) as a blue solid

(80mg, 35%). MPt. 48-49°C; EI m/e : 326 (M^+); Analysis found: C, 66.2; H, 4.5; N, 8.7. Calculated for $C_{18}H_{19}N_2S_2$: C, 66.3; H, 5.5; N, 8.6%; IR ν_{max} (KBr): 3020, 2920, 2840, 2190, 2160, 1600, 1380, 1360, 1340, 1180, 840, 700 and 540 cm^{-1} ; δ H(250MHz, $CDCl_3$) 7.21-6.98 (dd, 4H), 6.91 (s, 1H), 2.78 (t, 2H), 1.35 (m, 8H) and 0.92 (t, 3H) ppm.

7.6.3 1-Bromo-2-dodecanol (136)

To a stirred slurry of 1-dodecene (135) (40g, 0.24mol) in DMSO (400ml) and water (20ml) was added N-bromosuccinimide (85.4g, 0.48mol) portionwise over 2h. The solution was stirred at 25°C for 24h. Diethylether (200ml) and water (400ml) were added, the organic layer separated, dried ($MgSO_4$) and the solvent removed *in vacuo*. The alcohol (136) was obtained as a clear colourless liquid (34g, 54%). EI m/e : 263 (M^+); Analysis found: C, 54.8; H, 9.1. Calculated for $C_{12}H_{25}BrO$: C, 54.6; H, 8.9%; IR ν_{max} (Nujol): 3370, 1350, 1220, 1120, 1040, 860, 740, 660 and 570 cm^{-1} .

7.6.4 1-Bromo-2-dodecanone (137)

To a stirred solution of alcohol (136) (34g, 0.129mol) and water (20ml) was added a solution of sodium dichromate (64g, 0.39mol) in sulphuric acid (480ml, 3.6M) dropwise over 2h. Diethylether (200ml) was added and the mixture stirred vigorously for 1h. The organic layer was separated, washed

with water, dried (MgSO_4) and the solvent removed *in vacuo* to give the ketone (137) as a white solid (29.3g, 87%). MPt. 38-40°C; EI m/e : 263 (M^{+1}), 183 ($M^{+1}-\text{Br}$); Analysis found: C, 54.7; H, 8.4. Calculated for $\text{C}_{12}\text{H}_{23}\text{BrO}$: C, 55.0; H, 8.8%; IR ν_{max} (Nujol): 3370, 1740, 1120, 840, 740 and 570 cm^{-1} ; δH (250MHz, CDCl_3): 3.79 (s, 2H), 2.53 (t, 2H), 1.16 (s, 16H) and 0.77 (t, 3H) ppm.

7.6.5 *Q-Ethyl-1-xanthyl-dodecan-2-one* (138)

To a solution of ketone (137) (10.0g, 0.0383mol) in acetone (100ml) was added potassium ethyl xanthate (6.13g, 0.0383mol) and the mixture heated at reflux for 4h. On cooling to 0°C, diethylether (200ml) and water (400ml) were added. The organic layer was collected, washed with water, dried (MgSO_4) and the solvent removed *in vacuo* to give (138) as a tan solid (29.3g, 87%). MPt. 38-40°C; EI m/e : 305 (M^{+1}), 277 ($M^{+1}-\text{Et}$); Analysis found: C, 59.1; H, 9.0. Calculated for $\text{C}_{13}\text{H}_{26}\text{O}_2\text{S}_2$: C, 59.2; H, 9.2%; IR ν_{max} (Nujol): 1720, 1650, 1600, 1410, 1270, 1220, 1150, 1110, 1050, 870, 840 and 800 cm^{-1} .

7.6.6 *4-n-Decyl-1,3-dithiole-2-thione* (139)

To a solution of ketone (138) (5.0g, 0.016mol) in toluene (100ml) was added phosphorous pentasulfide (21.9g, 0.048mol) and the mixture heated at reflux for 24h.

On cooling to 0°C, diethylether (200ml) and water (200ml) were added. The organic layer was separated and washed with dilute sodium hydroxide (200ml, 1.0M). The organic layer was separated, dried (MgSO₄), and the solvent removed *in vacuo*. Silica column chromatography of the residue, eluting with dichloromethane, gave thione (139) as a clear red oil (3.68g, 84%); EI m/e : 275 (M⁺+1); Analysis found: C, 56.6; H, 7.8. Calculated for C₁₃H₂₂S₃: C, 56.9; H, 8.0%; IR ν_{max} (KBr): 2920, 2860, 1470, 1060, 890 and 710cm⁻¹; δ H (250MHz, CDCl₃): 6.59 (s, 1H), 2.51 (t, 2H), 1.19 (s, 16H) and 0.81 (t, 3H) ppm.

7.6.7 *4-n-Decyl-2-methylthio-1,3-dithiolium tetrafluoroborate (140)*

To thione (139) (2g, 7.3mmol) was added dimethylsulphate (0.92g, 7.3mmol) and the mixture heated at 90°C for 15min. On cooling to 0°C, tetrafluoroboric acid diethyletherate (54%w/v; 2.2ml, 7.3mmol) was added. Diethylether (400ml) was added and the precipitated white solid (140) collected, washed with cold diethylether and dried *in vacuo* (1.6g, 58%). MPt. 72-73°C; EI m/e : 291 (M⁺+2H-BF₄⁻); Analysis found: C, 44.4; H, 6.5. Calculated for C₁₄H₂₅BF₄S₃: C, 44.7; H, 6.7%.

7.6.8 4-n-Decyl-2-methylthio-2H-1,3-dithirole (141)

To a solution of salt (140) (1.5g, 4mmol) in ethanol (40ml) at 25°C under an atmosphere of nitrogen was added sodium borohydride (454mg, 12mmol) and the mixture stirred for 4h. The solvent was removed *in vacuo* and dichloromethane (100ml) added to the residue. Water was added to the mixture, the organic layer was separated, dried (MgSO₄) and the solvent removed *in vacuo* to give (141) as a clear colourless oil (0.96g, 82%). EI m/e : 290 (M⁺); Analysis found: C, 57.6; H, 8.8. Calculated for C₁₄H₂₆S₃: C, 57.9; H, 9.0%; δ H (250 MHz, CDCl₃): 6.63 (s, 1H), 5.59 (s, 1H), 2.25 (t, 2H), 2.14 (s, 3H), 1.19 (s, 16H) and 0.81 (t, 3H) ppm.

7.6.9 4-n-Decyl-1,3-dithiolium tetrafluoroborate (142)

To oil (141) (540mg, 1.86mmol) was added acetic anhydride (0.18ml, 1.86mmol) and tetrafluoroboric acid diethyletherate (54%w/v; 0.55ml, 1.86mmol) and the solution was stirred at 0°C for 2h. Diethylether (400ml) was added, the precipitated tan solid (142) was collected, washed with diethylether and dried *in vacuo* (510mg, 83%). MPt. 64-66°C; EI m/e : 243 (M⁺ - BF₄⁻); Analysis found C, 47.1; H, 6.8. Calculated for C₁₃H₂₅BF₄S₂: C, 47.3; H, 7.0%; IR ν_{max} (KBr): 2940, 2860, 1630, 1500, 1470, 1450, 1380, 1030, 750 and 720cm⁻¹.

7.6.10 4-*n*-Decyl-2-formylmethylene-1,3-dithiolo (143)

To a solution of salt (142) (500mg, 1.5mmol), under an atmosphere of nitrogen, was added tributylphosphine (333mg, 1.65mmol) and the solution heated at 40°C for 2h. Triethylamine (152mg, 1.5mmol) and aqueous glyoxal (40wt%; 2.18ml, 15mmol) was added and the solution stirred at 25°C for 2h. Water and dichloromethane were added, the organic layer separated, dried (MgSO₄) and the solvent removed *in vacuo*. Silica column chromatography of the residue, eluant dichloromethane, separated aldehyde(143) (290mg, 68%). Mpt. 36-38°C; EI m/e : 284 (M⁺); Analysis found: C, 63.2; H, 8.3. Calculated for C₁₅H₂₄OS₂ : C, 63.3; H, 8.5%; IR ν_{max} (nujol): 1640, 1320, 1260, 1190, 1100, 920, 880, 800, 740, 700 and 640cm⁻¹.

7.6.11 4-*n*-Decyl-2-(dicyanomethylene)methylene-1,3-dithiolo (129)

To a solution of aldehyde (143) (100mg, 0.35mmol) in ethanol (40ml) was added malononitrile (23mg, 0.35mmol) and piperidine (29mg, 0.35mmol) and the solution heated at reflux for 4h. The solvent was removed *in vacuo*. Water and dichloromethane were added, the organic layer was separated, dried (MgSO₄) and the solvent removed *in vacuo* to give

compound (129) as a red solid (44mg, 38%). Mpt. 47-49°C;
EI m/e : 332(M⁺); Analysis found: C, 64.8; H, 6.8; N, 8.3.
Calculated for C₁₆H₂₄N₂S₂: C, 65.0; H, 7.3; N, 8.4%; IR ν_{max} (KBr)
: 3060, 2940, 2860, 2210, 1410, 1270, 900, 740 and 710cm⁻¹.

APPENDICES

APPENDIX I - X-RAY CRYSTAL DATA

A. CRYSTAL DATA FOR 2,5-Dibromo-TCNQ (41d)

Chemical Formula: $C_{12}H_2Br_2N_4$; $M = 361.98$, monoclinic, space group $P2_1/C$ (No 14), $a = 6.184(1)$, $b = 6.445(1)$, $c = 14.653(2)$ Å, $\beta = 90.56(1)^\circ$, $U = 583.9(1)$ Å³, $Z = 2$, $D_c = 2.059$ g cm⁻³, $F(000) = 344$, $\lambda = 0.71069$ Å, μ (Mo-K α) = 68.6 cm⁻¹, crystal size (0.37 x 0.22 x 0.05 mm).

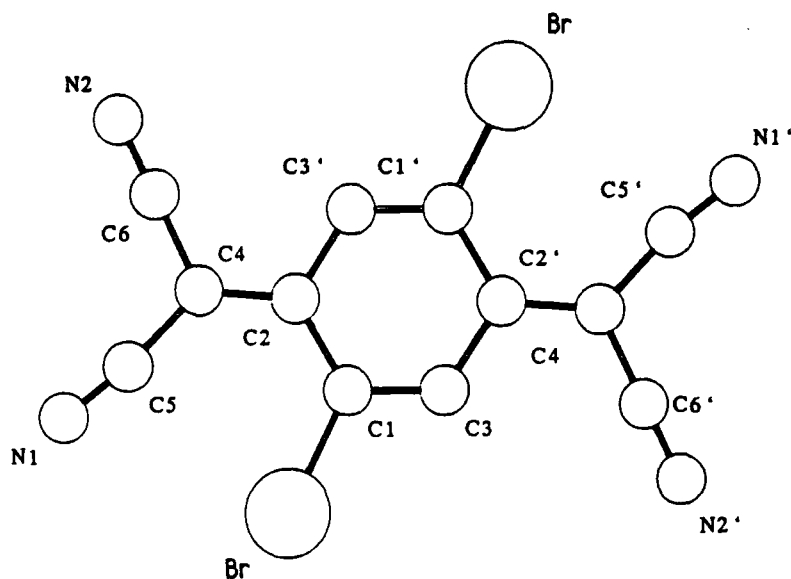
Data collection: Unit cell parameters and intensity data were obtained by following previously described procedures¹⁰⁴ using a CAD4 diffractometer operating in the ω -2 θ scan mode, with graphite monochromated Mo-K α radiation. A total of 1030 unique reflections were collected ($3 < 2\theta < 50^\circ$). The segment of reciprocal space scanned was: (h) 0 ... 7, (k) 0 ... 7, (l) -17 ... 17. The reflection intensities were corrected for absorption, using the azimuthal-scan method¹⁰⁵; maximum transmission factor 1.00, minimum value 0.66.

Structure solution and refinement: The structure was solved by the application of routine heavy-atom methods (SHELX-86¹⁰⁶), and refined by full matrix least squares (SHELX-76¹⁰⁷). After location, and isotropic refinement, of all non-hydrogen atoms, a further absorption correction was applied, program DIFABS¹⁰⁸; maximum correction 1.37, minimum 0.57. Refinement continued with all non-hydrogen treated

anisotropically. The single hydrogen atom of the asymmetric unit was allowed unrestricted isotropic refinement.

The final residue R and R_w were 0.031 and 0.033, respectively, for the 86 variables and 880 data for which $F_o > 3 \sigma(F_o)$. The function minimised was $\sum_w (F_o - F_c)^2$ with the weight, w , being defined as $1/[\sigma^2(F_o) + 0.0005 F_o^2]$. All computations were made on a DEC VAX-11/750 computer.

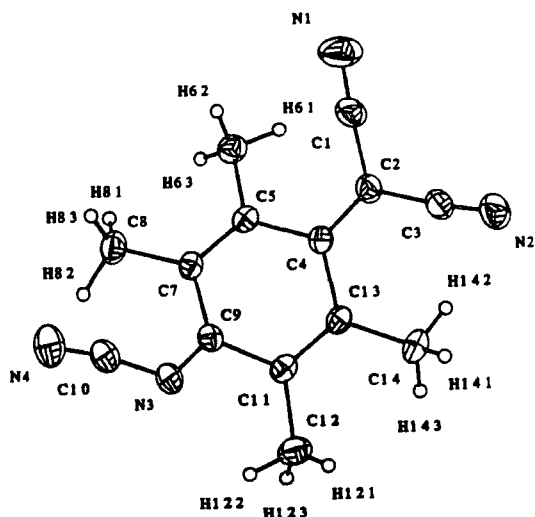
Atom numbering scheme for 2,5-dibromo-TCNQ (41d)



B. CRYSTAL DATA, INTENSITY DATA, COLLECTION PARAMETERS AND
DETAILS OF REFINEMENT FOR COMPOUND (72m)

Chemical Formula: $C_{14}H_{12}N_4$; $M = 236.26$; monoclinic; space group $P2_1/n$; $a = 15.047(6)$, $b = 8.117(3)$, $c = 10.466 \overset{\circ}{\text{Å}}$; $\beta = 91.31(3)^\circ$; $U = 1277.95 \overset{\circ}{\text{Å}}$; $Z = 4$; $D_c = 1.23 \text{ gcm}^{-3}$; $F(000) = 496$; $\lambda = 0.71069 \text{ Å}$; $\mu (\text{Mo-K}\alpha) = 0.44 \text{ cm}^{-1}$; $\theta \text{ min/max} = 1.5, 25.0$; $T = 293\text{K}$; Total data observed = 1627; significant test $F_o > 3\sigma F_o$; No. of parameters = 211; weighting scheme = $1/[\sigma^2(F_o) + 0.00169(F_o)^2]$; final $R = 0.045$; final $R_g = 0.067$.

Data were collected on a CAD 4 diffractometer following previously described procedures¹⁹⁴. The structure was solved by direct methods (SHELX-86¹⁹⁶) and developed and refined using standard Fourier and least-squares procedures. Non-hydrogen atoms were refined anisotropically, hydrogens isotropically. Bond angles and lengths are shown in Table A.2.



Atom Numbering Scheme for compound (72m)

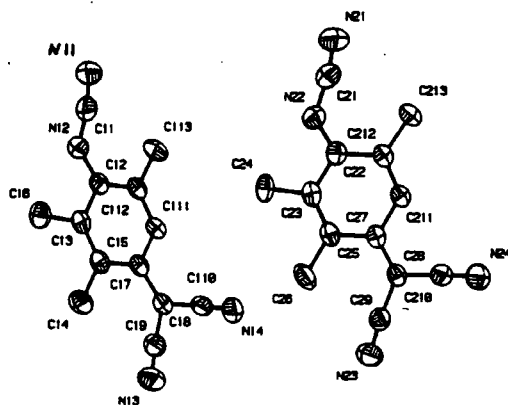
C(1)-N(1)	1.139(4)	C(2)-C(1)-N(1)	175.4(3)
C(3)-C(2)	1.436(4)	C(4)-C(2)-C(1)	123.7(3)
N(2)-C(3)	1.142(4)	N(2)-C(3)-C(2)	174.8(3)
C(13)-C(4)	1.469(4)	C(13)-C(4)-C(2)	121.9(3)
C(7)-C(5)	1.354(4)	C(6)-C(5)-C(4)	120.4(3)
C(9)-C(7)	1.466(4)	C(7)-C(5)-C(6)	122.4(3)
C(11)-C(9)	1.462(4)	C(9)-C(7)-C(5)	118.1(3)
N(4)-C(10)	1.151(4)	N(3)-C(9)-C(7)	126.4(3)
C(13)-C(11)	1.351(4)	C(11)-C(9)-N(3)	115.3(3)
C(2)-C(1)	1.431(4)	N(4)-C(10)-N(3)	170.4(3)
C(4)-C(2)	1.360(4)	C(13)-C(11)-C(9)	118.2(3)
C(5)-C(4)	1.476(4)	C(11)-C(13)-C(4)	117.5(3)
C(6)-C(5)	1.501(5)	C(14)-C(13)-C(11)	122.1(3)
C(8)-C(7)	1.501(5)	C(3)-C(2)-C(1)	110.7(3)
N(3)-C(9)	1.299(4)	C(4)-C(2)-C(3)	124.9(3)
C(10)-N(3)	1.332(4)	C(5)-C(4)-C(2)	120.9(3)
C(12)-C(11)	1.497(4)	C(13)-C(4)-C(5)	117.1(3)
C(14)-C(13)	1.503(5)	C(7)-C(5)-C(4)	117.1(3)
		C(8)-C(7)-C(5)	121.8(3)
		C(9)-C(7)-C(8)	120.1(3)
		C(11)-C(9)-C(7)	118.2(3)
		C(10)-N(3)-C(9)	123.9(3)
		C(12)-C(11)-C(9)	118.3(3)
		C(13)-C(11)-C(12)	123.4(3)
		C(14)-C(13)-C(4)	120.4(3)

Table A.2: Bond lengths (Å) and angles (°) for compound (72m).

C. CRYSTAL DATA, INTENSITY DATA, COLLECTION PARAMETERS AND
DETAILS OF REFINEMENT FOR COMPOUND (72n)

Chemical Formula: $C_{13}H_{10}N_4$; $M = 222.25$; monoclinic; space group $P21/c$; $a = 13.978(1)$, $b = 11.714(1)$, $c = 14.736(1)\text{\AA}$; $\beta = 98.96^\circ$; $U = 2325.18$; $Z = 8$; $D_c = 1.27\text{ g cm}^{-3}$; $F(000) = 928$; Cu-K α radiation; $\lambda = 1.5418$; $\mu = 6.07\text{ cm}^{-1}$; θ min/max = 3, 65; Total data observed = 3314; significant test $F_o > 3\sigma F_o$; No. of parameters = 350; weighting scheme = $1/[\sigma^2(F_o) + 0.00004669(F_o)^2]$; final $R = 0.055$; final $R_g = 0.076$.

Data were collected on a CAD 4 diffractometer following previously described procedures¹⁰⁴. The structure was solved by direct methods (SHELX-86¹⁰⁶) and developed and refined using standard Fourier and least-squares procedures. Non-hydrogen atoms were refined anisotropically, hydrogens isotropically. Bond lengths and angles are shown in Table A.3 and Table A.4 respectively.



Atom numbering scheme for compound (72n)

Table A. 3: Bond lengths (\AA) for compound (72n).

Molecule 1.			
C(11)-N(11)	1.151(4)	N(12)-C(11)	1.327(4)
C(12)-N(12)	1.303(4)	C(13)-C(12)	1.466(4)
C(112)-C(12)	1.462(4)	C(14)-C(13)	1.512(5)
C(15)-C(13)	1.362(4)	C(16)-C(15)	1.516(5)
C(17)-C(15)	1.457(4)	C(18)-C(17)	1.373(4)
C(111)-C(17)	1.451(4)	C(19)-C(18)	1.425(4)
C(110)-C(18)	1.434(4)	N(13)-C(19)	1.146(4)
N(14)-C(110)	1.144(4)	C(112)-C(111)	1.338(4)
C(113)-C(112)	1.505(5)	C(21)-N(21)	1.154(5)
Molecule 2.			
N(22)-C(21)	1.334(5)	C(22)-N(22)	1.309(4)
C(23)-C(22)	1.471(4)	C(212)-C(22)	1.456(4)
C(24)-C(23)	1.521(5)	C(25)-C(23)	1.349(4)
C(26)-C(25)	1.517(5)	C(27)-C(25)	1.452(4)
C(28)-C(27)	1.379(4)	C(211)-C(27)	1.451(4)
C(29)-C(28)	1.430(4)	C(210)-C(28)	1.436(4)
N(23)-C(29)	1.147(4)	N(24)-C(210)	1.134(4)
C(212)-C(211)	1.337(4)	C(213)-C(212)	1.504(5)

Table A. 4: Bond Angles ($^\circ$) for Compound (72n).

N(12)-C(11)-N(11)	169.8(3)	C(12)-N(12)-C(11)	126.8(3)
C(13)-C(12)-N(12)	114.5(3)	C(112)-C(12)-N(12)	126.0(3)
C(112)-C(12)-C(13)	119.6(3)	C(14)-C(13)-C(14)	117.0(3)
C(15)-C(13)-C(12)	121.4(3)	C(15)-C(13)-C(14)	121.6(3)
C(16)-C(15)-C(13)	121.2(3)	C(17)-C(15)-C(13)	118.8(3)
C(17)-C(15)-C(16)	120.0(3)	C(18)-C(17)-C(15)	124.5(3)
C(111)-C(17)-C(15)	118.6(3)	C(111)-C(17)-C(18)	116.8(3)
C(19)-C(18)-C(17)	128.1(3)	C(110)-C(18)-C(17)	121.4(3)
C(110)-C(18)-C(19)	110.5(3)	N(13)-C(19)-C(18)	173.3(3)
N(14)-C(110)-C(18)	175.7(3)	C(112)-C(111)-C(17)	123.8(3)
C(111)-C(112)-C(12)	117.7(3)	C(113)-C(112)-C(12)	122.4(3)
C(113)-C(112)-C(111)	119.9(3)	N(22)-C(21)-N(21)	168.7(3)
C(22)-N(22)-C(21)	126.9(3)	C(23)-C(22)-N(22)	114.6(3)
C(212)-C(22)-N(22)	126.1(3)	C(212)-C(22)-C(23)	119.4(3)
C(24)-C(23)-C(22)	116.4(3)	C(25)-C(23)-C(22)	121.5(3)
C(25)-C(23)-C(24)	122.1(4)	C(26)-C(25)-C(23)	121.8(3)
C(27)-C(25)-C(23)	118.9(3)	C(27)-C(25)-C(26)	119.2(3)
C(28)-C(27)-C(25)	124.6(3)	C(211)-C(27)-C(25)	118.7(3)
C(211)-C(27)-C(28)	116.8(3)	C(291)-C(28)-C(27)	127.9(3)
C(210)-C(28)-C(27)	121.1(3)	C(210)-C(28)-C(29)	111.0(3)
N(23)-C(29)-C(28)	173.4(3)	N(24)-C(210)-C(28)	177.1(3)
C(212)-C(211)-C(27)	123.6(3)	C(211)-C(212)-C(22)	117.8(3)
C(213)-C(212)-C(22)	122.1(3)	C(213)-C(212)-C(211)	120.1(3)

APPENDIX II - COLLOQUIA, LECTURES AND SEMINARS GIVEN BY
INVITED SPEAKERS IN THE DEPARTMENT OF CHEMISTRY DURING
THE PERIOD 1ST AUGUST 1988 TO 31ST JULY 1991

(A) 1ST AUGUST 1988 TO 31ST JULY 1989

- AVEYARD, Dr. R. (University of Hull) 15th March, 1989
Surfactants at your Surface
- * AYLETT, Prof. B.J. (Queen Mary College, London) 16th February, 1989
Silicon-Based Chips:- The Chemist's Contribution
- * BALDWIN, Prof. J.E. (Oxford University) 9th February, 1989
Recent Advances in the Bioorganic Chemistry of
Penicillin Biosynthesis
- BALDWIN & WALKER, Drs. R.R. & R.W. (Hull University) 24th November, 1988
Combustion: Some Burning Problems
- * BUTLER, Dr. A.R. (St. Andrews University) 15th February, 1989
Cancer in Linxiam: The Chemical Dimension
- CADOGAN, Prof. J.I.G. (British Petroleum) 10th November, 1988
From Pure Science to Profit
- CASEY, Dr. M. (University of Salford) 20th April, 1989
Sulphoxides in Stereoselective Synthesis
- * CRICH, Dr. D. (University College London) 27th April, 1989
Some Novel Uses of Free Radicals in Organic
Synthesis
- DINGWALL, Dr. J. (Ciba Geigy) 18th October, 1988
Phosphorus-containing Amino Acids: Biologically
Active Natural and Unnatural Products
- ERRINGTON, Dr. R.J. (University of Newcastle-upon-Tyne) 1st March, 1989
Polymetalate Assembly in Organic Solvents
- FREY, Dr. J. (Southampton University) 11th May, 1989
Spectroscopy of the Reaction Path: Photodissociation
Raman Spectra of NOCl
- * GRADUATE CHEMISTS, (Polytechs and Universities in 12th April, 1989
North East England)
R.S.C. Symposium for presentation of papers by
postgraduate students
- HALL, Prof. L.D. (Addenbrooke's Hospital, Cambridge) 2nd February, 1989
NMR - A Window to the Human Body
- HARDGROVE, Dr. G. (St. Olaf College, U.S.A.) December, 1988
Polymers in the Physical Chemistry Laboratory
- HARWOOD, Dr. L. (Oxford University) 25th January, 1988
Synthetic Approaches to Phorbols Via Intramolecular
Furan Diels-Alder Reactions: Chemistry under Pressure

- JÄGER, Dr. C. (Friedrich-Schiller University GDR) 9th December, 1988
NMR Investigations of Fast Ion Conductors of the NASICON Type
- JENNINGS, Prof. R.R. (Warwick University) 26th January, 1989
Chemistry of the Masses
- * JOHNSON, Dr. B.F.G. (Cambridge University) 23rd February, 1989
The Binary Carbonyls
- LUDMAN, Dr. C.J. (Durham University) 18th October, 1988
The Energetics of Explosives
- MACDOUGALL, Dr. G. (Edinburgh University) 22nd February, 1989
Vibrational Spectroscopy of Model Catalytic Systems
- * MARKO, Dr. I. (Sheffield University) 9th March, 1989
Catalytic Asymmetric Osmylation of Olefins
- McLAUCHLAN, Dr. K.A. (University of Oxford) 16th November, 1988
The Effect of Magnetic Fields on Chemical Reactions
- * MOODY, Dr. C.J. (Imperial College) 17th May, 1989
Reactive Intermediates in Heterocyclic Synthesis
- PAETZOLD, Prof. P. (Aachen) 23rd May, 1989
Iminoboranes $\text{XB}\equiv\text{NR}$: Inorganic Acetylenes?
- PAGE, Dr. P.C.B. (University of Liverpool) 3rd May, 1989
Stereocontrol of Organic Reactions Using 1,3-dithiane-1-oxides
- POLA, Prof. J. (Czechoslovak Academy of Sciences) 15th June, 1989
Carbon Dioxide Laser Induced Chemical Reactions - New Pathways in Gas-Phase Chemistry
- * REES, Prof. C.W. (Imperial College London) 27th October, 1988
Some Very Heterocyclic Compounds
- SCHMUTZLER, Prof. R. (Technische Universität Braunschweig) 6th October, 1988
Fluorophosphines Revisited - New Contributions to an Old Theme
- SCHROCK, Prof. R.R. (M.I.T.) 13th February, 1989
Recent Advances in Living Metathesis
- SINGH, Dr. G. (Teesside Polytechnic) 9th November, 1988
Towards Third Generation Anti-Leukaemics
- SNAITH, Dr. R. (Cambridge University) 1st December, 1988
Egyptian Mummies: What, Where, Why and How?
- STIBR, Dr. R. (Czechoslovak Academy of Sciences) 16th May, 1989
Recent Developments in the Chemistry of Intermediate-Sited Carboranes
- VON RAGUE SCHLEYER, Prof. P. (Universität Erlangen Nürnberg) 21st October, 1988
The Fruitful Interplay Between Computational and Experimental Chemistry
- WELLS, Prof. F.B. (Hull University) 10th May, 1989
Catalyst Characterisation and Activity

(B) 1ST AUGUST 1989 TO 31ST JULY 1990

- BADYAL, Dr. J.P.S. (Durham University) 1st November, 1989
Breakthroughs in Heterogeneous Catalysis
- * BECHER, Dr. J. (Odense University) 13th November, 1989
Synthesis of New Macrocyclic Systems using
Heterocyclic Building Blocks
- BERCAW, Prof. J.E. (California Institute of Technology) 10th November, 1989
Synthetic and Mechanistic Approaches to
Ziegler-Natta Polymerization of Olefins
- BLEASDALE, Dr. C. (Newcastle University) 21st February, 1990
The Mode of Action of some Anti-tumour Agents
- BOWMAN, Prof. J.M. (Emory University) 23rd March, 1990
Fitting Experiment with Theory in Ar-OH
- * BUTLER, Dr. A. (St. Andrews University) 7th December, 1989
The Discovery of Penicillin: Facts and Fancies
- * CHEETHAM, Dr. A.K. (Oxford University) 8th March, 1990
Chemistry of Zeolite Cages
- * CLARK, Prof. D.T. (ICI Wilton) 22nd February, 1990
Spatially Resolved Chemistry (using Nature's
Paradigm in the Advanced Materials Arena)
- COLE-HAMILTON, Prof. D.J. (St. Andrews University) 29th November, 1989
New Polymers from Homogeneous Catalysis
- CROMBIE, Prof. L. (Nottingham University) 15th February, 1990
The Chemistry of Cannabis and Khat
- DYER, Dr. U. (Glaxo) 31st January, 1990
Synthesis and Conformation of C-Glycosides
- FLORIANI, Prof. C. (University of Lausanne,
Switzerland) 25th October, 1989
Molecular Aggregates - A Bridge between
homogeneous and Heterogeneous Systems
- * GERMAN, Prof. L.S. (USSR Academy of Sciences -
Moscow) 9th July, 1990
New Syntheses in Fluoroaliphatic Chemistry:
Recent Advances in the Chemistry of Fluorinated
Oxiranes
- GRAHAM, Dr. D. (B.P. Reserch Centre) 4th December, 1989
How Proteins Absorb to Interfaces
- GREENWOOD, Prof. N.N. (University of Leeds) 9th November, 1989
Novel Cluster Geometries in Metalloborane
Chemistry

- HOLLOWAY, Prof. J.H. (University of Leicester)
Noble Gas Chemistry 1st February, 1990
- * HUGHES, Dr. M.N. (King's College, London)
A Bug's Eye View of the Periodic Table 30th November, 1989
- HUISGEN, Prof. R. (Universität München)
Recent Mechanistic Studies of [2+2] Additions 15th December, 1989
- * KLINOWSKI, Dr. J. (Cambridge University)
Solid State NMR Studies of Zeolite Catalysts 13th December 1989
- LANCASTER, Rev. R. (Kimbolton Fireworks)
Fireworks – Principles and Practice 8th February, 1990
- LUNAZZI, Prof. L. (University of Bologna)
Application of Dynamic NMR to the Study of
Conformational Enantiomerism 12th February, 1990
- PALMER, Dr. F. (Nottingham University)
Thunder and Lightning 17th October, 1989
- PARKER, Dr. D. (Durham University)
Macrocycles, Drugs and Rock 'n' roll 16th November, 1989
- PERUTZ, Dr. R.N. (York University)
Plotting the Course of C–H Activations with
Organometallics 24th January, 1990
- PLATONOV, Prof. V.E. (USSR Academy of Sciences –
Novosibirsk) 9th July, 1990
Polyfluoroindanes: Synthesis and Transformation
- POWELL, Dr. R.L. (ICI) 6th December, 1989
The Development of CFC Replacements
- POWIS, Dr. I. (Nottingham University) 21st March, 1990
Spinning off in a huff: Photodissociation of
Methyl Iodide
- ROZHKOVA, Prof. I.N. (USSR Academy of Sciences –
Moscow) 9th July, 1990
Reactivity of Perfluoroalkyl Bromides
- STODDART, Dr. J.F. (Sheffield University) 1st March, 1990
Molecular Lego
- SUTTON, Prof. D. (Simon Fraser University,
Vancouver B.C.) 14th February, 1990
Synthesis and Applications of Dinitrogen and Diazo
Compounds of Rhenium and Iridium
- THOMAS, Dr. R.K. (Oxford University) 28th February, 1990
Neutron Reflectometry from Surfaces
- THOMPSON, Dr. D.P. (Newcastle University) 7th February, 1990
The role of Nitrogen in Extending Silicate
Crystal Chemistry

(C) 1ST AUGUST 1990 TO 31ST JULY 1991

- * ALDER, Dr. B.J. (Lawrence Livermore Labs., California) 15th January, 1991
Hydrogen in all its Glory
- BELL[†], Prof. T. (SUNY, Stony Brook, U.S.A.) 14th November, 1990
Functional Molecular Architecture and Molecular Recognition
- BOCHMANN[†], Dr. M. (University of East Anglia) 24th October, 1990
Synthesis, Reactions and Catalytic Activity of Cationic Titanium Alkyls
- BRIMBLE, Dr. M.A. (Massey University, New Zealand) 29th July, 1991
Synthetic Studies Towards the Antibiotic Griseusin-A
- BROOKHART, Prof. M.S. (University of N. Carolina) 20th June, 1991
Olefin Polymerizations, Oligomerizations and Dimerizations Using Electrophilic Late Transition Metal Catalysts
- * BROWN, Dr. J. (Oxford University) 28th February, 1991
Can Chemistry Provide Catalysts Superior to Enzymes?
- BUSHBY[†], Dr. R. (Leeds University) 6th February, 1991
Biradicals and Organic Magnets
- * COWLEY, Prof. A.H. (University of Texas) 13th December, 1990
New Organometallic Routes to Electronic Materials
- * CROUT, Prof. D. (Warwick University) 29th November, 1990
Enzymes in Organic Synthesis
- DOBSON[†], Dr. C.M. (Oxford University) 6th March, 1991
NMR Studies of Dynamics in Molecular Crystals
- GERRARD[†], Dr. D. (British Petroleum) 7th November, 1990
Raman Spectroscopy for Industrial Analysis
- HUDLICKY, Prof. T. (Virginia Polytechnic Institute) 25th April, 1991
Biocatalysis and Symmetry Based Approaches to the Efficient Synthesis of Complex Natural Products
- JACKSON[†], Dr. R. (Newcastle University) 31st October, 1990
New Synthetic Methods: α -Amino Acids and Small Rings
- KOCOVSKY[†], Dr. P. (Uppsala University) 6th November, 1990
Stereo-Controlled Reactions Mediated by Transition and Non-Transition Metals

- * LACEY, Dr. D. (Hull University) 31st January, 1991
Liquid Crystals
- LOGAN, Dr. N. (Nottingham University) 1st November, 1990
Rocket Propellants
- * MACDONALD, Dr. W.A. (ICI Wilton) 11th October, 1990
Materials for the Space Age
- MARKAM, Dr. J. (ICI Pharmaceuticals) 7th March, 1991
DNA Fingerprinting
- * PETTY, Dr. M.C. (Durham University) 14th February, 1991
Molecular Electronics
- PRINGLE[†], Dr. P.G. (Bristol University) 5th December, 1990
Metal Complexes with Functionalised Phosphines
- PRITCHARD, Prof. J. (Queen Mary & Westfield College,
London University) 21st November, 1990
Copper Surfaces and Catalysts
- SADLER, Dr. P.J. (Birkbeck College London) 24th January, 1991
Design of Inorganic Drugs: Precious Metals,
Hypertension + HIV
- SARRE, Dr. P. (Nottingham University) 17th January, 1991
Comet Chemistry
- SCHROCK, Prof. R.R. (Massachusetts Institute of Technology) 24th April, 1991
Metal-ligand Multiple Bonds and Metathesis Initiators
- * SCOTT, Dr. S.K. (Leeds University) 8th November, 1990
Clocks, Oscillations and Chaos
- SHAW[†], Prof. B.L. (Leeds University) 20th February, 1991
Syntheses with Coordinated, Unsaturated Phosphine
Ligands
- SINN[†], Prof. E. (Hull University) 30th January, 1991
Coupling of Little Electrons in Big Molecules.
Implications for the Active Sites of (Metalloproteins
and other) Macromolecules
- * SOULEN[†], Prof. R. (South Western University, Texas) 26th October, 1990
Preparation and Reactions of Bicycloalkenes
- WHITAKER[†], Dr. B.J. (Leeds University) 28th November, 1990
Two-Dimensional Velocity Imaging of State-Selected
Reaction Products

* Attended by the author.

[†] Invited specifically for the postgraduate training programme.

APPENDIX III - REFERENCES

1. Williams, D. J., *Angew. Chem. Int. Ed. Engl.*, 23, 690 (1984).
2. Levine, B. F., *Chem. Phys. Lett.*, 37, 516 (1976).
3. Cojan, C., Agrawal, G. P. and Flytzanis, C., *Phys. Rev.*, B15, 909 (1977).
4. Morrell, J. A. and Albrecht, A. C., *Chem. Phys. Lett.*, 64, 46 (1979).
5. Lalama, S. J. and Garito, A. F., *Phys. Rev.*, A20, 1179 (1979).
6. Dulcic, A., Flytzanis, C., Tang, C. L., Pepin, D., Fitizon, M. and Hoppiliard., *J. Chem. Phys.*, 74, 1559 (1981).
7. Levine, B. F. and Bethea, C. G., *J. Chem. Phys.*, 63, 2666 (1975).
8. Kurtz, S. K. and Perry, T. T., *J. Appl. Phys.*, 39 (8), 3798 (1968).
9. Peterson, I. R., Russell, G. J., Earls, J. D. and Girling, I. R., *Thin Solid Films*, 161 (1988).
10. Blodgett, K. B., *J. Am. Chem. Soc.*, 57, 1007 (1935).
11. Michio, S., *J. Mol. Elect.*, 1, 3 (1985).
12. Nicond, J. F. and Twieg, R. J., "Non-linear Optical Properties of Organic Molecules and Crystals," Academic Press, 1, 277 (1987).
13. Aktsipetrov, O. A., Akhmediev, N. N., Baranova, I. M., Mishina, E. D. and Novak, V. R., *Sov. Phys. -JETP.*, 62, 524 (1985).

14. Hayden, L.M., Kowel, S.T. and Srinivasch, M.P., *Opt. Commun.*, 55, 289 (1985).
15. Decker, G., Tieke, B., Bosshard, C. and Gunter, P., *J. Chem. Soc. Chem. Commun.*, 933 (1988).
16. Gunter, P., Bosshard, C., Sutter, K., Arend, H., Chapius, G., Twieg, R.J. and Dobrowoloski, D., *Appl. Phys. Lett.*, 50, 486 (1987).
17. Yariv, A., "*Quantum Electronics*", Wiley, New York, (1975).
18. Girling, I.R., Cade, N.A., Kolinsky, P.V. and Montgomery, C.M., *Electron. Lett.*, 132, 101 (1985).
19. Grunfeld, F. and Pitt, C.W., *Electron. Lett.*, 99, 249 (1982).
20. Girling, I.R., Cade, N.A., Kolinski, P.V., Earls, J.D., Cross, G.H. and Peterson, I.R., *Thin Solid Films*, 132, 101 (1985).
21. Twieg, R.J. and Jain, K., *Non-linear Optical Properties of Organic and Polymeric Materials*, ACS symp. ser. 57, 233 (1983).
22. Hayden, L.M., Anderson, B.L., Lam, J.Y.S, Higgins, B.G., Stroeve, P. and Kowel, S.T., *Thin Solid Films*, 160, 379 (1988).
23. Girling, I.R., Jethwa, S.R., Stewart, R.T., Earls, J.D., Cross, G.H., Cade, N.A., Kolinsky, P.V., Jones, R.J. and Peterson, I.R., *Thin Solid Films*, 160, 355 (1988).

24. Ledoux, I., Josse, D., Fremaux, P., Piel, J-P., Post, G., Zyss, J., McLean, T., Hann, R.A., Gordon, P.F., *Thin Solid Films*, 160, 217 (1988).
25. Miller, L.S., Travers, P.J., Sethi, R.S., Goodwin, M.J., Marsden, R.M., Gray, G.W. and Scrowston, R.M., in "*Organic Materials for Non-linear Optics*", Hann, R.A., Bloor, D., Eds.; Royal Society of Chemistry: London, 1989, 361.
26. Aksipetrov, O.A., Akhmediev, N.N., Mishina, E.D. and Novak, V.R., *JETP Lett.*, 37, 207 (1983).
27. Ahmad, M.M., Feast, W.J., Neal, D.B., Petty, M.C. and Roberts, G.G., *J.Mol.Elect.*, 2, 129 (1986).
28. Mukherjee, S., Tsibouklis, J., Petty, M.C., Cresswell, J. and Feast, W.J., *J.Mol.Elect.*, 6, 221 (1990).
29. Bauer, J., Jeckeln, P., Lupo, D., Prass, W., Scheunemann, U., Keosian, R. and Khonerian, G., in ref. 25, p.348.
30. Era, M., Tsutsui, T. and Saito, S., *Langmuir*, 5, 1410 (1989).
31. Girling, I.R., Cade, N.A., Kolinsky, P.V., Jones, R.J., Peterson, I.R., Ahmad, M.M., Neal, D.B., Petty, M.C., Roberts, G.G. and Feast, W.J., *J. Opt. Soc. Am. B*, 4, 950 (1987).
32. Schildkraut, J.S., Penner, T.L., Willand, C.S. and Ulman, A., *Optics Lett.*, 13, 134 (1988).

33. Lupo, D., Praß, W., Scheunemann, U., Laschewsky, A., Ringsdorf, H. and Ledoux, I., *J. Opt. Soc. Am. B*, 5, 300 (1988).
34. Nakamura, K., Era, M., Tsutsui, T. and Saito, S., *Jap. Appl. Phys.*, 29, 628 (1990).
35. Ashwell, G. J., Dawnay, E. J. C., Kucynski, A. P., Szablewski, M., Savely, I. M., Bryce, M. R., Grainger, A. M. and Hasan, M., *J. Chem. Soc. Faraday. Trans.*, 86, 1117 (1990).
36. Era, M., Nakamura, K., Tsutsui, T., Saito, S., Niino, H., Takehara, K., Isomura, K. and Taniguchi, H., *Jap. J. Appl. Phys.*, 29, 2261 (1990).
37. Kalina, D. W. and Grubb, S. G., *Thin Solid Films*, 160, 48 (1989).
38. Blau, W., *Phys. Technol.*, 18, 250 (1987).
39. Oudar, J. L. and LePerson, H., *Opt. Commun.* 15(2), 258 (1975).
40. Levine, B. F., Bethea, C. G., Thurmond, C. D., Lynch, R. T. and Bernstein, J. L., *J. Appl. Phys.*, 50, 2523 (1979).
41. Meredith, G. R., Williams, D. J., Weagly, R. W., *J. Am. Chem. Soc.*, in press.
42. Singer, K. D., Sohn, J. E., Lalama, S. J., *Appl. Phys. Lett.*, 49, 248 (1986).
43. Bryce, M. R. and Murphy, L. C., *Nature*, 309, 119 (1984).
44. Baghdadchi, J. and Panetta, C. A., *J. Org. Chem.*, 48, 3852 (1983).
45. Acker, D. S. and Hertler, J. R., *J. Am. Chem. Soc.*, 84, 3370 (1962).

46. Uno, M., Seto, K., Masuda, M., Ueda, W. and Takahashi, S., *J. Chem. Soc. Chem. Commun.*, 932 (1984).
47. Uno, M., Seto, K., Masuda, M., Ueda, W. and Takahashi, S., *Tetrahedron Lett.*, 26, 1553 (1985).
48. Yamaguchi, S., Nagareda, K. and Hanafusa, T., *Synthetic Metals.*, 30, 401 (1989).
49. Rosenau, B., Krieger, C. and Staab, H. A., *Tetrahedron Lett.*, 26, 2081 (1985).
50. Lehnert, W., *Synthesis.*, 667 (1974).
51. Aumuller, A. and Hunig, S., *Liebigs. Ann. Chem.*, 618 (1984).
52. Kini, A., Mays, M. and Cowan, D. O., *J. Chem. Soc. Chem. Commun.*, 286 (1985).
53. Yamaguchi, S. and Hanafusa, T., *Chem. Lett.*, 689 (1985).
54. Wheland, R. C. and Martin, E. L., *J. Org. Chem.*, 40, 3101 (1975).
55. Whitten, J. P., McCarthy, J. R. and Matthews, D. P., *Synthesis.*, 470 (1988).
56. Bryce, M. R. and Howard, J. A. K., *Tetrahedron Lett.*, 24, 1205 (1983).
57. Stokes, J. P., Emge, T. J., Bryden, W. A., Chappell, J. S., Cowan, D. O., Poehler, T. O., Bloch, A. N. and Kistenmacher, T. J., *Mol. Cryst. Liq. Cryst.*, 79, 327 (1982).
58. Jorgensen, M. and Bechgaard, K., *Synthesis*, 208 (1989).
59. Ferraris, J., Cowan, D. O., Walatka, V. V. and Perstein, J. H., *J. Am. Chem. Soc.*, 95, 948 (1973).

60. Miller, J.S., Epstein, A.J. and Rieff, W.M., *Chem. Rev.*, 88, 201 (1988).
61. Metzger, R.M., Schumaker, R.R., Cava, M.P., Laidlaw, R.K., Panetta, C.A. and Torres, E., *Langmuir*, 4, 298 (1988).
62. Melby, L.R., Harder, R.J., Hertler, W.R., Mahler, W., Benson, R.E. and Mockel, W.E., *J. Am. Chem. Soc.*, 84, 3374 (1962).
63. Hunig, S., *Pure Appl. Chem.*, 62, 395, 1990.
64. Bryce, M.R. and Davies, S.R., *J. Chem. Soc. Chem. Commun.*, 328 (1989).
65. Czelanski, T., Hanack, M., Becker, J.Y., Bernstein, J., Bittner, S., Kaufman-Orenstein, L. and Peleg, D., *J. Org. Chem.*, 56, 1569 (1991).
66. Iwasaki, F., *Acta Crystallogr. Sect. B.*, B27, 1360 (1971).
67. Iwatsuki, S., Itoh, T. and Itoh, H., *Chem Lett.*, 1187 (1988).
68. Aumuller, A., Hunig, S., *Liebigs. Ann. Chem.*, 142 (1986).
69. Girling, I.R., Cade, N.A., Kolinsky, P.V. and Montgomery, C.M., *Electron. Lett.*, 21, 169 (1985).
70. Metzger, R.M., Heimer, N.E. and Ashwell, G.J., *Mol. Cryst. Liq. Cryst.*, 107, 133 (1984).
71. Ledoux, I. and Zyss, J., *Chem. Phys.*, 73, 203 (1982).
72. Ashwell, G.J., *Thin Solid Films*, 186, 155 (1990).
73. Mulliken, R.S. and Person, W.B., *Molecular Complexes* Wiley, New York, (1969).
74. Akhtar, S., Tanaka, J., Metzger, R.M. and Ashwell, G.J., *Mol. Cryst. Liq. Cryst.*, 139, 353 (1986).

75. Hertler, W.R., Hartzler, H.D., Acker, D.S. and Benson, R.E., *J. Am. Chem. Soc.*, 84, 3387 (1962).
76. Miller, J.S. and Calabrese, J.C., *J. Chem. Soc. Chem. Commun.*, 63 (1988).
77. Ashwell, G.J., Dawnay, E.J.C., Kuczynski, A.P. and Szablewski, M., *Mater. Res. Soc. Symp. Proc.*, 173, 507, (1990).
78. Ashwell, G.J., Dawnay, E.J.C. and Kuczynski, A.P., *J. Chem. Soc. Chem. Commun.*, 1335 (1990).
79. Popovitz-Biro, R., Hill, K., Landan, E.M., Lahav, M., Leiserowitz, L., Sagio, J., Hsiung, H., Meredith, G.R. and Vanherzeele, H., *J. Am. Chem. Soc.*, 110, 2672 (1988).
80. Marowsky, G., Chi, L.F., Mobius, D., Steinhoff, R., Shen, Y.R., Dorsch, D. and Reiger, B., *Chem. Phys. Lett.*, 147, 420 (1988).
81. Cross, G.H., Peterson, I.R., Girling, I.R., Cade, N.A., Goodwin, M.J., Carr, N., Sethi, R.S., Marsden, R., Gray, G.W., Lacey, D., McRoberts, A.M., Scrowston, R.M. and Toyne, K.J., *Thin Solid Films.*, 156, 39 (1988).
82. Dulcic, A. and Flytzanis, C., *Opt. Commun.*, 25, 402 (1978).
83. Netzer, L., Iscovici, R. and Sagiv, J., *Thin Solid Films*, 99, 235 (1983).
84. Ashwell, G.J., Dawnay, E.J.C., Kuczynski, A.P. and Martin, P.J., to be published.
85. Albright, J.D., DeVries, V.G., Du, M.T., Largis, E.E., Thomas, G., Reich, M.F. and Shepherd, R.G., *J. Med. Chem.*, 26, 1393 (1983).

86. Pugh, D. and Sherwood, J., *Chem. in Brit.*, 24, 544 (1988).
87. Bryce, M.R., *Aldrichimica Acta.*, 18 (3), 73 (1985).
88. Blanchard-Desce, M., Ledoux, I., Lehn, J.M., Malthete, J. and Zyss, J., *J. Chem. Soc. Chem. Commun.*, 737 (1988).
89. Dulcic, A., Flytzanis, C., Tang, C.L., Pepin, D., Fetizon, M. and Hopilliard, Y., *J. Chem. Phys.*, 74, 1559 (1981).
90. Oudar, J.L., *J. Chem. Phys.* 67, 446 (1977).
91. Kurtz, S.K. and Perry, T.T., *J. Appl. Phys.*, 39, 3798 (1988).
92. Barzoukas, M., Blanchard-Desce, M., Josse, D., Lehn, J-M. and Zyss, J., *Inst. Phys. Conf. Ser. No. 103. Section 2: 6.*, 239 (1989).
93. Dulcic, A. and Sauteret, C., *J. Chem. Phys.*, 69, 3453 (1978).
94. Morley, J.O., Docherty, V.J. and Pugh, D., *J. Chem. Soc. Perkin Trans. 2.*, 1351 (1985).
95. Palacin, S., Blanchard-Desce, M., Lehn, J.M. and Barraud, A., *Thin Solid Films*, 178, 387 (1989).
96. Vandevyver, M., Barraud, A., Ruaudel-Teixier, A., Maillard, P. and Gianotti, C., *J. Colloid Interface Sci.*, 85, 571 (1982).
97. Katz, H.E., Singer, K.D., Sohn, J.E., Dirk, C.W., King, L.A. and Gordon, H.M., *J. Am. Chem. Soc.*, 109, 6561 (1987).
98. Davis, W.A. and Cava, M.P., *J. Org. Chem.*, 48, 2774 (1983).

99. Sugimoto, T., Awaji, H., Sugimoto, I., Misaki, Y., Kawase, T., Yoneda, S. and Yoshida, Z., *Chem. Mater.*, 1, 535 (1989).
100. Hyatt, J. A., *J. Org. Chem.*, 48, 129 (1983).
101. Smith, L. I., Opie, J. W., Wawzonek, S. and Prichard, W. W., *J. Org. Chem.*, 4, 318 (1939).
102. Hahn, W. E., Wojciechowski, L., *Rocz. Chem.*, 41, 1067 (1967). (Chem. Abs. 68, 595104, 1968).
103. Gompper, R., Binder, R., Wagner, H. U., *Tetrahedron Lett.*, 27, 691 (1986).
104. Hursthouse, M. B., Jones, R. A., Malik, K. M. A. and Wilkinson, G., *J. Am. Chem. Soc.*, 101, 4128 (1979).
105. North, A. C. T., Phillips, D. C. and Mathews, F. S., *Acta Crystallogr., Sec. A*, A24, 351 (1968).
106. Sheldrick, G. M., SHELX-86 Program for Crystal Structure Solution, University of Gottingen, 1986.
107. Sheldrick, G. M., SHELX-76 Program for Crystal Structure Determination and Refinement, University of Cambridge, 1976.
108. Walker, N., Stuart, D., *Acta Crystallogr., Sec. A*, A39, 158 (1983).
109. Chatterjee, S., *J. Chem. Soc. (B)*, 1170, (1967).
110. Sandman, D. J. and Garito, A. F., *J. Org. Chem.*, 39, 1165, (1974).

